

GEOLOGICA ULTRAIECTINA

Mededelingen van de  
Faculteit Aardwetenschappen der  
Rijksuniversiteit te Utrecht

No. 86

**SOURCE, EVOLUTION, AND AGE OF  
CORONITIC GABBROS FROM THE ARENDAL-  
NELAUG AREA, BAMBLE, SOUTHEAST NORWAY**

**G.J.L.M. de Haas**

GEOLOGICA ULTRAIECTINA

Mededelingen van de  
Faculteit Aardwetenschappen der  
Rijksuniversiteit te Utrecht

No. 86

**SOURCE, EVOLUTION, AND AGE OF  
CORONITIC GABBROS FROM THE ARENDAL-  
NELAUG AREA, BAMBLE, SOUTHEAST NORWAY**

24 - 006

CIP-GEGEVENS KONINKLIJKE BIBLIOTHEEK, DEN HAAG

Haas, Gerardus Johannes Lambertus Maria de

Source, evolution, and age of coronitic gabbros from the  
Arendal-Nelaug area, Bamble, Southeast Norway/ Gerardus  
Johannes Lambertus Maria de Haas. - [Utrecht : Faculteit  
Aardwetenschappen der Rijksuniversiteit Utrecht]. -  
(Geologica Ultraiectina, ISSN 0072-1026 ; no. 86)  
Proefschrift Rijksuniversiteit Utrecht - Met lit. opg. -  
Met samenvatting in het Nederlands.  
ISBN 90-71577-38-4  
Trefw.: coronitische gabbros; Noorwegen; geschiedenis.

**SOURCE, EVOLUTION, AND AGE OF  
CORONITIC GABBROS FROM THE ARENDAL-  
NELAUG AREA, BAMBLE, SOUTHEAST NORWAY**

**OORSPRONG, EVOLUTIE EN OUDERDOM VAN CORONITISCHE  
GABBROS UIT HET ARENDAL-NELAUG GEBIED, BAMBLE,  
ZUIDOOST NOORWEGEN**

(MET EEN SAMENVATTING IN HET NEDERLANDS)

PROEFSCHRIFT

TER VERKRIJGING VAN DE GRAAD VAN DOCTOR  
AAN DE RIJKSUNIVERSITEIT TE UTRECHT  
OP GEZAG VAN DE RECTOR MAGNIFICUS, PROF.DR. J.A. VAN GINKEL,  
INGEVOLGE HET BESLUIT VAN HET COLLEGE VAN DEKANEN  
IN HET OPENBAAR TE VERDEDIGEN OP MAANDAG  
27 APRIL 1992 DES NAMIDDAGS OM 12.45 UUR

DOOR

**GERARDUS JOHANNES LAMBERTUS MARIA DE HAAS**  
GEBOREN OP 1 FEBRUARI 1964, TE GOIRLE

PROMOTORES: PROF.DR. R.D. SCHULING  
PROF.DR. J.L.R. TOURET  
CO-PROMOTOR: DR. C. MAIJER

Aan Anne  
Aan mijn ouders

Is 't zoo goed mister...  
Ge doet mar zô as ge denkt det goed is...  
As 't mar goed is.

Cees Robben

## **VOORWOORD**

Bij het tot stand komen van dit proefschrift, wil ik graag de volgende personen bedanken voor hun bijdrage, in welke vorm dan ook.

Mijn co-promotor Dr. C. Maijer. Cees, bedankt voor de meer dan voortreffelijke samenwerking. Jouw nimmer aflatend enthousiasme en schier onuitputtelijke kennis van Zuid-Noorwegen zijn voor mij van grote waarde geweest.

Mijn promotores Prof. Dr. R.D. Schuiling en Prof. Dr. J.L.R. Touret voor hun constructieve reviews van mijn manuscripten en waardevolle suggesties.

Tony Senior, Ben Jansen, Rob Verschure, Timo Nijland, Bas Dam en Diederik Visser voor de vele discussies, in het veld dan wel op de kamer.

Joep Huijsmans voor zijn begeleiding 'op afstand'.

Andries Krijgsman, Dick Liefink, Roland Vogels en Maarten Broekmans voor hun interesse en hun bijdrage aan de prettige werksfeer binnen de afdeling Petrologie.

Marius Maarschalkerweerd voor het verlenen van duizend-en-één hand en spandiensten.

Sven Scholten, Pieter Vroon, Hans Eggenkamp, Bertil van Os, Giuseppe Frapporti, Paulien van Gaans, Simon Vriend, Manfred van Bergen, Else Henneke, Pier de Groot, Jurian Hoogewerff, René Poorter, Ineke Kalt, Vian Govers, Chiel Eussen, Berta Djie-Kwee, Thea van Meerten, de medewerkers van de bibliotheek, de slijpkamer en de A.V. dienst.

Mijn collega-promovendi, werkzaam bij het Laboratorium voor Isotopen Geologie te Amsterdam: Paul Saager, Kay Beets, Peter Valbracht, José van Duin, Marjan van der Wiel, Jan Schijf en Max Röhrman.

Medewerkers van bovengenoemd laboratorium: Paul Andriessen, Ed Verdurmen, Lodewijk IJlst, Jan Wijbrands, Piet Remkes, Coos van Belle, Richard Smeets, Rob Scheveers en Frans Benavente.



I also thank my SvecoNorwegian Friends Tom Andersen, Lars Kullerud, Sven Dahlgren, Per Hagelia, Peter Padget, Inge-Anne Munz, Karl-Inge Åhäll, Leif Johansson, Stephen Daly and Julian Menuge for their interest in my work and the fruitful discussions.

Mijn ouders dank ik voor hun onvoorwaardelijke steun die ik altijd ondervonden heb tijdens mijn studie.

Anne, bedankt voor het vele geduld en vertrouwen.

# CONTENTS

<b>Voorwoord</b> .....	vii
<b>Contents</b> .....	ix
<b>Summary</b> .....	xi
<b>Samenvatting</b> .....	xiii
<b>Chapter I Introduction</b> .....	1
1.1 Evolution of the Baltic Shield .....	3
1.2 Magmatic evolution of the Southwest Scandinavian Domain .....	5
1.3 The geology of the Bamble Sector .....	9
1.3.1 Introduction .....	9
1.3.2 Evolution of the Bamble Sector .....	11
1.3.2.1 The Gothian Orogeny (1.75-1.50 Ga) .....	11
1.3.2.2 The Gothian-Sveconorwegian interlude (1.50-1.25 Ga) .....	13
1.3.2.3 The Sveconorwegian Orogeny (1.25-0.90 Ga) .....	13
1.4 The Bamble hyperites and the scope of this thesis .....	15
1.4.1 The term hyperite .....	15
1.4.2 The Bamble hyperites .....	15
1.4.3 The scope of this thesis .....	18
<b>Chapter II The magmatic history of the Vestre Dale Gabbro</b> .....	19
2.1 Introduction .....	19
2.2 Geological setting .....	20
2.3 Petrography .....	23
2.4 Whole rock and mineral chemistry .....	25
2.4.1 Analytical techniques .....	25
2.4.2 Whole rock chemistry .....	28
2.4.3 Sr isotopes .....	31
2.4.4 Mineral chemistry .....	31
2.5 Discussion .....	32
2.5.1 Crystallization of the Vestre Dale Gabbro .....	32
2.5.2 Parental magma composition .....	35
2.5.3 Emplacement .....	36
2.5.4 Regional implications .....	37
<b>Chapter III Igneous layering and magma replenishment in a 500 m thick gabbroic intrusion in the Proterozoic crust of South Norway</b> .....	39
3.1 Introduction .....	39
3.2 Geological setting .....	39
3.3 Igneous structures .....	40
3.3.1 Basal Zone .....	40
3.3.2 Slumped Unit .....	41
3.3.3 Upper Zone .....	44
3.4 Petrography .....	45
3.5 Whole rock chemistry .....	46
3.6 Magmatic evolution .....	48
3.7 Lower crustal implications .....	52
<b>Chapter IV Sm-Nd age determinations of some coronitic gabbros and the nature of the Proterozoic mantle below Bamble</b> .....	55
4.1 Introduction .....	55
4.2 Geology .....	56
4.3 Petrography .....	58

4.4 Analytical methods	59
4.5 Age calculations	59
4.6 Discussion	63
4.6.1 Interpretation of the isochron ages	63
4.6.2 Age correlations	64
4.6.3 Depletion and evolution of the sub-Bamble mantle	65
4.7 Conclusions	67
<b>Chapter V Rb-Sr isotope systematics of the Vestre Dale Gabbro and its country rocks</b>	<b>69</b>
5.1 Introduction	69
5.2 Petrography	70
5.3 Results	70
5.4 Discussion and conclusions	76
<b>Chapter VI Identification of the source and petrogenesis of the coronitic gabbros from the Arendal-Nelaug area</b>	<b>79</b>
6.1 Introduction	79
6.2 Petrography	81
6.3 Chemical correlations between the gabbros	81
6.3.1 Harker diagrams	81
6.3.2 REE patterns	83
6.3.3 Incompatible trace element plots	86
6.4 Petrogenesis	89
6.4.1 Parental magma composition	89
6.4.2 LILE and LREE enrichments	94
6.4.3 Sr and Nd isotopes	95
6.4.4 Comparison with other mafic rocks from the SWSD	96
6.4.5 Origin of the LILE and LREE enrichments	99
6.5 Conclusions	104
Appendix 1	105
Appendix 2	108
<b>Chapter VII The Bamble Gabbros: implications for the evolution of the Bamble Sector and the underlying mantle</b>	<b>111</b>
<b>References</b>	<b>116</b>
<b>Curriculum Vitae</b>	<b>129</b>

**Chapter II** will appear in *Neues Jahrbuch für Mineralogie/Abhandlungen* under the title "The magmatic history of a gabbroic intrusion in the Bamble Sector, Vestre Dale, Norway" (in press). Co-authors: T.G. Nijland, J.P.P. Huijsmans, C. Maijer and B.P. Dam.

**Chapter III** has been accepted for publication in *Norsk Geologisk Tidsskrift* (with revisions). Co-authors: T.G. Nijland, A. Senior and B.P. Dam.

**Chapters IV and VI** (combined) will appear in *Precambrian Research* under the title "Isotopic constraints on the timing of crustal accretion of the Bamble Sector, Norway, as evidenced by coronitic gabbros" (in press). Co-authors: R.H. Verschure and C. Maijer.

**Chapter V** has been submitted to *Geologiska Föreningens i Stockholm Förhandlingar* under the title "Isotopic age determinations in South Norway III: Rb-Sr isotope systematics of the coronitic Vestre Dale Gabbro and its country rocks, Bamble Sector". Co-authors: R.H. Verschure and C. Maijer.

## SUMMARY

In this thesis the results of a petrological, geochemical and isotopic study of five coronitic gabbros (hyperites) from the Arendal-Nelaug area, Bamble Sector, South Norway, are presented. The scope of this study was 1) to determine the age of these gabbros, 2) to study their magmatic and chemical evolution, 3) to study the nature of the Proterozoic mantle below Bamble from Nd isotope data, and 4) to infer the composition of the mantle source(s) of the gabbros.

In **Chapter I**, an outline of the geological evolution of the Southwest Scandinavian Domain and, in more detail, of the Bamble Sector is presented. A review of previous studies of the Bamble coronitic gabbros is given. The chapter ends with the scope of the thesis.

**Chapter II** deals with the magmatic evolution of the Vestre Dale Gabbro. This gabbro, which is built up by four groups of cumulates ranging in composition from troctolitic gabbro via olivine gabbro to ferro gabbro, crystallized from one single, tholeiitic magma. Whole rock chemical variations in the cumulate sequence are governed by varying amounts of cumulus olivine and plagioclase. During crystallization, the magma became enriched in incompatible elements like K, Rb, P, Zr and REE. Sr isotope data betray limited progressive contamination of the magma by wall rock assimilation. The Vestre Dale Gabbro has finally been emplaced as a crystal mush.

In **Chapter III**, an account on primary igneous layering in the Flosta Gabbro is given. In this 500 meter thick gabbro, at least three separate magma pulses have been detected on basis of the whole rock chemical profiles of Mg#, TiO<sub>2</sub>, FeO, Nb and Zr. The pulses coincide with maximum anorthite contents of plagioclase. A fourth pulse could not be established with certainty. The igneous structures indicate that current deposition was the main cumulate forming process. These features were preserved in spite of a granulite facies overprint.

Sm-Nd isotope data for the coronitic gabbros, presented in **Chapter IV**, demonstrate that intrusion of the Bamble coronitic gabbros is not bound to the Sveconorwegian Orogeny (1.25 - 0.90 Ga). The Vestre Dale Gabbro has been dated at  $1.11 \pm 0.14$  Ga; the Jomåsknutene and Flosta Gabbros yield much older, Gothian, ages:  $1.77 \pm 0.19$  Ga and  $1.64 \pm 0.23$  Ga respectively. Initial Nd isotope ratios of these gabbros indicate that a depleted mantle below Bamble, with an  $\epsilon_{Nd}$  of  $\approx +5.5$ , was present at  $T = 1.7$  Ga.

This highly positive value differs significantly from the Nd isotope evolution curve for the Southwest Scandinavian mantle postulated by Mearns et al. (1986), which assumes that depletion of the mantle beneath this part of Scandinavia started c. 1.74 Ga ago.

**Chapter V** deals with Rb-Sr isotope systematics of the Vestre Dale Gabbro and its country rocks. Rb-Sr whole rock errorchron ages of the Vestre Dale Gabbro and the agmatitic contact zone fall within the error limits of the Sm-Nd whole rock age of the Vestre Dale Gabbro. This suggests that, at hand-specimen scale, the Rb-Sr system remained closed during the Sveconorwegian Orogeny. Emplacement of the Vestre Dale Gabbro disturbed the Rb-Sr systematics of surrounding migmatites; it appears that complete homogenization of the Rb-Sr system was not achieved. Rb-Sr and K-Ar ages of biotites and muscovites are related to Sveconorwegian cooling.

From the geochemical study, presented in **Chapter VI**, it is concluded that none of the gabbros crystallized from primary, mantle-derived magmas. Some trace element ratios (Ti/Zr, Zr/Y) suggest a close genetic relationship between the gabbros. Variable LREE (La, Ce, Nd) enrichment, associated with LILE (K, Rb, Ba) enrichment indicates that this is only partly true. It is proposed that enrichment was caused by introduction of LILE/LREE-bearing fluids into the mantle during Gothian subduction. This is also responsible for the range in  $\epsilon_{Nd}$  values and  $^{87}Sr/^{86}Sr$  ratios at 1.1 Ga, indicating that the mantle retained its enriched nature for more than 0.5 Ga.

**Chapter VII** synthesises the conclusions of this study and considers their implications for the evolution of the Bamble Sector. It is inferred that accretion of the Bamble Sector was contemporaneous with crustal growth in the Östfold-Marstrand Belt at c. 1.76 Ga and occurred at an active plate margin. The Sveconorwegian gabbros have been derived from a mafic underplate, which also provided the heat for amphibolite-granulite facies metamorphism.

## SAMENVATTING

In dit proefschrift worden de resultaten gepresenteerd van een petrologisch, geochemisch en isotopisch onderzoek van vijf coronitische gabbro's uit het Arendal-Nelaug gebied, Bamble Sector, Zuid-Noorwegen. Het doel van dit onderzoek was om 1) de ouderdom van deze gabbro's te bepalen, 2) de magmatische en chemische evolutie van deze gabbro's te bestuderen, 3) de aard van de mantel onder Bamble ten tijde van het Proterozoïcum te bestuderen aan de hand van Nd isotopen, en 4) de samenstelling van het oorsprongsgesteente van de gabbro's in de mantel te achterhalen.

In **Hoofdstuk I** wordt de geologische evolutie van Zuidwest Scandinavië (Southwest Scandinavian Domain) en, in meer detail, van de Bamble Sector geschetst. Daarnaast wordt een overzicht gegeven van eerdere onderzoeken van de coronitische gabbro's uit de Bamble Sector. Het hoofdstuk eindigt met de doelstelling van dit proefschrift.

**Hoofdstuk II** behandelt de magmatische evolutie van de Vestre Dale Gabbro. Deze gabbro, die opgebouwd is uit vier groepen cumulaten, in samenstelling variërend van troctolitische gabbro via olivijn gabbro tot ferro gabbro, kristalliseerde uit één tholeiitisch magma. Variaties in de whole rock chemie worden bepaald door variërende hoeveelheden olivijn en plagioklaas. Tijdens kristallisatie werd het magma aangerijkt in incompatibele elementen zoals K, Rb, P, Zr en de REE. Sr isotopen geven aan dat kristallisatie, zij het op geringe schaal, gepaard ging met progressieve contaminatie van het magma door assimilatie van korstmateriaal. De Vestre Dale Gabbro intrudeerde uiteindelijk als een 'crystal mush'.

In **Hoofdstuk III** wordt gewag gemaakt van primaire magmatische gelaagdheden in de Flosta Gabbro. In deze 500 m dikke gabbro zijn, op grond van whole rock chemische profielen van Mg#, TiO<sub>2</sub>, FeO, Nb en Zr, op zijn minst drie afzonderlijke magma pulsen te onderscheiden. De pulsen vallen samen met maxima in de anorthietgehalten van plagioklaas. Een vierde puls kon niet met zekerheid worden vastgesteld. De magmatische structuren geven aan dat de cumulaten vooral gevormd zijn door stroomafzetting. De structuren zijn bewaard gebleven ondanks een daaropvolgende granuliet facies metamorfose.

Uit Sm-Nd isotoop data, gepresenteerd in **Hoofdstuk IV**, blijkt dat intrusie van de coronitische gabbro's uit de Bamble Sector niet alleen plaats vond tijdens de Sveconorwegische Orogenese (1,25 - 0,9 miljard jaar geleden). De Vestre Dale Gabbro

is gedateerd op  $1,11 \pm 0,14$  miljard jaar. De Jomåsknutene en Flosta Gabbro's leveren veel hogere, Gothische, ouderdommen op, respectievelijk  $1,77 \pm 0,19$  en  $1,64 \pm 0,23$  miljard jaar. Initiële Nd isotoop verhoudingen van deze gabbro's geven aan dat de mantel onder Bamble 1,7 miljard jaar geleden verarmd ('depleted') was, met een  $\epsilon_{Nd}$  waarde van ca. +5.5. Deze hoge, positieve waarde wijkt aanzienlijk af van de door Mearns et al. (1986) gepostuleerde Nd isotopische evolutie curve voor Zuid-Scandinavië, die er vanuit gaat dat de depletie van de mantel onder dat deel van Scandinavië pas ongeveer 1,74 miljard jaar geleden startte.

**Hoofdstuk V** behandelt de Rb-Sr isotopen systematiek van de Vestre Dale Gabbro en zijn nevangesteente. Rb-Sr whole rock errorchron ouderdommen van de Vestre Dale Gabbro en de agmatitische contactzone vallen binnen de foutenmarge van de Sm-Nd whole rock ouderdom van de Vestre Dale Gabbro. Dit suggereert dat, op handstuk schaal, het Rb-Sr systeem gesloten bleef tijdens de Sveconorwegische Orogenese. De intrusie van de Vestre Dale Gabbro verstoortte het Rb-Sr systeem van de omliggende migmatieten. Het blijkt dat dit niet leidde tot volledige homogenizatie van het Rb-Sr systeem. Rb-Sr en K-Ar ouderdommen van biotieten en muscovieten zijn gerelateerd aan Sveconorwegische afkoeling.

Uit de geochemische studie in **Hoofdstuk VI** wordt geconcludeerd dat geen van de coronitische gabbro's gekristalliseerd zijn uit primaire, uit de mantel afkomstige magma's. Enkele spore-element ratio's (Ti/Zr, Zr/Y) suggereren dat de gabbro's genetisch aan elkaar verwant zijn. De variabele aanrijking in LREE (La, Ce, Nd) samen met de aanrijking in LILE (K, Rb, Ba) duidt erop dat dit slechts ten dele waar is. Er wordt voorgesteld dat deze aanrijking veroorzaakt is door de introductie van LILE/LREE-houdende fluïde fase in de mantel tijdens Gothische subductie. Dit proces is ook verantwoordelijk voor de spreiding in  $\epsilon_{Nd}$  waarden en  $^{87}\text{Sr}/^{86}\text{Sr}$  ratio's 1,1 miljard jaar geleden. Dit geeft aan dat de mantel aangerijkt bleef gedurende meer dan een half miljard jaar.

**Hoofdstuk VII** vat de conclusies van dit onderzoek samen en overweegt de implicaties die deze hebben voor de evolutie van de Bamble Sector. Er wordt afgeleid dat accretie van de Bamble Sector gelijktijdig was met die van de Östfold-Marstrand Belt, ca. 1,76 miljard jaar geleden en dat dit plaats vond langs een actieve plaat grens. De Sveconorwegische gabbro zijn afkomstig uit een mafische onderplaat die ook de warmte leverde voor de amphiboliet-granuliet facies metamorfose.

# CHAPTER I

## INTRODUCTION

One of the salient features of the Proterozoic Bamble Sector is the occurrence of coronitic gabbros or *hyperites*. These rocks have attracted the attention of many geologists since the classical study of Brøgger (1934a). Attention in later studies mainly focused on the coronitic microstructures. The geochemistry and the age of the Bamble hyperites have gained little attention. Except for a few K-Ar mineral ages (O’Nions et al., 1969), no isotope data were available previous to this study. Because of the preservation of very fresh, obviously magmatic features in the cores, it was more or less tacitly accepted that the hyperites were late phenomena in Bamble’s complicated history. This thesis presents a study on the geochemical and magmatic evolution of five hyperites from the Bamble Sector and their isotope systematics, with the emphasis on the Sm-Nd system.

The aim of this chapter is to inform the reader about the evolution of the Bamble Sector, its relationship with other Proterozoic domains in southwestern Scandinavia, and the present-day state of knowledge of the Bamble hyperites. In the last part of this chapter the scope of this thesis will be highlighted.

The Proterozoic polymetamorphic Bamble Sector is situated in the southeastern part of Norway along the Skagerrak coast, extending for 150 km with a maximum width of 30 km (Fig. 1.1). It is separated from the adjacent Telemark Sector on its northwestern margin by the ‘great breccia’ or ‘friction breccia’ (Bugge, 1928) or Porsgrunn-Kristiansand-Fault (Morton et al., 1970). Its contact with the Oslo Rift in the northeast is obscured by Cambro-Ordovician sediments. The Bamble Sector is part of the Southwest Scandinavian Domain of the Baltic (Fennoscandian) Shield (Gaál and Gorbatshev, 1987; Gorbatshev and Gaál, 1987), the latter comprising most of Scandinavia and the Kola Peninsula. Before going into details of the geology of the Bamble Sector, an outline of the evolution of the Baltic Shield, and especially the Southwest Scandinavian Domain, is presented.



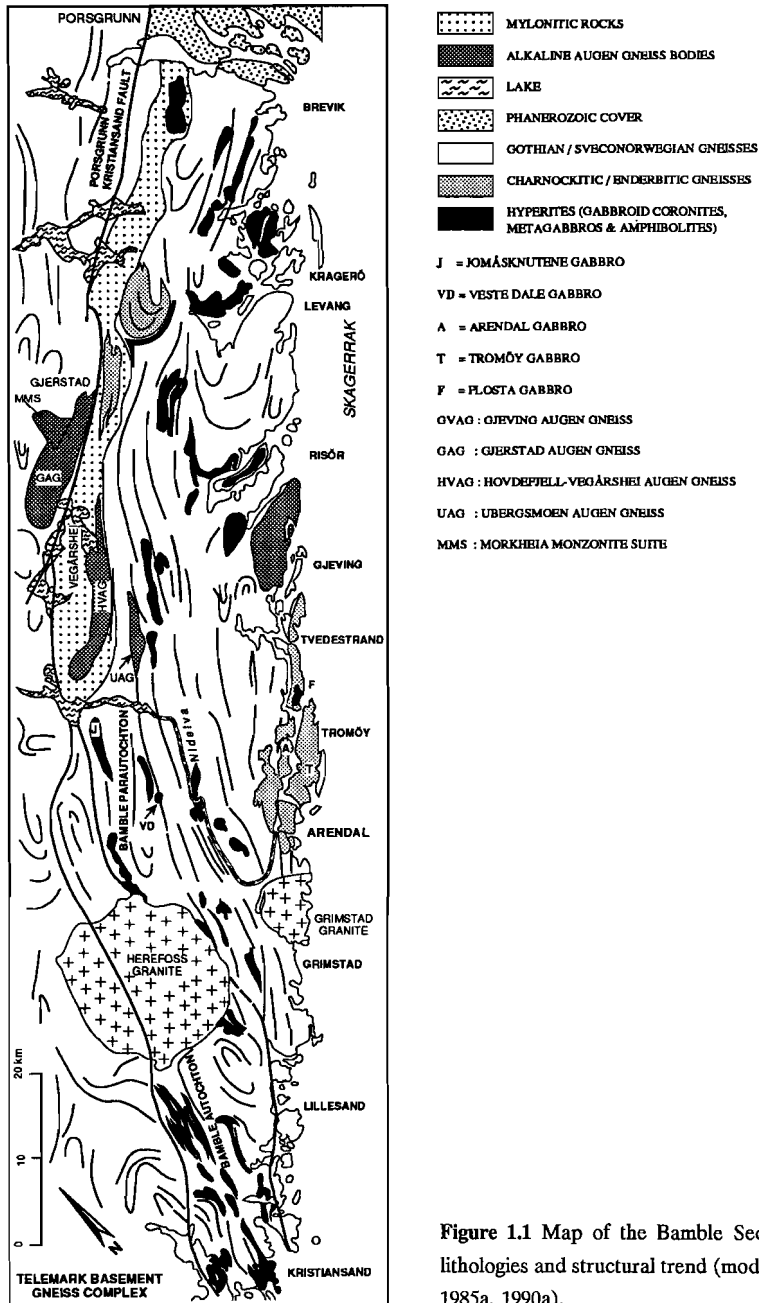


Figure 1.1 Map of the Bamble Sector with the main lithologies and structural trend (modified after Starmer, 1985a, 1990a).

## 1.1 EVOLUTION OF THE BALTIC SHIELD

The Archaean, the Svecofennian and Southwest Scandinavian Domains constitute the Precambrian lithosphere of the Baltic Shield (Fig. 1.2). The **Archaean Domain**, situated in the northeast, represents the oldest continental crust of the Baltic Shield. Oldest recognizable rocks are 3.1 - 2.9 Ga old tonalitic-trondjhemitic granitoids (Gaál and Gorbatshev, 1987), but there is indirect evidence for pre - 3.1 Ga crust. Claesson et al. (1991) reported the occurrence of 3.4 - 3.3 Ga old detrital zircons in Svecofennian metasediments from southern Finland and south and central Sweden. Most of the Archaean continental lithosphere was formed during the Lopian Orogeny (2.9 - 2.6 Ga).

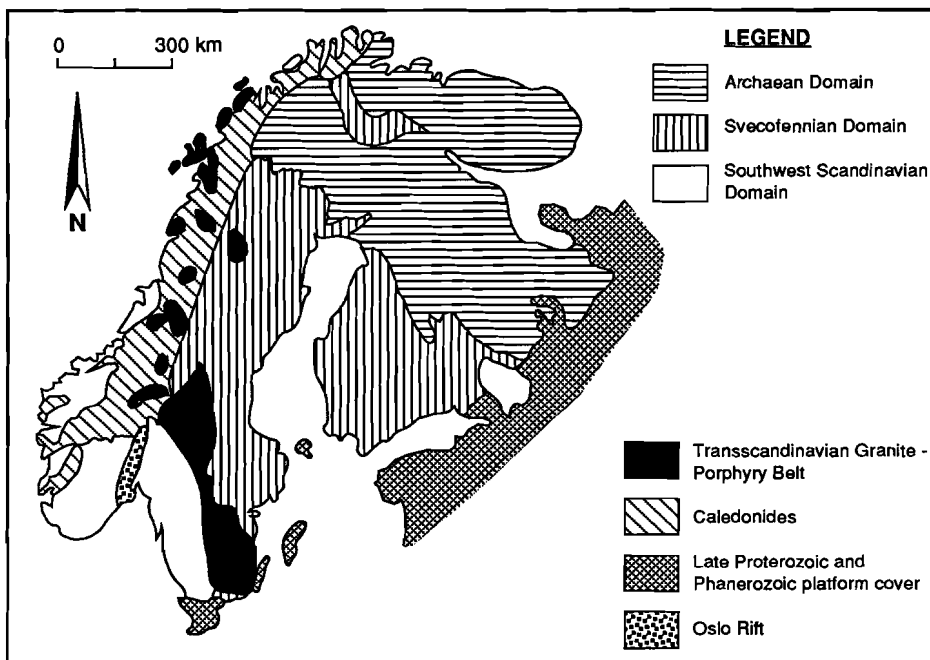


Figure 1.2 Map of the Baltic Shield (modified after Gaál and Gorbatshev, 1987)

The major part of the **Svecofennian Domain**, which occupies the central part of the Baltic Shield, was accreted in a relatively short interval (1.92 - 1.87 Ga; Pharaoh and Brewer, 1990) of the Svecofennian Orogeny (2.0 - 1.75 Ga), and involved deposition of volcanic rocks and the emplacement of synorogenic granites. The Svecofennian Domain is bordered on its western edge by the 1.78 - 1.70 Ga Transscandinavian Granite-

Porphyry Belt (Patchett et al., 1987). The granitoids of this 1600 km long, N-S trending belt, that extends from south Sweden into the Archaean Domain in the north, have granitic to quartz monzonitic or quartz monzodioritic compositions, and are accompanied by abundant felsic volcanics (porphyries) (Larson et al., 1990).

It is now commonly accepted that crustal accretion of the youngest part of the Baltic Shield, the **Southwest Scandinavian Domain (SWSD)**, took mainly place between 1.75 and 1.5 Ga, during the so-called **Gothian Orogeny** (Gaál and Gorbatshev, 1987). Isotopic data suggest a westward younging of the Gothian continental crust (Gaál and Gorbatshev, 1987; Falkum, 1990). The SWSD bears the mark of metamorphic imprint at about 1.25 - 0.9 Ga, ending with the emplacement of intrusive granites and associated pegmatites. This has been called the **Sveconorwegian Orogeny** (Welin, 1966), but as in the case of the Phanerozoic **Caledonian Orogeny** (0.6 - 0.4 Ga), it is largely limited to reworking of older crust. Exceptions are the emplacement of igneous, mantle-derived complexes, the most notable being the Rogaland Anorthosite Complex (RAC), intruded at about 1.0 Ga. Much smaller, but to some extent comparable, intrusions exist also in the Bamble Sector, e.g. the Morkheia Monzonite Suite, as well as charnockitic augen gneiss bodies.

Nowadays, it is generally accepted that the Baltic and Canadian Shields, together with Greenland and the northwestern British isles, evolved as a single mass after amalgamation of the Archaean domains between 1.98 and 1.83 Ga (Gower et al., 1990). The Makkovic Province in Canada and the Ketilidian Mobile Belt in Greenland have been correlated with the Svecofennian Domain. The Trans-Labrador Batholith is regarded as the Canadian equivalent of the Transscandinavian Granite-Porphyry Belt. The Grenville Province has since long been correlated with the SWSD (e.g. Barth and Dons, 1960). Gower (1990) demonstrated that this correlation is only valid in terms of pre-Sveconorwegian - Grenvillian crustal history. Palaeomagnetic studies show a 90° clockwise rotation of the Baltic Shield relative to the Canadian Shield (Poorter, 1981; Stearn and Piper, 1984). This rotation between 1.2 and 1.0 Ga resulted in the oblique opposition of the Grenville Province and the SWSD, which formerly constituted the same tectonic margin (Gower, 1990).

## 1.2 MAGMATIC EVOLUTION OF THE SOUTHWEST SCANDINAVIAN DOMAIN

The SWSD comprises South Norway and the southwestern part of Sweden (Fig. 1.3). East of the Oslo Rift, the SWSD is traditionally subdivided in three segments, which are separated by major N-S trending shear zones (Gorbatshev, 1980; Verschure, 1985; Lindh, 1987). West of the Oslo Rift, the SWSD comprises the Bamble, Kongsberg, Telemark and Rogaland/Vest-Agder Sectors (Fig. 1.3). The boundary between the Kongsberg and Bamble Sectors and the Telemark Sector is defined by the ductile Kristiansand-Bang Shear Zone (Hageskov, 1980; Sigmond, 1984), which has later (post - 0.95 Ga) partly been reactivated as the brittle Porsgrunn-Kristiansand Fault. An outline on the evolution of the SWSD is presented in Table 1.1.

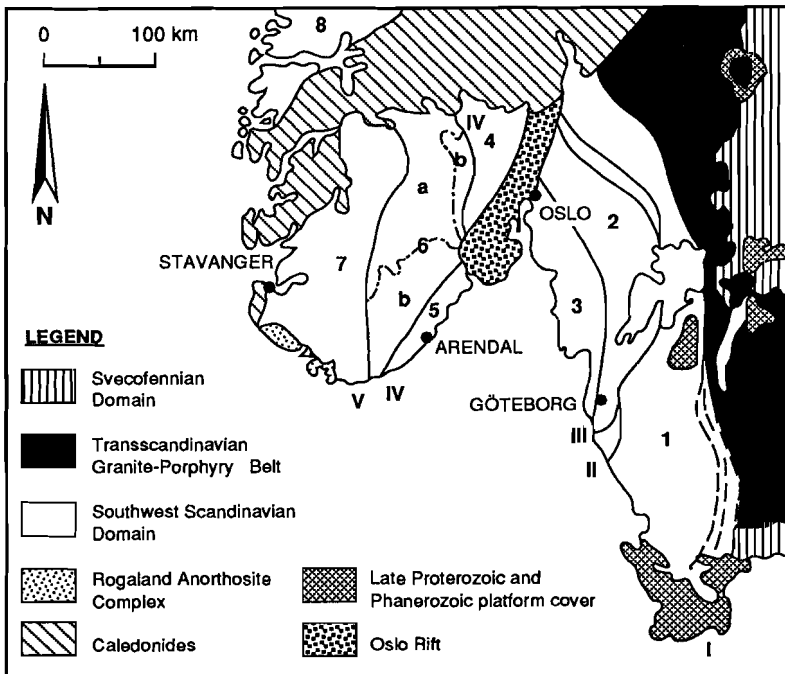


**Figure 1.3** Map of the Southwest Scandinavian Domain (after Verschure, 1985). Crustal segments: 1 Eastern Segment; 2 Median Segment; 3 Western Segment; 4 Kongsberg Sector; 5 Bamble Sector; 6 Telemark Sector: a) supracrustals, b) basement gneisses; 7 Rogaland/Vest-Agder Sector. 8 Western Gneiss Region. Major tectonic zones: I Protogine Zone; II Mylonite Zone; III Dalsland Boundary Thrust; IV Kristiansand-Bang Shear Zone; V Mandal-Ustaoset Line.

**Table 1.1** Evolution of the Southwest Scandinavian Domain. Data from Åhäll et al. (1990); Åhäll and Daly (1989); Bingen et al. (1990); Demaiffe and Michot (1985); Gorbatshev (1980); Menuge (1988); Ploquin (1980); Priem et al. (1973); Starmer (1985a, 1991); Verschure (1985).

	Rogaland/Vest-Agder Sector	Telemark Sector	Bamble Sector	Østfold-Marstrand Belt
↑ Gothian Orogeny ↓	↑ Deposition of sediments (e.g. Faurefjell Formation); accretion of charnockitic and granitic gneiss precursors ↓	Deposition of Rjukan Group (possibly also Selfjord and Bandak Groups)	Deposition of supracrustals	Deposition of SLM/Åmål sediments; contemporaneous volcanics. Emplacement of calc-alkaline granitoids (Group A) <i>amphibolite facies metamorphism</i> Calc-alkaline granitoids (Åmål I; Østfold augen gneisses) (Group B) <i>amphibolite facies metamorphism</i> Mafic-acid dykes (e.g. Värmland dykes) (Group C1) <i>amphibolite facies metamorphism</i>
	granulite-amphibolite (?) facies <i>metamorphism</i>	<i>High-grade metamorphic,            gneiss-forming event</i>	Intrusion of charnockites/enderbites Levang granite; calc-alkaline basic sheets <i>Upper amphibolite-granulite facies</i>	Tonalite-granite dykes; gabbro-dolerite sheets; bimodal augen granite-dolerite sheets; augen granite bodies (Group C2)
T(Ga)			↑ ?	
↑ Sveonorwegian Orogeny ↓	Pyroxene-syenites (e.g. Gløppurdi)	Anorogenic magmatism (e.g. Kallingsheia adamellite)	'Anorogenic' alkaline augen gneiss bodies; Morkheia Monzonite Suite; early phase hyperites	Mafic dykes (Kattsund-Koster; Orust); Håstefjorden Group granites (Group C3)
	Porphyratic granite-granodiorites (e.g. Fedda)	<i>Low- to high-grade metamorphism</i>	Emplacement of granitic sheets  Main phase hyperites; granites <i>amphibolite-granulite facies metamorphism</i>	<i>amphibolite facies metamorphism</i>
	Emplacement of massif-type anorthositic (e.g. Egersund-Ogna)  <i>HT granulite facies metamorphism</i> Mangerite-charnockitic intrusions (e.g. Farsund, Bjerkheim-Sokndal)	Post-tectonic granites (e.g. Vrårdal granite)	Granitic and pegmatitic activity; late phase hyperites  Post-tectonic granities (Herefoss and Grimstad)	Granites and pegmatites (Bohus-type) (Group D)

## Introduction

A 1.76 Ga Sm-Nd whole rock age for amphibolites from the supracrustal Stora Le-Marstrand Formation, Östfold-Marstrand belt (Western Segment in Fig. 1.3), provides an estimate for the onset of crustal growth in the SWSD (Åhäll and Daly, 1989). Skjernaa and Pedersen (1982) reported Rb-Sr whole rock ages of 1.71 and 1.85 Ga (calculated with fixed initial  $^{87}\text{Sr}/^{86}\text{Sr}$  ratio of 0.703) for augen gneisses from the Norwegian part of the Östfold-Marstrand belt. Crustal accretion proceeded with intrusion of voluminous granitoids, the so-called Åmål-I group of granitoids, between 1.7 and 1.6 Ga (Welin et al., 1982). Crust generating processes in this part of the SWSD terminated at c. 1.5 Ga with the emplacement of mafic dyke swarms (Värmland Dolerites) in the Eastern Gneiss Segment (Fig. 1.3) (Priem et al., 1968; Johansson and Johansson, 1990) and gabbro-dolerite bodies west of the Mylonite zone (Åhäll et al., 1990).

The timing of the crustal accretion of the SWSD west of the Oslo Rift is less well constrained. Verschure (1985) remarked that this part of the SWSD has been less systematically dated, but another, probably more important reason, is the westward increasing intensity of crustal reworking during the Sveconorwegian Orogeny (e.g. Zeck and Wallin, 1980; Gaál and Gorbatshev, 1987). Most ages have been obtained by 'conventional' techniques: first K-Ar and then Rb-Sr, both isotopic systems which are very susceptible to metamorphism and therefore yielded ages which were difficult to interpret (e.g. Priem et al., 1973; Verschure et al., 1990). Field and Råheim (1979) presented the first 1.6 - 1.5 Ga ages by proper interpretation of Rb-Sr data for the Bamble Sector, now followed by the Sm-Nd ages of the gabbros (this thesis).

The oldest ages have been reported from the Bamble Sector. Sm-Nd whole rock ages of  $1.77 \pm 0.19$  Ga and  $1.64 \pm 0.23$  Ga have been obtained for the Jomåsknutene Gabbro and the Flostå Gabbro respectively (de Haas et al., 1992b; Chapter IV of this thesis). Ages of c. 1.6 - 1.5 Ga have been reported for charnockitic and tonalitic gneisses (Field et al., 1985; Hagelia, 1989; see also section 1.3.2.1). Jacobsen and Heier (1978) concluded that there is no isotopic evidence for crust older than 1.6 Ga in the Kongsberg Sector, but they do not exclude the possibility that this crust formed by melting of crust, much older than 1.6 Ga.

The accretionary history of the Telemark Sector has still to be elucidated. Field relations between the Telemark gneisses and the Telemark supracrustals, a 6 km thick sequence of metamorphosed and deformed acid and basic volcanics and sediments, are not clear (Dons, 1960). Naterstad et al. (1973) claimed that the contact between the supracrustals and the gneisses at the Nyastøl bridge is depositional. Verschure et al. (1990), however, described a clear intrusive contact between the supracrustals and a gneissose granite at the same locality, but in a new exposure. In most cases, foliations

are concordant and the supracrustals progressively grade into the migmatitic gneiss, in which dispersed remnants can be followed step by step throughout the migmatitic domain until the high-grade Bamble supracrustals, which are obviously older than the Gothian metamorphism (Touret, 1969). Precise age relations are still a matter of debate (Verschure, 1985; Verschure et al., 1990). Rb-Sr systems are strongly disturbed and give only disputable evidence. Priem et al. (1973) inferred from Rb-Sr data of Rjukan and Bandak acid metavolcanics that deposition of the Telemark supracrustals took place around 1.57 Ga and considered the Telemark supracrustals as protoliths for the basement gneisses. Menuge (1985) inferred a period of crustal accretion between 1.6 and 1.5 Ga from Sm-Nd data of the basement gneisses and consequently regards the Telemark gneisses as the basement upon which the Telemark supracrustals were deposited. Sm-Nd whole rock dating by Menuge (1985) of the oldest lithostratigraphic unit of the Telemark supracrustals, the Rjukan Group, yielded an age of 1.19 Ga. Verschure (1985) however inferred a 1.6 Ga age from Menuge's data for the stratigraphically younger Bandak Group. Recently, Dahlgren et al. (1990) reported a 1.5 Ga U-Pb zircon age for one of the Rjukan metarhyolites and a slightly younger age for a dike intruding these metarhyolites. This makes the Sm-Nd age of Menuge even more questionable. Dahlgren et al.'s 1.2 - 1.1 Ga Rb-Sr and U-Pb ages for the basement gneisses support the earlier view of Priem et al. (1973).

Oldest ages in the Rogaland/Vest-Agder Sector range between 1.5 and 1.4 Ga. Pasteels and Michot (1975) obtained  $^{207}\text{Pb}/^{206}\text{Pb}$  zircon ages from metasedimentary rocks in the range of 1.5 and 1.4 Ga and a Rb-Sr age of  $1.42 \pm 0.04$  Ga for an anatectic granite. Verstevee (1975) reported an 'age-estimate' of 1.45 Ga for the Drangsdalen charnockitic migmatites. Van der Wel (cited in Sigmond, 1978) dated the Langeidvatn augen gneiss at  $1.48 \pm 0.04$  Ga (Rb-Sr whole rock). Evidently, a pre-Sveconorwegian basement existed in the Rogaland/Vest-Agder Sector (Demaiffe and Michot, 1985), like in other parts of the SWSD. Based on Sm-Nd data from charnockitic and granitic gneisses, Menuge (1988) concluded that crustal accretion of the Rogaland/Vest-Agder Sector took place between 1.85 and 1.55 Ga.

The interval between the Gothian and Sveconorwegian Orogenies (1.5 - 1.25 Ga) is characterized by sporadic, but significant magmatic activity in the SWSD. In the Östfold-Marstrand belt this is manifested by the emplacement of gabbro-dolerite massifs, basic to acidic dykes, bimodal augen granite-dolerite sheets and discrete bodies of augen granite between 1.42 and 1.3 Ga (Åhäll and Daly, 1985). These authors tentatively correlated the bimodal magmatism with the Gjerstad-Morkheia complex (Fig. 1.1; Milne and Starmer, 1982). The exact emplacement age of this complex and genetically related

## *Introduction*

alkaline augen gneisses from the Bamble Sector (Starmer, 1985a), however, is still a matter of debate (see section 1.3.2.2). Anorogenic magmatism in the eastern part of the SWSD continued until c. 1.22 Ga with the emplacement of the alkaline granites of the Håstefjorden Group (Åhäll et al., 1990).

The early Sveconorwegian orogenic phase (1.25 - 1.20 Ga) in the western part of the SWSD was accompanied by the intrusion of voluminous granite sheets at the contact of the (Kongsberg-) Bamble belt and the Telemark Sector (Starmer, 1991). Magmatism in this part of the SWSD continued during the Sveconorwegian anorogenic phase between 1.2 - 1.1 Ga (Starmer, 1985a) with the intrusion of the 'main hyperite' gabbroic stocks in the Bamble and Kongsberg Sectors, and pyroxene syenites in the Rogaland/Vest-Agder Sector (Wielens et al., 1980).

The main Sveconorwegian orogenic phase between 1.1 and 0.9 Ga was essentially a phase of crustal reworking. Substantial crustal formation was limited to the Rogaland/Vest-Agder Sector where huge volumes of anorthosites-norites and associated monzonorites, mangerites and charnockites were emplaced (DemaiFFE and Michot, 1985). The Sveconorwegian Orogeny ended with the emplacement of large, post-tectonic granites and associated pegmatites throughout most of the SWSD at about 0.9 Ga (Brueckner, 1972; Priem et al., 1973; Killeen and Heier, 1975; Skiöld, 1976; Eliasson and Schöberg, 1991).

## **1.3 THE GEOLOGY OF THE BAMBLE SECTOR**

### **1.3.1 Introduction**

The Bamble Sector (**Fig. 1.1**) is one of the classic Proterozoic high-grade metamorphic terrains, which has attracted attention for more than a century. In the nineteenth century, the Bamble Sector was especially known for its large diversity of mineralizations, among which the apatite and skarn iron ore deposits were the most famous (Kjerulf and Dahll, 1861; Helland, 1874; Brøgger and Reusch, 1875; Michel-Levy, 1878). Forbes (1857) and Kjerulf and Dahll (1861) discussed the general geology of the Arendal district.

Major contributions to the understanding of the geology of the Bamble Sector in the first half of this century were made by Brøgger (1934a,b), A. Bugge (1936), J.A.W. Bugge (1940, 1943) and Barth (1925, 1933). A. Bugge (1936) gave a description of the Bamble and Kongsberg lithologies, in which he made a distinction between the Bamble and Kongsberg Formations (as distinct from the Sectors!). The Kongsberg



Formation, mainly constituted by gneissic rocks, occupied the westernmost parts of the Kongsberg and Bamble Sectors. The Bamble Formation, a term of W.C. Brøgger for the coastal rocks between the Oslo Rift and Kristiansand, consisted of a great variety of rocks which were, according to A. Bugge (1936), altered to a variable extent by pneumatolitic hydrothermal activity, initiated by injection of rather small bodies of gabbro. Of particular interest are the works of J.A.W. Bugge (1940, 1943). Not only did he give a detailed petrographical account of the different lithologies from the Bamble and Kongsberg Sectors, but he also tentatively deduced a stratigraphical scheme for these areas. He made a distinction between the *Older Complex* and the *Younger Complex*. The *Older Complex* comprised rocks, formed before migmatitization: metasediments, which were interpreted as geosyncline and flysch formations, volcanics and basic intrusives, among which the hyperites. The *Younger Complex* consisted of rocks, which were formed after the migmatitization event: metataxites (migmatitic banded gneisses), arendalites (norite-charnockitic rocks from the Arendal region), cordierite-anthophyllite-bearing rocks, nodular gneisses, synkinematic granites and pegmatites, post-kinematic granites and skarns. J.A.W. Bugge's studies had a great impact and served as a basis for many later studies, e.g. Barth and Dons (1960) and Touret (1968, 1969). Touret (1968) estimated the migmatitization event to have taken place at c. 1.0 Ga, based up on concordant geochronological measurements by Broch (1964).

Although the first isotopic ages from the Bamble Sector were already published in the early thirties (Gleditsch and Quiller, 1932 in Neumann, 1960), research on the evolution of the Bamble Sector got a new impulse in the sixties when the first K-Ar isotopic ages of micas and hornblendes became available (Kulp and Neumann, 1961; O'Nions et al., 1969). The Rb-Sr whole rock age of 1.58 Ga age for the Levang gneiss dome, reported by O'Nions and Baadsgaard (1971), was the first isotopic evidence for the existence of Gothian rocks in the Bamble Sector. However, it was not clear at that time if this age did represent the (still unknown) basement on which the Bamble supracrustals must have been deposited, or a metamorphic age (J. Touret, pers. com.). At the end of the seventies and the early eighties, D. Field and co-workers extensively dated the coastal charnockitic gneisses from the Arendal region (Field and Råheim, 1979, 1981; Field et al., 1985). They concluded that the only high-grade metamorphic event took place during the Gothian and that the Sveconorwegian Orogeny was only a low-grade event (see next section).

Based upon his own observations, and with data from others and the then available isotopic data, Starmer (1985a) inferred an evolutionary scheme for the Bamble and the Kongsberg Sectors. A slightly modified version of this scheme was published by

Starmer in 1991. Starmer (1990a, 1991) divided the Bamble Sector in a parautochthon and an autochthon (Fig. 1.1). The parautochthon, which comprises the northeastern part of the Bamble Sector, is the equivalent of the Kongsberg Sector whereas the autochthon, which occupies the southwestern part of the Bamble Sector, is more similar to the Telemark Basement Gneiss Complex in the southern half of the Telemark Sector.

### **1.3.2 Evolution of the Bamble Sector**

#### **1.3.2.1 *The Gothian Orogeny (1.75 - 1.50 Ga)***

Obviously older than the Gothian metamorphism, the Bamble supracrustals were deposited at c. 1.7 Ga (Starmer, 1985a, 1991). In the autochthon as well as the parautochthon, the supracrustals comprise variable (qtz-bt-plag-hbl) gneisses, which include thin layers of quartzite, quartz-rich gneisses, sulphidic and graphitic schists and amphibolites (Starmer, 1985a). Minor calc-silicates, skarns and marbles occur as well. The variable gneisses are thought to be of mixed volcanic-sedimentary origin (Beeson, 1978). In the parautochthon, the variable gneisses are underlain by massive quartzites and quartz-rich ( $\pm$  sillimanite and biotite) gneisses, which now outcrop as the Coastal Quartzite Complex and the Nidelva Quartzite Complex (Starmer, 1985a). The Quartzite Complexes also comprises nodular gneisses (Brøgger, 1934b) and small lenses of cordierite-orthoamphibole rocks (Brøgger, 1934a; Bugge, 1943), which generally do not exceed 2-3 meters (Nijland and Maijer, 1991). According to Starmer (1985a), deposition of the supracrustals took place in a marginal basin. Touret (1966, 1969) interpreted the Selås banded gneisses as ancient metagreywackes, deposited by turbidity currents. Nijland and Maijer (1991) concluded from primary sedimentary structures in the Nidelva Quartzite Complex, like mudcracks, small scale fluvial cross stratification and large scale, possibly, aeolian cross stratification, and the association with the alleged meta-evaporites (cf. Touret, 1979; Beeson, 1988; Hulzebos-Sijen et al., 1990), that deposition probably took place in an inland basin. Apparently, deposition of the Bamble supracrustals took place in a variety of environments.

The NE-SW trending structures in the Bamble Sector (Fig. 1.1) were established during a first deformation phase (D1 of Starmer, 1991) after deposition of the supracrustals (Starmer, 1985a). The first deformation phase was followed by the intrusion of charnockitic-enderbitic rocks along the coast near Arendal and near Gjerstad and a large granite near Levang (Fig. 1.1). An U-Pb zircon age of 1.59 Ga (A. Råheim, unpubl. data in Lamb et al., 1986) was interpreted as an intrusion age. O'Nions and Baadsgaard (1971) reported a similar Rb-Sr whole rock age of  $1.58 \pm 0.04$  Ga for

the Levang granite. This phase of the Gothian Orogeny was accompanied by high-grade granulite facies metamorphism. Rb-Sr data of the charnockitic gneisses near Arendal indicate 1.54 Ga as the time of peak metamorphism (Field et al., 1985). Field et al. (1980) and Touret (1985) inferred that the charnockitic gneisses directly crystallized under these high-grade conditions. This, and the conclusion of Field and Råheim (1979) that the low initial  $^{87}\text{Sr}/^{86}\text{Sr}$  ratios (c. 0.703) of these gneisses exclude a crustal history for the gneiss precursors of more than 50 Ma, indicate a period of significant crustal growth at 1.6 Ga. Recently, Visser et al. (1991) questioned the synkinematic intrusive origin of part of these rocks. The absence of intrusive textures and the random succession of layers with variable compositions led Alberti and Comin-Chiaromonti (1976) to propose a metasedimentary origin for these rocks. Moine et al. (1972) associated these rocks with keratophyre-spilite series, containing greywackes, contaminated by this volcanism. Cooper and Field (1977) did not exclude a paragneiss component in these rocks.

Peak metamorphic conditions have been estimated to have been 700-800 °C at a pressure between 6 and 8 kbar (Touret, 1971a). Lamb et al. (1986) reported a P-T box of  $800 \pm 60$  °C and  $7.3 \pm 0.5$  kbar for the Arendal granulite terrain and concluded (on a limited amount of samples from the granulite zone only) that no P-T gradient existed across the amphibolite-granulite transition zone. According to these authors, the transition from the amphibolite facies terrain to granulite facies terrain reflects the increasing dominance of  $\text{CO}_2$  over  $\text{H}_2\text{O}$  in the fluids (cf. Touret, 1971b, 1985). Visser and Senior (1990), however, reported slightly lower peak metamorphic temperatures of  $740 \pm 60$  °C at a pressure of 7 kbar for the amphibolite facies terrain around Froland. In addition, Nijland and Maijer (1992) obtained P-T estimates of  $752 \pm 34$  °C,  $7.1 \pm 0.4$  kbar for the amphibolite facies terrain and  $836 \pm 49$  °C,  $7.7 \pm 0.3$  kbar for the core of the granulite facies terrain, which appears to be situated on the main land and not on the islands of Tromøy and Hisøy, as has always been assumed.

Visser and Senior (1990) inferred a clockwise Gothian P-T path for the Bamble Sector, and suggested that the D1 deformation phase might be related to a continent-continent collisional event. The peak metamorphic temperatures were, according to Visser and Senior (1990), established due to the possible emplacement of the charnockitic-enderbitic suites and the subsequent calc-alkaline basic sheets (cf. Starmer, 1991).

### ***1.3.2.2 The Gothian-Sveconorwegian interlude (1.50 - 1.25 Ga)***

The 'anorogenic' interlude between the Gothian and the Sveconorwegian Orogenies (1.5 - 1.25 Ga) was in fact marked by a discrete but constant magmatic activity (Hagelia, 1989; Starmer, 1990a,b and 1991), envisaged by the alkaline augen gneiss complexes (the Hovdefjell-Vegårshei (HVAG), Ubergsmoen (UAG), Gjeving (GVAG) and Gjerstad augen gneiss (GAG); Fig. 1.1), the Morkheia Monzonite Suite (MMS) and the widespread intrusion of small sheets of alkaline gabbros ('early hyperites'). Age determinations of the alkaline augen gneisses are far from unambiguous. Rb-Sr and U-Pb zircon ages of the UAG and HVAG, ranging between 1.13 and 1.28 Ga, are internally not consistent (cf. Nijland and Senior, 1991). Smalley et al. (1988) inferred a 1.25 Ga intrusive age for the MMS and a slightly younger age,  $1.24 \pm 0.05$  Ga, for the intruding GAG (Smalley et al., 1983a). Smalley et al. (1988) correlated the MMS with Gardar-age alkaline magmatic activity on Greenland and in Labrador, which is commonly regarded as an expression of a large-scale tensional regime in the North Atlantic regions. Starmer (1990a,b) argued, on structural grounds and on petrological similarities with the 1.42 Ga Varberg charnockite (Welin and Gorbatshev, 1978a), that the augen gneisses were intruded between 1.40 and 1.45 Ga. On the basis of the chemistry of these intrusions, which is similar to those of Finnish Rapakivi granites, both Starmer and Smalley regard these rocks as anorogenic. However, there are fundamental textural differences between undeformed Finnish Rapakivis and the strongly deformed, blastomylonitic augen gneisses. Touret (1968) and Hagelia (1989) consider them as synkinematic intrusions. Hagelia (1989) recognized the anorogenic chemistry of the augen gneisses and suggested that the magmas of these intrusions originated in an anorogenic environment, closely followed by emplacement under an orogenic regime.

### ***1.3.2.3 The Sveconorwegian Orogeny (1.25 - 0.90 Ga)***

At the onset of the Sveconorwegian Orogeny, voluminous granite sheets were emplaced. During the 1.2 - 1.1 Ga period of Sveconorwegian anorogeny, renewed magmatic activity resulted in the intrusion of the 'main' hyperites and granites. Hyperites from the Kongsberg Sector, which are supposed to be contemporaneous with the Bamble 'main hyperites' have been dated at  $1.18 \pm 0.05$  Ga (Rb-Sr, WR; Jacobsen and Heier, 1978) and  $1.22 \pm 0.02$  Ga (Sm-Nd, WR + min; Munz and Morvik, 1991). The emplacement of numerous sheets of dolerites (the 'late hyperites') marks the end of this period (Starmer, 1991).

The main Sveconorwegian orogenic phase (1.1 - 0.9 Ga) was a period of repeated

deformation (D6 and D7 of Starmer, 1991), alternating with granitic and pegmatitic activity (Starmer, 1985a). Baadsgaard et al. (1984) obtained an  $1.06 \pm 0.01$  Ga age (Rb-Sr K-feldspar) for the Gloserheia pegmatite. Field and Råheim (1979) reported a Rb-Sr whole rock age of  $1.06 \pm 0.02$  Ga for a granitic sheet from Tromøy. Fluids, associated with this granitic and pegmatitic activity caused low-grade alterations in the adjacent country rocks and resetting of their Rb-Sr systematics (Field and Råheim, 1979).

During the last decade, the metamorphic grade of the Sveconorwegian has become a matter of much discussion. From pioneering isotope studies (K-Ar and Rb-Sr) in the Bamble Sector at the end of the sixties and the onset of the seventies, O'Nions et al. (1969) and O'Nions and Baadsgaard (1971) recognized the Sveconorwegian Orogeny as a major orogenic event, involving high-grade metamorphism. Rb-Sr dating studies in the Arendal region at the end of the seventies and the early eighties led D. Field and co-workers to the conclusion that the Gothian Orogeny was the only high-grade event in the Bamble Sector and that Sveconorwegian Orogeny was in fact a myth, involving only pegmatitic and granitic activity, without any significant crustal reworking (e.g. Field et al., 1985 and references therein). The preservation of Gothian ages in the other parts of the charnockites and enderbites, however, does not exclude a possible high-grade Sveconorwegian event (Maijer, 1990). Field et al.'s claim for a low-grade Sveconorwegian event is also contradicted by field observations, which favour amphibolite, locally even granulite, facies conditions during the Sveconorwegian Orogeny (Starmer, 1985a and 1991; Hagelia, 1989; Maijer, 1990; Nijland and Senior, 1991; Nijland et al., 1991; Chapter II of this thesis).

From their P-T path for the Bamble Sector, Visser and Senior (1990) concluded that the Bamble Sector enjoyed prolonged isobaric cooling after the Gothian Orogeny. The path, which is more or less similar to that of Touret and Olsen (1985), suggests that the Bamble Sector resided at deep crustal levels for some 0.3 Ga, before uplift during the Sveconorwegian (D6 of Starmer, 1991). The c. 1.1 Ga Sm-Nd ages for granulite facies mineral assemblages in gneisses from Flostå (Kullerud and Dahlgren, 1990) indeed suggest that high-grade metamorphic conditions persisted until Mid-Sveconorwegian times.

Large, post-tectonic granitic plutons like the Herefoss Granite, dated at  $0.96 \pm 0.06$  Ga (Rb-Sr whole rock; Brueckner, 1972), and the Grimstad Granite, dated at  $0.99 \pm 0.01$  Ga (U-Pb zircon and titanite; Kullerud and Machado, 1991a) (Fig. 1.1), are the last representatives of Sveconorwegian magmatic activity in the Bamble Sector.

Post-Sveconorwegian magmatism is evidenced by c. 0.6 Ga old (Fen-age) volcanic breccias in the northern parts of the Bamble Sector (Verschure et al., 1983) and by late

## *Introduction*

Permian volcanic breccias near Kristiansand (Verschure et al., 1989). This magmatism is, like the late Carboniferous-Permian mafic alkaline dykes near Kristiansand (Halvorsen, 1970), Arendal (Halvorsen, 1972) and Kragerö (Støretvedt, 1968), commonly associated with epeirogeny in southern Norway, that finally resulted in the formation of the Oslo Rift. One of the Kragerö dykes has a Tertiary age (Støretvedt, 1968).

## **1.4 THE BAMBLE HYPERITES AND THE SCOPE OF THIS THESIS**

### **1.4.1 The term hyperite**

Hyperite is a common term among Scandinavian geologists, and may apply to all kinds of gabbroic rocks. The name hyperite is Swedish and was, according to Morthorst et al. (1983), introduced by A. Erdmann and J.H. af Forselles as a general petrographic term for a granular rock composed mainly of labradorite and hypersthene (Erdmann, 1855), occurring as voluminous intrusives of black doleritic gabbro in the Värmland gneiss basement. According to Tröger (1935) the term was already introduced around 1830 by Elie de Beaumont to describe noritic rocks. Naumann (1849) used the term hyperite as a synonym for diabase. When more precise optical determination data for hypersthene became available, it became clear that hypersthene was lacking in many hyperites. Törnebohm (1877) therefore proposed to use hyperite as a descriptive term for the whole rock suite, i.e. the term hyperite got a lithostratigraphic character. According to Brøgger (1934a) the use of the term hyperite should be limited to coronitic gabbros. In some parts of the hyperites, first assumed to be in the margin, but later demonstrated to be widespread within the hyperites as a whole, the rock grades into amphibolites. This amphibolitization is complex, and J.A.W. Bugge (1943) did even include under the name hyperite practically all kinds of massive amphibolite occurring in southern Norway. These are most of the hyperites occurring in the Bamble Sector (not along the coast) in Bugge's sketch maps. Finally, the American Commission on Stratigraphic Nomenclature (1970), introduced the more formal stratigraphic denomination "Värmland Hyperite Formation", which not only includes the hyperites from Sweden, but also the hyperites from east Norway. The confusing term hyperite will not be used for the five gabbros, which are subject of this thesis.

### **1.4.2 The Bamble hyperites**

The Bamble hyperites have attracted much attention after the classical study of Brøgger

(1934a), mainly on the Kragerö hyperites. This study was followed by detailed studies on hyperites from the Ödegårdens Verk district (Ryan, 1966), the Risör district (Starmer, 1969), eastern Bamble (Morton et al., 1970) and on the Hiåsen Gabbro (Frodesen, 1968a,b, 1973).

The hyperites occur all over the Bamble Sector as stock-like bodies and as elongate, sheet-like bodies. The size of the stock-like bodies varies between a few 100 m<sup>2</sup> and several km<sup>2</sup>. Some of the Bamble hyperites are associated with Fe-Ni-Cu sulphide deposits, situated at the margins of the intrusions (Brickwood, 1986).

Bugge (1943) noted that the Bamble hyperites were probably not all of the same age. The presence of more than one generation of hyperite was also noticed by Touret (1969). Later, Starmer (1985a) even distinguished three types of hyperites: the 'early phase' hyperites, which were contemporaneous with the granitic-charnockitic augen gneisses, the 'main phase' hyperites, and the 'late phase' (olivine-free) hyperites. The primary magmatic mineralogy of the hyperites considerably varies. Plagioclase and clinopyroxene are the most common phases encountered in the hyperites; olivine and orthopyroxene occur in variable amounts but are not always present. All intrusions have been affected by amphibolitization, especially along their margins, but locally also in the core of the intrusions.

The most striking feature in the olivine-bearing hyperites is the development of coronitic microstructures on the former interface between olivine and plagioclase, and between ilmenite and plagioclase. The olivine-plagioclase coronas have a variable mineralogy, but they generally consist of an inner shell of orthopyroxene, rimmed by amphibole, and an amphibole/spinel symplectite. Locally an outer rim of garnet is present.

The coronitic microstructures in the Bamble hyperites have been subject of many studies. Although it is commonly thought that Törnebohm (1877) gave the first description of the coronitic microstructures, it was Sjögren who published in 1883 the first descriptions of olivine coronas in samples of the Ödegården Gabbro from the Bamble Sector (Fig. 1 and 2, p. 471). Lacroix (1889) studied the coronas in gabbros from Tvedestrand, Kragerö and Ödegården and noticed the presence of garnet in the coronas. Much attention in later studies on the coronas was focused on the growth mechanism of the coronas, the timing of the growth, and the prevailing P-T conditions. According to Bugge (1943), the coronas formed through a reaction in the solid state, usually in connection with magmatic processes. Reynolds and Frederickson (1962) stressed the role of water in the corona-forming processes. They regarded corona growth, like Morton et al. (1970), as a metamorphic process, caused by introduction of silica-bearing solutions. Frodesen (1968a) proposed a combined late-magmatic

## *Introduction*

('deuteric') - metamorphic origin for the coronas. The orthopyroxene and spinel-free amphibole were, according to his model, formed in the late-magmatic stage of the gabbro; the amphibole/spinel symplectite, and the pseudomorphic replacement of olivine by orthopyroxene and magnetite, would then be formed during regional metamorphism. Starmer (1969) attributed corona-formation to isochemical recrystallizations in the solid-state, promoted by intergranular diffusion. Brickwood and Craig (1987) noted, like Frodesen (1968a), the apparent contrast between the P-T conditions, required for corona-forming reactions, and the relatively low regional metamorphic conditions. They therefore proposed, like Starmer (1969), that the coronas started to grow early in the cooling history, and continued to develop in response to isobaric cooling at elevated pressures. Joesten (1986) inferred in his study on coronas in a troctolitic gabbro from Risør, an entirely magmatic origin for the coronas. This was heavily disputed by Ashworth (1986) who favoured a solid-state origin for the coronas. Davidson and van Breemen (1988) concluded from U-Pb ages of baddeleyite and radiating columnar zircon coronas in coronitic gabbros from the Grenville Province, that the coronas are a metamorphic phenomenon.

In a TEM, SEM and microprobe study, Dam (in prep.) modelled an isochemical reaction for corona formation in the Mesel and Vestre Dale Gabbros. This reaction, which took place at c. 850 °C, is accompanied with a 6.6 volume % decrease, which may explain the ortho-enstatite - clino-enstatite transition, observed in the orthopyroxene.

From both the great extension of the olivine hyperites and the thickness of the intrusions, Bugge (1943) concluded that the rocks crystallized from a common mother magma. These two observations, in combination with the major element chemistry of the olivine hyperites, were used by Bugge (1943) to compare the olivine hyperites with plateau basalts. Touret (1969) noted the tholeiitic affinities of the hyperites.

From major element data of the hyperites from the Risør-Söndeled area, Starmer (1969) concluded that all these series belong to one and the same differentiation trend and suggested that the individual intrusions crystallized from differentiated fractions from a large, underlying mass of magma, probably of olivine-gabbro composition. Morton et al. (1970), on the other hand, suggested that the corona-bearing gabbros, norites and the olivine-norites from eastern Bamble crystallized from two different parental magmas: a nepheline-normative magma and a high-hypersthene or quartz-normative magma.

Clinopyroxenes in several gabbroic intrusions from the Bamble Sector show transitional alkaline-tholeiitic affinities (Brickwood and Craig, 1987). Starmer (1990a) also inferred a transitional alkaline-tholeiitic parental magma for the gabbros.



### 1.4.3 The scope of this thesis

The scope of this thesis is:

- a) To study the chemical and magmatic evolution of five gabbros from the Arendal-Nelaug area from major and trace element data (including the REE) combined with field and petrographic observations.
- b) To determine the age of these gabbros by the Sm-Nd, and for one gabbro also the Rb-Sr, method.
- c) To study the nature of the Proterozoic mantle below Bamble. Nd isotope data from the Rogaland/Vest-Agder and Telemark Sectors indicate that the mantle below these part of the SWSD had a depleted character during the Gothian (Menuge, 1985, 1988), like the mantle below other Proterozoic terrains throughout the world. These data fit the model of DePaolo (1981) that depletion already started in the early days of earth's history. Mearns et al. (1986) however postulated a deviating evolution curve for southern Scandinavia, which assumes that depletion started at 1.74 Ga. The Nd isotope data of the gabbros will provide more information about the depletion of the mantle below this part of the SWSD.
- d) To determine the composition of the mantle source(s) of the gabbros. Incompatible trace element data of the gabbros and their Nd isotope systematics may yield information about the source(s) of the gabbros: 1) do they originate from the same source, or are more sources involved, 2) what is the composition of the mantle below Bamble like, and 3) how do the gabbro data compare with trace element data of other basic intrusions from other parts of the SWSD.

### Acknowledgements

Discussions with J.L.R. Touret and T.G. Nijland have been most valuable and are greatly appreciated. D. Visser and C. Maijer are acknowledged for critical comments on earlier versions of the manuscript.

## CHAPTER II

### THE MAGMATIC HISTORY OF THE VESTRE DALE GABBRO

#### 2.1 INTRODUCTION

The Bamble Sector (Fig. 2.1) of the Southwest Scandinavian Domain of the Baltic Shield (Bugge, 1940; Gaál and Gorbatshev, 1987) is one of the classical high-grade metamorphic terrains in which the presence of coronitic gabbros has attracted much attention since Brøgger's (1934a) classical study (e.g. Frodesen, 1968a,b, 1973; Starmer, 1969; Brickwood and Craig, 1987). As is the case with coronitic gabbros from elsewhere, this attention was mainly focused on the mechanism of corona growth and the implications for the geological history of the terrains in which they occur. Less attention has been paid to the magmatic, "pre-corona", evolution of these intrusions. Frodesen (1968b) discerned in major element whole rock analyses of the Hiåsen coronitic gabbro a magmatic differentiation trend. Starmer (1969) recognized troctolite-troctolitic norite series, troctolite-olivine gabbro series and a number of late-stage, olivine-free gabbros in coronites from the Risør-Söndeled area (Fig. 2.1), which, according to him, all belong to one regional differentiation trend. In-situ differentiation of the intrusions was observed by Brickwood and Craig (1987) in their mineral chemical study of coronites from the Bamble and Kongsberg Sectors.

In this chapter, a unique dataset for one of the coronitic gabbros from the Bamble Sector, the Vestre Dale Gabbro (co-ordinates: 32VMK 4770-4895; Nelaug-sheet 1612 III, 1:50.000; Norges geografiske oppmåling 1967) is presented. Major and trace element analyses, including the REE, mineral data and Sr isotope data will be used to unravel the magmatic evolution of the Vestre Dale Gabbro and to infer some constraints on the origin of the parental magma. Little is known about the source of the coronitic gabbros. Touret (1969) reported their tholeiitic affinities, and Starmer (1985a,b) classified the coronites as transitional alkali basalt-tholeiite-high alumina intrusions with alkaline affinities and alkali and Fe-enrichment trends. Field data, together with mineral and whole rock data, will be used to elucidate the emplacement mechanism of the Vestre Dale Gabbro.

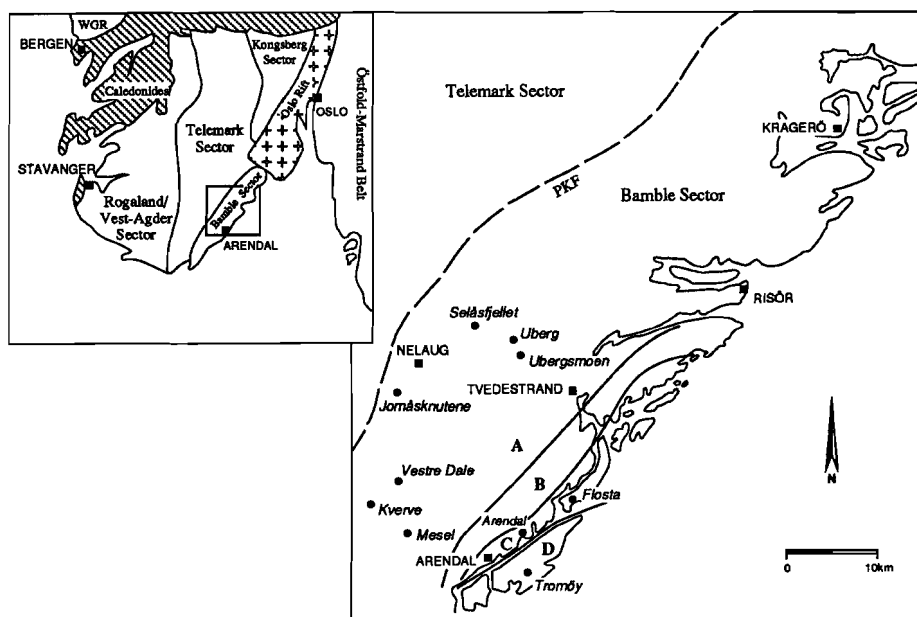


Figure 2.1 Map of the Bamble Sector. Black spots mark the location of the main gabbro bodies in the Arendal-Nelaug area. Zone A represents amphibolite facies metamorphism; zone B contains orthopyroxene in metabasic rocks while in zone C orthopyroxene is also present in acidic rocks; zone D is, in addition to zone C, LILE depleted. Zonation after Smalley et al. (1983b). Inset shows the major geological divisions of the Southwest Scandinavian Domain; WGR = Western Gneiss Region (modified after Verschure, 1985).

## 2.2 GEOLOGICAL SETTING

The geology of the Bamble Sector has largely been determined by the Gothian (Kongsbergian, 1.75 - 1.5 Ga) and the Sveconorwegian (Grenvillian, 1.25 - 0.9 Ga) Orogenies. The Gothian Orogeny resulted in an amphibolite-granulite facies transition zone with a fourfold division of the Nelaug-Arendal area (Fig. 2.1; Smalley et al., 1983b). Basic plutonic rocks in the area include small to medium-sized discordant, often layered and multiple intrusive coronitic metagabbros (e.g. Brickwood and Craig, 1987), small (< 1 km<sup>2</sup>) coronitic metagabbros and discordant, entirely amphibolitized plutons. The Vestre Dale Gabbro belongs to the second category. Starmer (1985a) argued that emplacement of the coronitic gabbros (his "main phase hyperites") was bounded to the Sveconorwegian Orogeny and correlated their intrusion with the emplacement of the basic Vinor intrusions in the Kongsberg Sector (Fig. 2.1). Recent Sm-Nd dating however

revealed that some of the coronitic gabbros (the Jomåsknutene and the Flosta Gabbros; Fig. 2.1) were already emplaced at the onset or during the Gothian Orogeny (de Haas et al., 1992b; Chapter IV of this thesis). The Vestre Dale Gabbro intruded during the Sveconorwegian Orogeny at  $1.11 \pm 0.14$  Ga (de Haas et al., 1992b; Chapter IV of this thesis).

The Vestre Dale Gabbro is a lens-shaped body surrounded by migmatitic gneisses (Fig. 2.2). The inner part of the outcrop consists of fine-grained, coronitic gabbro with purple-coloured plagioclase and greenish olivine. Dark rims around olivine are occasionally visible. The grain size increases towards the contact, where the gabbro displays a subophitic texture built up by cm-scale plagioclase and dark-green clinopyroxene crystals. The latter are generally rimmed by dark-green hornblende. Primary igneous layering has not been observed.

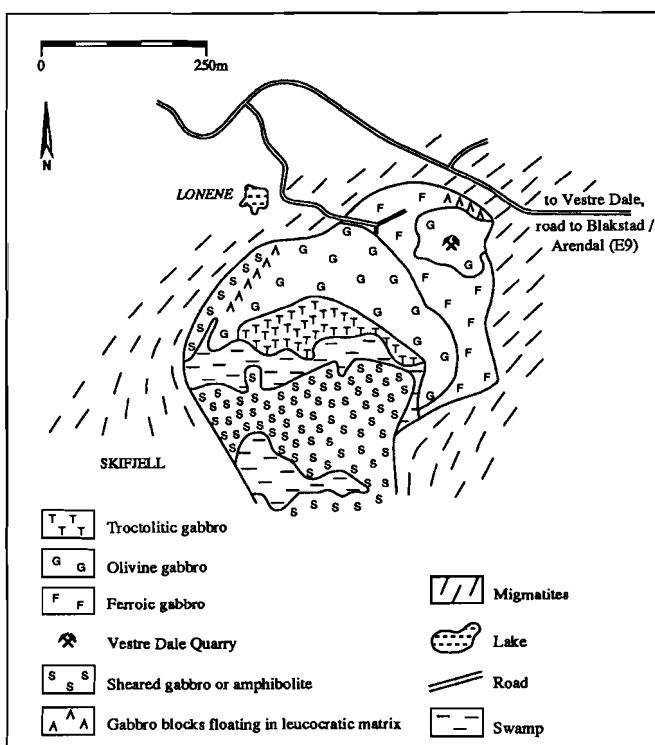


Figure 2.2 Geological map of the Vestre Dale Gabbro.

The foliation in the gneisses wraps around the gabbro. The gneisses are migmatitic, especially along the contact between gneisses and the late-stage, pegmatoid ferroic gabbro in the northeast. At the entrance of the quarry, the gabbro lies above migmatitic gneisses; the contact is subhorizontal. Just above the contact, dark, angular to subrounded gabbroic blocks float in a leucocratic matrix (Fig. 2.3), constituting an agmatitic structure. The gabbroic blocks nearest to the contact seem to be dragged into it (Fig. 2.3). The foliated parts of the gabbro are strongly amphibolitized along the contact. Amphibolitization also occurred along late hydrothermal veins that cut across the gabbro. The southern extension of the gabbro consists of strongly foliated garnet-amphibolite. In the southeastern part of the quarry the gabbro is cut by a 30 cm thick felsic pegmatite.



**Figure 2.3** Contact relations between the gabbro and the country rock: the gabbro (upper left corner) is separated from the country rock (below) by an agmatitic structured zone.

### 2.3 PETROGRAPHY

The gabbros in the core are fine- to medium-grained, ophitic to subophitic mesocumulates (Irvine, 1982), with variable amounts of cumulus olivine and plagioclase and intercumulus clinopyroxene, plagioclase and ilmenite. The gabbros in the inner core, hereafter called **troctolitic gabbros**, contain up to 67 modal % euhedral olivine and 25 modal % plagioclase (Table 2.1). Plagioclase is concentrated in clusters, irregularly distributed in the olivine mesocumulate which locally tends to an adcumulate. The outer core consists of olivine gabbro mesocumulates in which the modal amount of olivine roughly decreases outward and finally disappears. These gabbros fall apart in **olivine-rich gabbros**, containing 20-40 modal % olivine, and **olivine-poor gabbros** (less than 20 modal % olivine). Both types have 40-50 modal % plagioclase. The modal amount of intercumulus clinopyroxene varies between 15 and 40 %. In a few samples subsolidus alteration aggregates provide evidence for the former presence of olivine. **Ferroic gabbros** constitute the outer rim of the intrusion. These are coarse-grained, subophitic meso- to orthocumulates, with cumulus plagioclase and intercumulus clinopyroxene in approximately equal amounts. Fine-grained brownish aggregates of cummingtonite and chlorite, occasionally rimmed by garnet, are interpreted as former olivine. Ilmenite occasionally occurs as a cumulus phase. In the olivine-poor and ferroic gabbros intercumulus apatite occurs; minor amounts of zircon are also present.

Mostly, plagioclase has a cloudy appearance due to the presence of small spinel inclusions orientated parallel to (010) cleavage planes. Intercumulus clinopyroxene has exsolved Ca-poor pyroxene lamellae parallel to (100) and ilmenite flakes parallel to (100) and (001) planes. Clinopyroxene often displays a rim of brown hornblende. Brown hornblende also occurs as thin lamellae along cleavage planes of clinopyroxene, growing inwards from the brown amphibole rim. These amphiboles may represent a late-stage magmatic overgrowth (cf. Otten, 1984). Inverted pigeonite is present in one sample from the olivine-poor gabbro, recognizable at the lamellar exsolutions. In gabbros from the Bamble Sector, pigeonite has only been reported from an hyperite on Tromøy (Bugge, 1940) and the Selåsfjellet Gabbro (A. Senior, pers. com.). Intercumulus orthopyroxene has only been observed once in the olivine-poor gabbro.

Equidimensional coronas between olivine and plagioclase and between ilmenite and plagioclase occur in the troctolitic and olivine gabbros. The coronas around olivine consist of successive shells of orthopyroxene and/or clinopyroxene, amphibole and amphibole-spinel symplectites. Coronas between ilmenite and plagioclase are mainly

composed of amphibole, and sporadically contain minor biotite. Similar coronas have been described from other Bamble gabbros (Brøgger, 1934a; Frodesen, 1968a; Brickwood and Craig, 1987; among others). The thickness of the coronas increases from troctolitic gabbros to olivine-poor gabbros.

Late alteration of the gabbro includes the development of fibrous or patchy, pale-green actinolite within intercumulus clinopyroxene in samples from the margin. In the ferroic gabbros, late amphibolitization is characterized by the occurrence of granular aggregates of blue-green amphibole around intercumulus clinopyroxene. According to Mongkoltip and Ashworth (1986) this replacement results in excess quartz. In the samples from the Vestre Dale Gabbro, quartz blebs are observed along the amphibole-clinopyroxene contacts.

Gabbroic blocks in the agmatite have been extensively altered. Clinopyroxene is entirely absent and replaced by aggregates of amphibole and quartz. Hornblende is replaced by actinolite and biotite. Biotite itself is replaced by chlorite and often surrounded by small rims of titanite. Prehnite and pumpellyite occur as lenses in the biotite parallel to its cleavage. The blocks contain remarkably high amounts of zircon and allanite. Late calcite is present in interstices and veinlets.

**Table 2.1** Modal analyses of the igneous mineralogy for seven samples from the Vestre Dale Gabbro. Coronitic orthopyroxene and the bordering spinel-bearing symplectites have been counted as olivine and plagioclase respectively; clinopyroxene includes the brown hornblende and late actinolite. Group 1: Troctolitic gabbro; Group 2: Olivine-rich gabbro; Group 3: Olivine-poor gabbro; Group 4: Ferroic gabbro.

Sample	Group	Olivine	Plagioclase	Clinopyroxene	Ilmenite
DT10	1	67	25	8	< 1
WT203	2	40	45	14	1
WT208	2	42	44	13	1
WT217	2	31	44	23	2
WT225	2	27	38	33	2
WT209	3	12	51	35	2
DT3	4	-	55	42	3

## 2.4 WHOLE ROCK AND MINERAL CHEMISTRY

### 2.4.1 Analytical techniques

Major element, Ni, Cu, Sr, Y, Zr, Nb, Ba and some Rb analyses were performed at the Department of Geochemistry, Utrecht, by XRF using an automated Philips PW1400 spectrometer. Most Rb analyses were obtained at the Isotope Geology Laboratory, Vrije Universiteit, Amsterdam, by XRF using an Philips 1450/AHP automatic spectrometer. Samples of approximately 1.5 to 3 kg were broken in a tungsten-carbide coated jaw-crusher. After homogenization, a split of about 75 gram was ground in a tungsten-coated swing-mill. About 2.5 gram of the ground sample was ignited in an oven for four hours at 900 °C. Ignited splits of rock powder were mixed with  $\text{LiBO}_2/\text{Li}_2\text{B}_4\text{O}_7$  (66/34) spectroflux in a ratio of 1:10 and fused at 1000 °C in a Herzog HAG1200 automated oven to obtain glass beads for major element analyses. Pressed pellets for trace elements were made from eight grams of rock sample using Elvacite as a cementing medium. Whole rock data are listed in **Table 2.2**. Part of the samples have also been analyzed for REE (**Table 2.3**). Sm and Nd concentrations were obtained by isotope dilution techniques at the Isotope Geology Laboratory, Vrije Universiteit, Amsterdam (see Chapter IV of this thesis for analytical techniques); the concentrations have an uncertainty of  $\approx 1\%$ . Other REE, Co, Cr and Hf were analyzed by INAA at the IRI in Delft. The precision is better than 10% for the REE and better than 5% for Co and Hf.

Sr isotope analyses were performed at the Isotope Geology Laboratory, Vrije Universiteit, Amsterdam. About 450 mg whole rock powder was dissolved in a mixture of  $\text{HClO}_4$  and HF at 140 °C. After evaporation to dryness the residue was redissolved in 3M HCl at 120 °C prior to aliquotting. The aliquot was dried at 140 °C after addition of 1 ml  $\text{HClO}_4$ . The residue was redissolved in 2 ml  $\text{HClO}_4$  and 5 ml 3.25 M HCl. After separation of Sr and Rb, using cation exchange columns, the sample was dried after addition of one drop of  $\text{HNO}_3$ . This process was repeated twice. Sr mass spectrometry analyses were made using a Finnigan MAT 261 mass spectrometer equipped with a fixed multicollector array. Analytical uncertainties are estimated to be within 0.002% for  $^{87}\text{Sr}/^{86}\text{Sr}$  and 0.5% for  $^{87}\text{Rb}/^{86}\text{Sr}$ . The results are presented in **Table 2.4**.

Mineral compositions (**Table 2.5**) were partly determined at the Department of Geochemistry, Utrecht, with an automated TPD microprobe using energy-dispersive techniques and the Tracor-Northern ZAF correction program. Operating conditions were 15 kV acceleration voltage, 30-40 nA sample current and counting times between 70 and 100 seconds. Additional analyses were performed with a Cambridge Mark 9 automated microprobe at the Vrije Universiteit, Amsterdam, using wavelength dispersive techniques. On-line data reduction included correction for deadtime, background, absorption, fluorescence and atomic number. Operating conditions were 20 kV accelerating voltage, 20 nA sample current and 20 seconds counting time.



**Table 2.2** Major and trace element chemistry of sixteen gabbros, a gabbroic block from the agmatitic margin (WT218) and a migmatitic gneiss (WT224). Major element oxides and LOI in wt.%, other elements in ppm. Group 1: Troctolitic gabbro; Group 2: Olivine-rich gabbro; Group 3: Olivine-poor gabbro; Group 4: Ferroic gabbro. All iron as FeO. na = not analyzed; dl = below detection limit (detection limit for Rb, analyzed in Utrecht, is 5 ppm). Bold printed Rb analyses have been obtained at the Isotope Geology Laboratory, Amsterdam (detection limit for Rb less than 1 ppm).

Sample	DT10	WT203	WT223	WT208	WT217	WT214	WT225	WT215	WT220
Group	1	2	2	2	2	2	2	2	2
SiO <sub>2</sub>	40.77	45.29	43.93	44.19	42.56	45.35	44.35	42.77	47.29
TiO <sub>2</sub>	0.28	0.52	0.41	0.53	0.80	0.91	0.84	0.78	0.67
Al <sub>2</sub> O <sub>3</sub>	8.19	13.11	15.05	12.92	9.66	11.15	10.86	10.93	18.11
FeO	16.16	12.92	11.46	13.89	16.47	13.87	15.88	14.77	9.54
MnO	0.24	0.20	0.18	0.21	0.25	0.22	0.24	0.21	0.15
MgO	25.45	17.37	13.64	16.48	19.39	15.99	18.25	16.79	9.79
CaO	5.15	9.01	9.12	8.18	6.42	8.80	6.73	7.77	11.12
Na <sub>2</sub> O	0.80	1.33	1.71	1.50	1.40	1.74	1.71	1.64	2.10
K <sub>2</sub> O	0.10	0.20	0.25	0.21	0.30	0.31	0.33	0.35	0.29
P <sub>2</sub> O <sub>5</sub>	0.09	0.10	0.10	0.11	0.14	0.13	0.13	0.13	0.14
LOI	1.44	dl	2.22	dl	dl	dl	dl	1.87	0.02
Cr	165	332	na	na	135	na	92	na	na
Co	165	118	na	na	121	na	131	na	na
Ni	499	364	322	369	449	315	400	408	156
Cu	30	29	25	34	55	49	61	50	39
Rb	dl	3	dl	dl	<b>6</b>	<b>6</b>	<b>6</b>	dl	4
Sr	134	233	271	251	194	217	214	197	324
Y	4	11	9	11	16	17	16	15	13
Zr	18	39	33	42	57	60	60	55	46
Nb	0	2	2	2	3	3	3	2	3
Ba	56	89	97	103	138	148	151	125	121
Hf	0.42	0.70	na	na	1.18	na	1.70	na	na
Mg#	73.7	70.5	68.0	67.9	67.7	67.3	67.2	66.9	64.6

*The magmatic history of the Vestre Dale Gabbro*

Sample Group	WT210 3	WT211 3	WT222 3	WT221 3	WT209 3	DT3 4	WT216 4	WT218	WT224
SiO <sub>2</sub>	48.02	46.21	47.50	45.83	48.87	49.60	46.62	50.39	72.59
TiO <sub>2</sub>	0.87	1.10	0.88	0.88	1.20	1.22	1.84	1.23	0.34
Al <sub>2</sub> O <sub>3</sub>	15.10	13.69	17.46	18.20	15.81	14.24	12.96	15.84	12.23
FeO	10.93	11.35	9.87	10.01	11.13	11.28	13.64	10.41	2.15
MnO	0.19	0.19	0.17	0.17	0.19	0.18	0.22	0.18	0.02
MgO	9.29	9.45	7.98	7.96	8.03	6.87	7.12	6.41	1.22
CaO	11.45	11.14	10.98	10.86	11.80	11.89	10.79	8.76	0.35
Na <sub>2</sub> O	2.06	1.77	2.42	2.13	2.50	2.72	2.32	2.55	1.15
K <sub>2</sub> O	0.70	0.90	0.54	0.78	0.45	0.57	0.67	1.98	7.58
P <sub>2</sub> O <sub>5</sub>	0.12	0.13	0.14	0.14	0.16	0.16	0.15	0.16	0.09
LOI	0.56	1.88	1.12	1.26	dl	0.72	1.06	1.45	1.40
Cr	342	na	na	na	270	143	131	na	na
Co	76	na	na	na	72	97	65	na	na
Ni	115	115	122	136	93	59	69	87	dl
Cu	62	70	37	61	71	62	113	99	5
Rb	27	35	dl	30	8	10	19	89	220
Sr	289	236	328	317	307	271	288	249	78
Y	16	19	16	16	21	21	25	23	35
Zr	50	55	55	59	71	55	68	86	244
Nb	2	3	3	2	4	2	3	5	8
Ba	195	173	134	206	185	161	153	253	773
Hf	1.20	na	na	na	1.60	1.93	1.66	na	na
Mg#	60.2	59.7	59.1	58.6	56.2	52.0	48.2	52.4	

**Table 2.3** REE contents of eight samples; concentrations in ppm. Groups as defined in Table 2.2.

Sample	DT10	WT203	WT217	WT225	WT210	WT209	DT3	WT216
Group	1	2	2	2	3	3	4	4
La	1.04	2.52	4.20	5.33	4.36	6.63	6.50	6.65
Ce	2.65	dl	10.70	10.80	10.2	13.1	17.10	17.0
Nd	na	4.23	7.27	7.89	6.32	9.38	na	11.41
Sm	0.54	1.20	1.97	2.11	1.84	2.61	3.24	3.32
Eu	0.33	0.65	0.74	0.84	1.05	1.18	1.30	1.29
Tb	0.16	0.38	0.28	0.48	0.43	0.63	0.60	0.67
Yb	0.60	1.10	1.21	1.33	1.23	1.81	2.10	1.95
(La/Sm) <sub>N</sub>	1.06	1.15	1.17	1.38	1.30	1.39	1.10	1.10

### 2.4.2 Whole rock chemistry

Harker diagrams for major and trace elements have been made with the magnesium number Mg# ( $= 100 \cdot \text{molar MgO}/(\text{MgO} + \text{FeO})$ ) as differentiation index (**Fig. 2.4a-h**). Troctolitic gabbro DT10 has a Mg# of 73.7; Mg# for the olivine-rich gabbro ranges from 70.5 to 64.6; for the olivine-poor gabbro from 60.2 to 56.2; and for the ferroic gabbro from 52.0 to 48.2. SiO<sub>2</sub> slightly increases with decreasing Mg#, although within group variations exist (**Fig. 2.4a**). Troctolitic and olivine-rich gabbros are on the average are high in FeO (9.54 - 16.47 wt.%), and low in CaO (5.15 - 11.12 wt. %; **Fig. 2.4b-c**). The olivine-poor gabbros, in which plagioclase is the dominant cumulus phase, are low in FeO (9.87 - 11.35 wt.%) and high in CaO (10.86 - 11.80 wt.%). The shift from olivine-rich cumulates to plagioclase-dominated cumulates is also visualized by the trends of Sr (**Fig. 2.4f**) and Ni (**Fig. 2.4g**). TiO<sub>2</sub> and P<sub>2</sub>O<sub>5</sub> show a steady increase (**Fig. 2.4d-e**), reflecting the fractionation of these elements in the intercumulus liquid from which ilmenite respectively apatite ultimately crystallize. The olivine-rich gabbros however display a remarkable variation in TiO<sub>2</sub> (up to 0.5 wt.%) and P<sub>2</sub>O<sub>5</sub> (up to 0.04 wt.%). Incompatible trace elements like Zr, Rb (not shown) and the REE (see below) also become steadily enriched towards more evolved cumulates. The trend shown by Zr (**Fig. 2.4h**) is similar to that of TiO<sub>2</sub>, including the variation observed within the olivine-rich gabbros.

The magmatic history of the Vestre Dale Gabbro

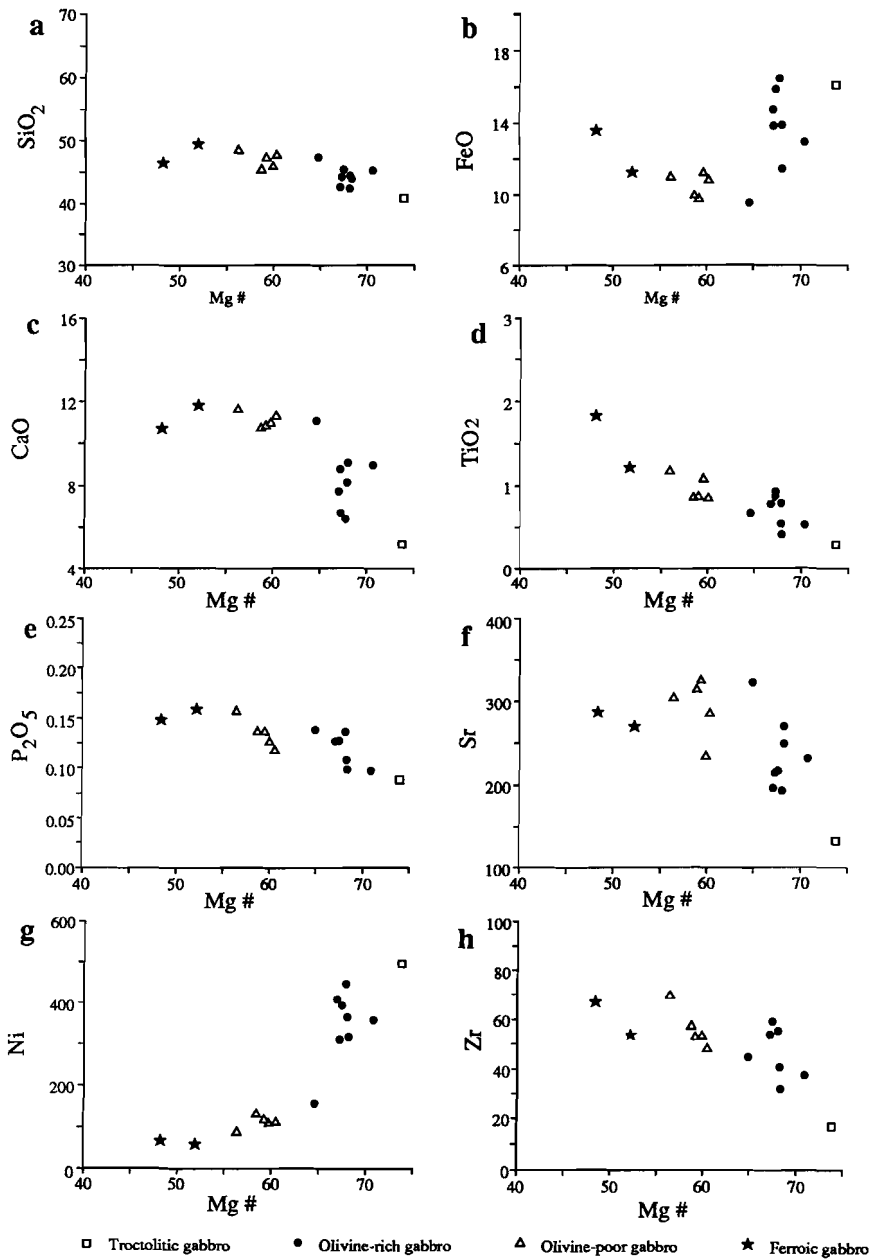


Figure 2.4a-h Whole rock variation diagrams with Mg# as differentiation index. SiO<sub>2</sub>, FeO, CaO, TiO<sub>2</sub>, P<sub>2</sub>O<sub>5</sub> in wt.%; Sr, Ni and Zr in ppm.

**Table 2.4** Sr isotopic composition of ten gabbro samples, a sample of a gabbroic block from the agmatitic margin (WT218) and a sample from the country rock gneisses (WT224).  $^{87}\text{Sr}/^{86}\text{Sr}(0)$  is the measured ratio.

Sample	Rb (ppm)	Sr (ppm)	$^{87}\text{Rb}/^{86}\text{Sr}$	$^{87}\text{Sr}/^{86}\text{Sr}(0)$	$^{87}\text{Sr}/^{86}\text{Sr}(1.11 \text{ Ga})$
WT203	3	233	0.0375	0.703712	0.703117
WT217	6	194	0.0864	0.704599	0.703226
WT214	6	217	0.0814	0.704584	0.703291
WT225	6	214	0.0839	0.704628	0.703294
WT220	4	324	0.0383	0.703829	0.703220
WT209	8	307	0.0743	0.704486	0.703306
WT216	19	288	0.1905	0.706533	0.703507
WT210	27	289	0.2669	0.706908	0.702668
WT211	35	236	0.4340	0.709626	0.702731
WT221	30	317	0.2705	0.705105	0.700808
WT218	89	249	1.0504	0.721720	0.705032
WT224	220	78	8.6590	0.878596	0.741032

**Table 2.5** Mean mineral compositions.

Sample	Group	Olivine Fo%	Plagioclase An%	Clinopyroxene En, Fs, Wo %
DT10	1	74	76	48, 9, 43
WT203	2	66	68	45, 11, 44
WT225	2	66	61	45, 11, 44
WT217	2	65	63	43, 9, 48
WT214	2	66	61	43, 10, 47
WT210	3	53	60	39, 15, 46
WT209	3	47	60	39, 16, 45
DT3	4	-	52	38, 16, 46

The anomalously high Rb and  $\text{K}_2\text{O}$  contents of olivine-poor gabbros WT210 and WT221 (Table 2.2) are almost certainly due to interaction with the neighbouring pegmatite. The high Rb and  $\text{K}_2\text{O}$  of WT221 may be explained by its position near the agmatitic margin.

Chondrite normalized REE abundances increase from 3 for the troctolitic gabbro to 20 for the ferroic gabbro (Fig. 2.5). The negative Ce anomaly for WT210 and WT225 is an analytical artefact (Th. van Meerten, pers. com.). The pronounced positive Eu

anomaly in DT10 is due to preferential Eu incorporation by the first accumulating plagioclase. The variations in the height of the Eu anomaly in other gabbros are ascribed to a combination of depletion of the fractionating magma in Eu and the amount of cumulus plagioclase present in a sample. All gabbros are slightly LREE enriched (**Fig. 2.5**; **Table 2.3**).

Despite the gabbros being cumulates, their REE patterns yield information about the REE pattern of the parental magma. Because of the low partition coefficients for olivine/melt and plagioclase/melt, with exception of Eu (*e.g.* McKay, 1989), accumulation of olivine and plagioclase will only result in 'dilution' of the REE and in an Eu anomaly. Thus, the parental magma probably had a rather flat REE pattern, with REE abundances about 30 times the chondritic values, assuming 10 wt.% of trapped liquid in ad- to mesocumulate DT10 (see also Chapter VI of this thesis).

### 2.4.3 Sr isotopes

**Table 2.4** presents the results of Sr isotope determinations on ten gabbro samples, a sample of a gabbroic block from the agmatitic margin, and a sample from the country rock gneisses.  $^{87}\text{Sr}/^{86}\text{Sr}$  analyses have been recalculated to ratios at  $T = 1.11$  Ga, the crystallization age of the Vestre Dale Gabbro as determined by Sm-Nd dating (de Haas et al., 1992b; Chapter IV of this thesis). Seven samples (WT203, WT209, WT214, WT216, WT217 and WT225) have  $^{87}\text{Sr}/^{86}\text{Sr}(1.11 \text{ Ga})$  ratios between 0.7031 and 0.7035 (**Table 2.4**). Detailed inspection of these ratios reveals a slight increase of the  $^{87}\text{Sr}/^{86}\text{Sr}(1.11 \text{ Ga})$  ratios with decreasing Mg# (**Fig. 2.6**): WT203 with a Mg# of 70.5 has an  $^{87}\text{Sr}/^{86}\text{Sr}(1.11 \text{ Ga})$  of 0.703117, whereas WT216 (Mg# = 48.2) has an  $^{87}\text{Sr}/^{86}\text{Sr}(1.11 \text{ Ga})$  ratio of 0.703507. WT210, WT211 and WT221 have anomalously high Rb contents, and lower  $^{87}\text{Sr}/^{86}\text{Sr}(1.11 \text{ Ga})$  ratios, 0.7008 - 0.7027, whereas WT218D from the agmatitic margin, has a higher initial ratio of 0.7050.

### 2.4.4 Mineral chemistry

**Olivine** exhibits a Fe-enrichment trend from  $\text{Fo}_{74}$  in the troctolitic gabbro via  $\text{Fo}_{66}$  in the olivine-rich gabbro to  $\text{Fo}_{47}$  in the olivine-poor gabbro (**Table 2.5**). Zonation of the olivine has not been observed. Core compositions of the **plagioclase** decrease from  $\text{An}_{76}$  in the troctolitic gabbro to  $\text{An}_{68}$  -  $\text{An}_{60}$  in the olivine gabbro (**Table 2.5**). The maximum core composition observed in the ferroic gabbro is  $\text{An}_{52}$ . The maximum difference between

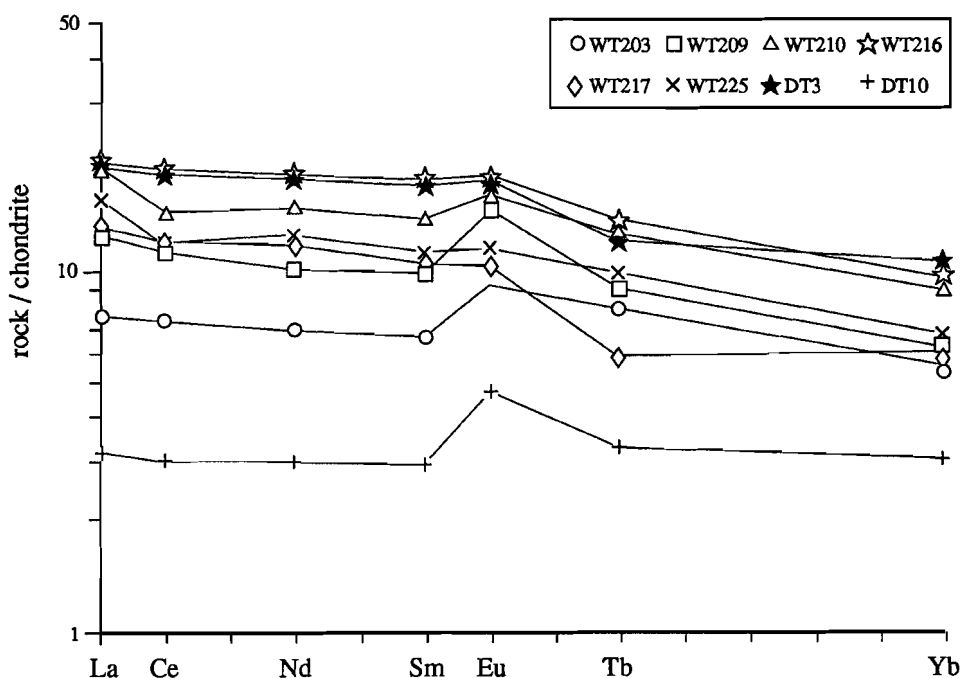


Figure 2.5 REE patterns of samples from the Vestre Dale Gabbro; normalization after Haskin et al. (1968).

core and rim compositions ranges between 5-13 An%. **Clinopyroxene** closely follows the Fe-enrichment trend shown by olivine (Table 2.5).  $\text{TiO}_2$  and  $\text{Al}_2\text{O}_3$  contents in the clinopyroxene decrease with increasing FeO contents. The decreasing  $\text{TiO}_2$  content of clinopyroxene is probably due to the fact that the spot analyses of this mineral were not integrated with exsolved ilmenite flakes.

## 2.5 DISCUSSION

### 2.5.1 Crystallization of the Vestre Dale Gabbro

Mineral and whole rock chemistry reveal that crystallization of the Vestre Dale Gabbro involved fractionation of both olivine and plagioclase. The observed outcrop pattern of the Vestre Dale Gabbro (Fig. 2.2) suggest an outward or upward crystallization order of the cumulate succession in the original magma body. These cumulate groups represent different stages in the crystallization process. The omnipresence of intercumulus clinopyroxene and ilmenite indicates that all cumulates trapped a certain

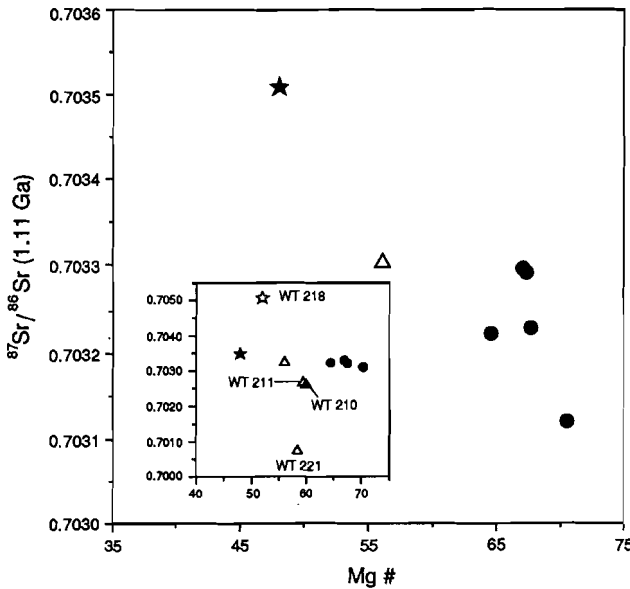


Figure 2.6 Increase of  $^{87}\text{Sr}/^{86}\text{Sr}(1.11 \text{ Ga})$  ratios with decreasing Mg#; disturbed samples WT210, WT211, WT221 and WT218 have been omitted. Inset shows a plot of all samples. Symbols as in Figure 2.4.

amount of interstitial liquid. The primary assemblage of olivine-plagioclase-clinopyroxene constrains crystallization conditions to less than 1200 °C and less than 8 kbar (Thompson, 1975; Presnall et al., 1978). The occurrence of inverted pigeonite, though sparse, points to relatively high temperatures of crystallization (Lindsley, 1980).

The troctolitic gabbros represent the least fractionated cumulates. Their mineralogy indicates that olivine was the dominant fractionating phase at the onset of the crystallization. The olivine-rich and olivine-poor gabbros demonstrate that proceeding differentiation resulted in a shift towards a plagioclase-dominated fractionation process. The transition to more plagioclase-rich cumulates was accompanied by an increase in the amount of intercumulus clinopyroxene, as witnessed by the change from an adcumulate texture to a clear mesocumulate texture. This points to a higher amount of liquid trapped in the cumulates. The ferroic gabbros represent the most evolved cumulates, in which olivine is only sporadically present.

The sympathetic decrease in Fo and An contents observed throughout the whole sequence suggests that progressive fractionation of olivine and plagioclase occurred in a closed-system. However, the observed increase in initial  $^{87}\text{Sr}/^{86}\text{Sr}$  ratios suggests that the fractionation of the magma was attended with assimilation of wall- and roof-rock



material, albeit on a rather restricted scale.

Increasing incompatible element concentrations in the cumulates indicate that the magma became progressively enriched in these elements during crystallization. Enrichment in Zr and  $P_2O_5$  resulted in intercumulus crystallization of zircon and apatite in the olivine-poor and ferroic gabbros. Ilmenite is present as an intercumulus phase in all groups, and becomes a cumulus phase in the ferroic gabbro. The increased abundance of incompatible elements with the modal amount of intercumulus clinopyroxene, indicates that the concentration of these elements is controlled by the amount of trapped liquid (cf. Chalokwu & Grant, 1987), for which the amount of clinopyroxene may serve as a minimum estimate. This may explain the more than doubled increase in Zr concentrations between adcumulate DT10 (18 ppm) and mesocumulate WT203 (39 ppm). Variations in the amount of trapped liquid also account for the large ranges in Zr, Y, REE,  $TiO_2$  and  $P_2O_5$  concentrations observed within the olivine-rich gabbros. This can be demonstrated in a quantitative way using the approach of DeLong and Chatelain (1989). They demonstrated how weight fractions of trapped liquid in cumulates and the concentration of trace elements in the trapped liquid can be estimated by means of simple Rayleigh fractionation calculations for an incompatible and a compatible element. The results of our calculations with Zr and Ni (Table 2.6) reveal that weight percentages of trapped liquid for WT217 and WT225 are 50 % higher than those for WT208 and WT203, whereas the Zr concentration in the trapped liquid is approximately constant for these four samples.

**Table 2.6** Calculated weight percentages of trapped liquid and Zr and Ni concentrations in the trapped liquid ( $c_{Zr}^l$  and  $c_{Ni}^l$ ) in four olivine-rich gabbros. Calculations have been performed after DeLong & Chatelain (1989) assuming crystallization of olivine and plagioclase in the ratio 1:1 and with  $D^{ol/liq} = 15$ . Initial Ni and Zr concentrations, 190 and 133 ppm respectively, are from a tholeiite from Mt. Gellibrand, Australia (Frey et al., 1978; p. 482).

Sample	Whole rock Zr (ppm)	Wt.% trapped liquid	$c_{Zr}^l$ (ppm)	$c_{Ni}^l$ (ppm)
WT203	39	24	154	73
WT208	42	26	156	66
WT217	57	38	148	94
WT225	60	39	151	83

During solidification of the ferroic gabbro, water activities were probably higher, which evidently resulted in its coarse-grained to pegmatoid character and the subsolidus growth of amphibole. It also enhanced diffusion, which stimulated corona growth and resulted in increasing thickness of the coronas towards the outer margins. This higher water activity can be attributed to an increasingly water-rich residual liquid produced from fractional crystallization, but in addition may have resulted from the infiltration of aqueous fluids from the country rock.

The absence of felsic differentiation products like granophyres (cf. Naslund, 1989) indicates that the crystallization of the ferroic gabbro was not a closed-system process. The residual liquid, which most probably accumulated under the roof and along the outer margins, has been removed. The residual liquid was still basic, since it was still able to crystallize olivine.

### **2.5.2 Parental magma composition**

As chilled margins have not been found, it is not possible to determine the composition of the parental magma directly. The melt in equilibrium with the most forsterite-rich olivine present, i.e. Fo<sub>75</sub> of sample DT10, must have had a minimum Mg# of 47, using the olivine-melt partitioning coefficient of Roeder and Emslie (1970). Chalokwu and Grant (1987, 1990) propose re-equilibration of olivine with trapped liquid as a mechanism to lower the forsterite content of primary olivine. Since the olivine in DT10 shows no signs of post-cumulus overgrowth, the effect of re-equilibration is considered to be negligible. Primary mantle-derived melts have a Mg# of 68 to 83 when in equilibrium with residual mantle olivine compositions of Fo<sub>88</sub> to Fo<sub>94</sub>. Hence, it appears that the Vestre Dale Gabbro crystallized from a melt which had been subject to some degree of fractional crystallization before intrusion into the magma chamber. The low initial <sup>87</sup>Sr/<sup>86</sup>Sr ratios of the Vestre Dale Gabbro as well as the high Ni and MgO contents indicate a basaltic magma as a parental liquid for the Vestre Dale Gabbro. The marked trend of Fe-enrichment observed in olivine and clinopyroxene, the enrichment in TiO<sub>2</sub> with increasing differentiation and the inferred REE pattern for the parental magma are typical for a magma with a tholeiitic signature, which stems with the observation of Starmér (1985a).

### 2.5.3 Emplacement

For the Vestre Dale Gabbro, much of the evidence to elucidate the emplacement mechanism has been obscured by Sveconorwegian metamorphism and deformation. However, the non-sheared parts of the Vestre Dale Gabbro show features which may in part reveal the emplacement mechanism: 1) the absence of chilled margins, 2) the absence of modally and grain-size graded layering, and 3) the agmatitic structures (see: **Geological Setting**). In these, the gabbroic blocks have a whole rock chemistry comparable to that of evolved samples from the margin (**Table 2.2**), although the interaction with the matrix resulted in a slight enrichment of SiO<sub>2</sub> and in a significant increase in the K<sub>2</sub>O, Rb and Ba contents.

Observation 1) may indicate that the gabbro was not emplaced in a completely molten state, like 2). Alternatively, it may have been due to a too small temperature contrast between the magma and the country rocks. The agmatitic structure indicates that the gabbro, because it could break up, was already partly solidified (cf. Sutcliffe et al., 1989). This indicates that the gabbro did not crystallize in-situ but was emplaced as a crystal mush, a mechanism which has often been invoked for cumulate sequences like anorthosites (cf. Duchesne et al., 1985a; Czamanske and Bohlen, 1990). The emplacement as a crystal mush did apparently not disturb the original cumulate sequence. However it would be expected that during the upward transfer of the crystal mush the interstitial magma was at least partly homogenized. Indeed, the composition of intercumulus clinopyroxene from the olivine-poor and ferroic gabbros (**Table 2.5**) is nearly identical. In the internal part of the mush, the compositional relationship between intercumulus liquid and corresponding cumulates remained largely undisturbed.

The ultimate residual liquid may have been driven outward by compaction of the cumulates. An alternative mechanism would have been provided by tectonic squeezing, for which an argument could be found in the lensoid shape of the intrusion. However, tectonic squeezing would require a compressional stress regime. The absence of crystal preferred orientation and the roughly equidimensional nature of the olivine and ilmenite coronas favour final solidification under static or extensional rather than compressional conditions. The time span (1.2 - 1.1 Ga) in which the Vestre Dale Gabbro was emplaced was considered a static/extensional interval separating two compressive stages of the Sveconorwegian orogenic cycle by Starmer (1991).

The transformation of the marginal parts of the Vestre Dale Gabbro into garnet amphibolites indicates the presence of a metamorphic fluid. The exact timing of this

amphibolitization with respect to the emplacement of the Vestre Dale Gabbro is uncertain. It seems likely that infiltration of metamorphic aqueous fluids from outside into the solidifying body diluted the residual liquid, which not only facilitated its removal but also increased water activities, resulting in the growth of the late-stage amphibole around clinopyroxene in the otherwise not amphibolitized part of the intrusion. The gabbroic intrusion formed a water sink, thus buffering the aqueous metamorphic fluid phase, as amphibolitization was not completed. Compression during the second phase of the Sveconorwegian orogenic cycle (Starmer, 1991) probably squeezed the diluted residual liquid.

Summarized, the emplacement mechanism proposed above implies that the cumulates crystallized at a level in the crust, which was deeper than the final solidification and thus at higher temperature and pressure. Rb-Sr systematics show that the residual liquid was contaminated at a restricted scale during crystallization. As the average crustal rocks are more siliceous than a gabbroic liquid, this will have resulted in slightly enhanced silica activities. The effect will have been that higher temperature cumulus minerals came in contact with a lower temperature, slightly more siliceous liquid. The re-equilibration between these phases may have initiated corona growth.

#### **2.5.4 Regional implications**

Mineral and whole rock chemistry of other basic intrusions from the Bamble Sector indicate that the extend of Fe/Mg fractionation displayed by the Vestre Dale Gabbro is unique. Olivine compositions of the Vestre Dale Gabbro cover the whole range of olivine compositions in fifteen basic intrusions, scattered over the Bamble Sector (Brickwood and Craig, 1987). All coronitic gabbros from the Risør-Söndeled area together comprise a range in whole rock Mg# from 71 to 53 (Starmer, 1969) which is smaller than that of the Vestre Dale Gabbro alone. Olivine compositions in these gabbros run from Fo<sub>74</sub> to Fo<sub>64</sub>. Moreover, the troctolitic coronites from the Risør-Söndeled area, with Mg# comparable to the olivine-rich gabbros of Vestre Dale, have much lower MgO contents (12.15-12.95 wt. %) and higher Al<sub>2</sub>O<sub>3</sub> (18.83-17.97 wt.%) and CaO (9.93-10.15 wt. %) than the olivine-rich gabbros. This suggests that crystallization of these gabbros was mainly governed by fractionation of plagioclase rather than of olivine. The only well-documented set of trace element data for a coronitic gabbro from the Bamble Sector published so far is for the Hiåsen Gabbro, also from the Söndeled area (Frodesen, 1973). Eight samples which define the differentiation trend of the

Hiåsen Gabbro, have lower MgO contents (10.3-5.8 wt. %) and Mg# (62.3-44.1) than the Vestre Dale Gabbro (Frodesen, 1968b). The Hiåsen Gabbro has in addition significantly lower Zr/Y, Ba/Nb and Ba/La ratios than the Vestre Dale Gabbro. The deviating trace element chemistry suggests that the Vestre Dale Gabbro and the Hiåsen Gabbro had a different origin.

It is tempting to correlate the intrusion of the Vestre Dale Gabbro and other Bamble coronitic gabbros during the Sveconorwegian Orogeny with contemporaneous basic magmatism in the Bamble Sector as well as the adjacent Telemark Sector (Menuge, 1985), which is generally considered to represent a higher crustal level (e.g. Ploquin, 1980). The similarity between  $\epsilon_{Nd}(T)$  values for the Vestre Dale Gabbro and the basic volcanics ( $+1.8 \pm 0.5$  for the Vestre Dale Gabbro at  $T = 1.11 \pm 0.14$  Ga and  $+2.1 \pm 0.7$  for the Rjukan basic volcanics at  $T = 1.19 \pm 0.04$  Ga) strengthen this temptation. However more information about the chemistry of the basic volcanics is required to substantiate this hypothesis.

The crystallization conditions of the Vestre Dale Gabbro,  $< 1200$  °C and  $< 8$  kbar, correspond with other gabbros from the area (Brickwood and Craig, 1987) and imply emplacement at mid crustal levels. This matches reasonably well with the 740°C and 7 kbar of the M 3b metamorphic stage of Visser and Senior (1990) as result of thermal stabilization between the Gothian and Sveconorwegian orogenies (1.5 - 1.1 Ga). This stabilization involved repeated magmatic addition, which process may also count for many of the amphibolites present (Bugge 1943). The magmatic evolution and transformation of the margins of the Vestre Dale Gabbro into garnet amphibolite show that these conditions have prevailed until the early Sveconorwegian and that the Bamble Sector enjoyed prolonged burial at lower to mid crustal levels.

### Acknowledgements

This chapter benefitted from comment on earlier versions by M. v. Bergen, L.C.G.M. Bol, J.B.H. Jansen, A. Senior and J.L.R. Touret. W. Theulings and G.P. van Ditshuizen kindly provided the samples. Blakstad Yrkesskole kindly provided lodging during field work.

## **CHAPTER III**

### **IGNEOUS LAYERING AND MAGMA REPLENISHMENT IN A 500 M THICK GABBROIC INTRUSION IN THE PROTEROZOIC CRUST OF SOUTH NORWAY.**

#### **3.1 INTRODUCTION**

The Flosta Gabbro (co-ordinates: 32VMK 4952-4870; Tvedestrand-sheet 1612 II, 1:50.000; Norges geografiske oppmåling, 1967) is a small intrusion located at southwestern Flostaøya, an islet in the South Norwegian skaergaard, 13 km northeast of Arendal (Fig. 2.1). The gabbro, one of the so-called "hyperites" (Brøgger, 1934), was previously mapped as an amphibolite of undetermined origin by Touret (1968) and as a composite amphibolite-coronitic gabbro body by Starmer (1985a).

Detailed field investigations have revealed primary igneous layering and other igneous structures. The aim of this chapter is to document these structures, and to interpret them and the chemistry of the gabbro in terms of igneous processes. The implications of layering in small intrusions like the Flosta Gabbro for the nature of the Mid-Proterozoic lower continental crust will be considered.

#### **3.2 GEOLOGICAL SETTING**

The Bamble Sector is part of the Proterozoic, Southwest Scandinavian Domain of the Baltic Shield (Gaál and Gorbatshev, 1987). Its geology is characterized by early Gothian supracrustals (Verschure, 1985) that were metamorphosed and intruded by basic and acidic magmas during the Gothian (Kongsbergian, 1.75 - 1.5 Ga) and Sveconorwegian (Grenvillian, 1.25 - 0.9 Ga) Orogenies (Bugge, 1940, 1943; Starmer, 1985b, 1991).

The Flosta Gabbro is situated in the granulite facies part of the area (Zone C of Smalley et al., 1983b); it is surrounded by migmatites, gneiss-quartzite transition rocks and charnockitic to enderbitic gneisses. The gneisses yield Rb-Sr whole rock isochron ages of  $1.51 \pm 0.08$  Ga and  $1.54 \pm 0.12$  Ga (Field and Råheim, 1979), and an U-Pb zircon age of  $1.54 \pm 0.01$  Ga with a Sveconorwegian lower intercept age of  $1.11 \pm 0.01$  Ga (Kullerud and Machado, 1991a). Rb-Sr mineral isochrons from the

gneisses give ages around 1.04 Ga (Field and Råheim, 1979). Dahlgren (1991) presented a Sm-Nd mineral isochron of approximately 1.1 Ga for one of the granulites. The gabbro itself has dated at  $1.64 \pm 0.23$  Ga (Sm-Nd whole rock; de Haas et al., 1992b; Chapter IV of this thesis).

A coronitic microstructure is absent in most of the Flosta Gabbro, in contrast to many other Bamble gabbros (Brögger, 1934; Frodesen, 1968a; Starmer, 1969; Joesten, 1986; Theulings et al., 1986; Brickwood and Craig, 1987). The Flosta Gabbro displays distinct primary igneous layering, which dips moderately southeast. Such layering has only been reported twice before from gabbros in the Bamble Sector (Touret, 1968, 1969), but in fact occurs in many small gabbros e.g. the Kverve, Selåsfjellet and Ubergsmoen Gabbros (Fig. 2.1). Igneous layering has also been described from the Morkheia Monzonite Suite (Fig. 1.1; Smalley et al., 1988; Smalley, 1990).

Emplacement of the gabbro was accompanied by melting of the country rocks and back veining. Gneissic xenoliths are mainly present in the contact zones of the intrusion. Deformation was limited to low angle shear zones and local tight folding. An axial planar cleavage to these folds is sporadically developed and is accompanied by the appearance of biotite in the gabbro. The gabbro was later intruded by several pegmatites, among them the Narestö pegmatite (e.g. Eakin, 1989), which was the first pegmatite in Norway to be economically exploited. Most pegmatites dip 40-50° southeast and seem to have intruded along pre-existing shear zones.

### 3.3 IGNEOUS STRUCTURES

The Flosta Gabbro can be divided into a Basal Zone and an Upper Zone. These are separated by the Slumped Unit (Fig. 3.1). All features suitable for determining the upward direction of the layered series consistently indicate top to the southeast. The thickness of the entire sequence amounts to approximately 500 m. The terminology used is according to Irvine (1982).

#### 3.3.1 Basal Zone

The BZ consists of medium- (10-15 mm) and fine-grained ( $\approx 5$  mm) layered gabbro. Though locally homogeneous, medium-grained layers occasionally exhibit the following specific structures: 1) diffuse monomineralic layers, usually only one grain thick;

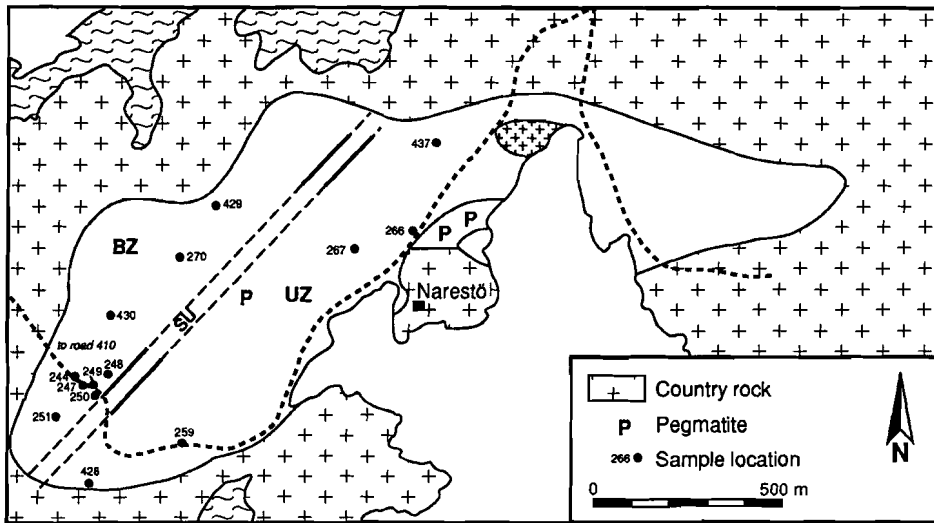


**Figure 3.1** Map of the Flostá Gabbro, modified after Starmer (1985a).

2) thin (1-2 cm) mafic laminae (**Fig. 3.2**); 3) mafic schlieren that wedge out within the layers (**Fig. 3.3**); 4) elongate patches of plagioclase, oriented parallel to the layer boundaries (**Fig. 3.4**).

The fine-grained layers lack this variety of internal structures, but may exhibit modal grading (**Fig. 3.5**) and grain-size grading. Fine-grained layers with distinctly different mineralogical compositions and separated by thin ( $\pm 1$  mm) mafic laminae also occur (**Fig. 3.6**).

Contacts between the layers are generally concordant. These contacts may be either sharp (between medium and fine-grained layers) or grain-size gradational. In the middle of the BZ, a low angle discordant contact is present between packages of medium and fine-grained layers (**Fig. 3.7**). In one place in the upper part of the BZ, the contact between more and less mafic fine-grained layers has a wavy appearance, and resembles sedimentary cross bedding.

### 3.3.2 Slumped Unit

In the middle part of the layered series there is a unit with disrupted layering, that extends laterally throughout the intrusion. Subrounded blocks of medium-grained gabbro float in a matrix of fine-grained gabbro with contorted layering. Similar structures have been described from the Tugtutôq Younger Giant Dike Complex of South Greenland (Upton, 1987).





Figure 3.2 Mafic laminae in a medium-grained layer from the BZ.

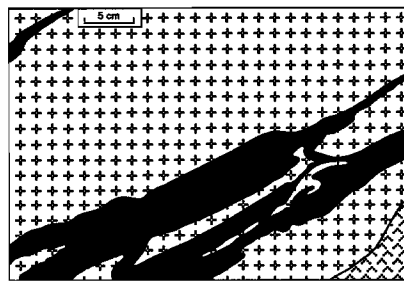
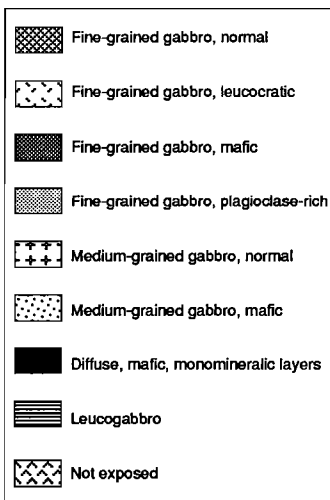


Figure 3.3 Mafic schlieren in the BZ.

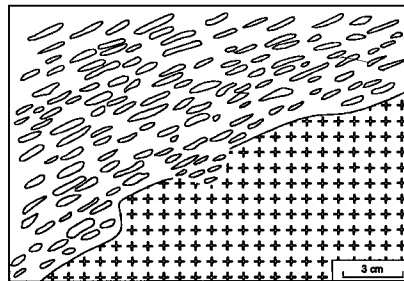


Figure 3.4 Oriented elongate patches of plagioclase in the lower part of the BZ.

*Igneous layering and magma replenishment*

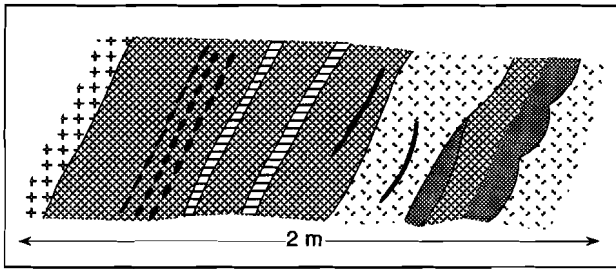


Figure 3.5 Modal grading in medium-grained layers from the upper part of the BZ (right).

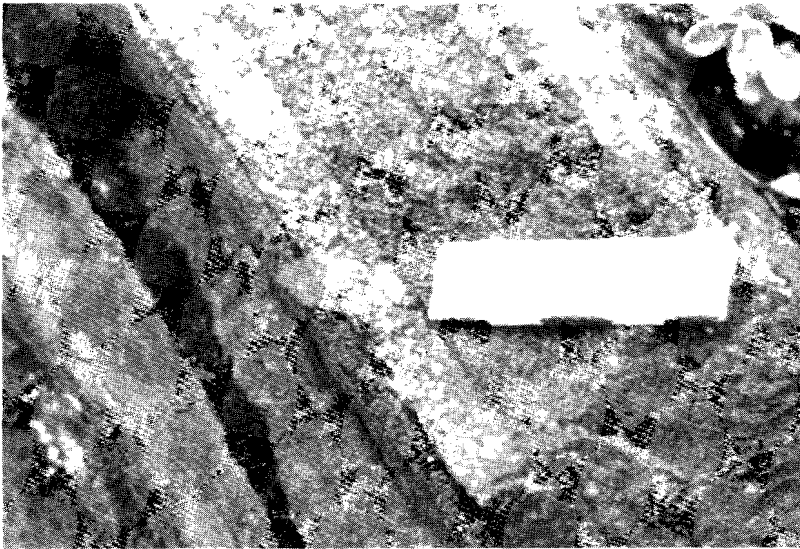


Figure 3.6 Mafic laminae separating two compositionally different types of fine grained gabbro in the upper part of the BZ.

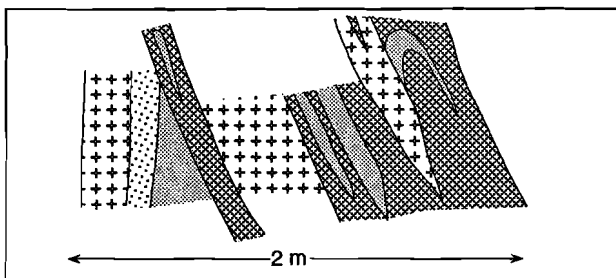


Figure 3.7 Low angle unconformity between two layered units in the middle of the BZ.

3.3.3 Upper Zone

Just above the SU is a thinly layered unit. In the upper part, disturbed layering occurs beneath a homogeneous medium-grained unit. These disturbances include pouches of medium-grained gabbro which have sunk into the underlying layers (Fig. 3.8), and troughs.

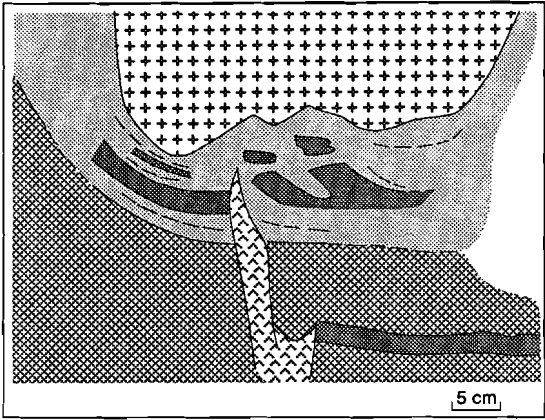


Figure 3.8 Load casts of medium-grained gabbro disturbing the underlying layering in the lowermost part of the UZ.

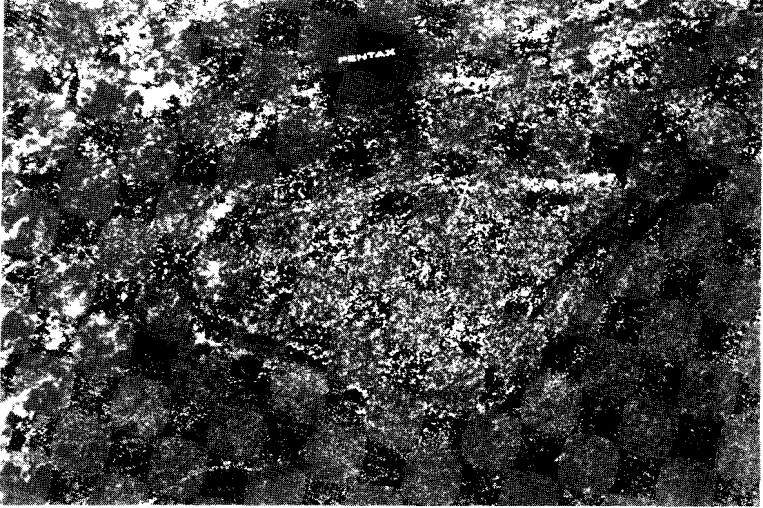


Figure 3.9 Trough filled with medium-grained gabbro and discontinuously overlain by medium-grained gabbro in the lowermost part of the UZ.

Below the load casts, thin mafic as well as plagioclase-rich laminae are present. In the mafic laminae, a foliation has been developed parallel to the base of the medium-grained gabbro. Troughs filled up by medium-grained gabbro are covered by a blanket of the same material (Fig. 3.9)

Units of medium-grained gabbro, up to several meters thick and intercalated with thinly layered units, build up the rest of this zone. The thick medium-grained units locally show a gradation from finer medium-grained at their basis to coarser medium-grained at their tops. Apart from a few intercalated mafic laminae, these units are relatively homogeneous with respect to the thinner medium-grained layers in the BZ. The thinly (up to a few decimeters) layered units consists of fine and medium-grained layers. Medium-grained layers in these units tend to become thicker in the higher units.

### 3.4 PETROGRAPHY

Medium- and fine-grained layers in the Flosta Gabbro display relic subophitic textures. Plagioclase and orthopyroxene are cumulus minerals, clinopyroxene and ilmenite intercumulus. Evidence for the former presence of olivine has not been found. Cumulus clinopyroxene and ilmenite occur in the mafic laminae. Clinopyroxene is altered to hornblende and orthopyroxene, probably due to the action of late-stage magmatic fluids (Otten, 1984).

During subsequent metamorphism, magmatic clinopyroxene reacted to hornblende and quartz, initially along the cleavage planes. The hornblende was later overgrown by ortho- and clinopyroxene. These metamorphic pyroxenes form a foam texture together with hornblende and recrystallized plagioclase. Interstitial carbonates occur locally. Biotite is present in some samples and is always younger than the hornblende. The biotite encloses small zircons and apatite. Apatite is locally remarkably coarse-grained.

Microscopically, the transition from more leucocratic medium-grained to more mafic medium-grained gabbro layers in the BZ is characterized by a decrease in the modal amount and grain-size of plagioclase, an increase in the modal amount of ilmenite, and an increase in the size of ortho- and clinopyroxene grains. The transition from fine- to medium-grained gabbro is simply a result of an increase in the size of cumulus plagioclase as well as of intercumulus clinopyroxene and ilmenite. Furthermore, there is a small increase in the modal amount of ilmenite, while the amount of

plagioclase decreases.

Samples were selected for whole rock chemistry, using the following criteria: 1) to represent one single layer; 2) to be out of the vicinity of granitic pegmatites and shear zones; 3) to represent normal gabbroic cumulates and not exclusively mafic or felsic minerals; 4) to display relic magmatic textures. No samples from the slumped group have been included. Samples from the eastern part have also been excluded since it was impossible to correlate their stratigraphic position with certainty. Modal mineralogy and optically determined anorthite contents of plagioclase are presented in **Table 3.1**. Anorthite contents are for the cores of plagioclases which preserved their original magmatic habit.

**Table 3.1** Point counted modal analyses and anorthite percentages of plagioclase (optically determined).

Sample	Plagioclase	An %	Pyroxene/ Hornblende	Ilmenite	Biotite
GA429	82.9	50	15.5	0.3	1.3
GA270	48.9	55	44.8	6.3	-
GA244	56.6	58	39.6	1.4	2.4
GA247F	35.7	-	51.0	5.0	8.3
GA248	49.8	37	31.9	2.9	15.4
GA249	67.9	58	24.3	2.3	5.5
GA250	24.9	57	66.6	8.4	0.1
GA251	41.7	48	46.9	9.9	1.5
GA256	57.6	52	31.0	4.8	6.6
GA428	59.6	56	36.4	4.0	-
GA437	46.9	37	44.9	8.2	-
GA267	43.9	60	54.8	1.3	-
GA259	43.1	36	38.6	-	18.3
GA266	66.7	52	29.1	1.9	2.3

### 3.5 WHOLE ROCK CHEMISTRY

Analytical techniques for major and trace element determinations have been described in Chapter II of this thesis. Analyses are listed in **Table 3.2**.

Major and trace elements and the Mg-number,  $Mg\# = 100 * \text{molar MgO}/(\text{MgO} + \text{FeO})$ , of fifteen samples have been plotted versus their stratigraphic height in the Flostá Gabbro (**Fig. 3.10**). The profiles reveal two sharp discontinuities, one at c. 170 m in the lower part of the BZ and one at c. 390 m in the UZ. Both are defined by a strong increase of the Mg# (**Fig. 3.10**).

*Igneous layering and magma replenishment*

**Table 3.2** Whole rock analyses of fifteen samples. All iron as FeO; dl = below detection limit; na = not analyzed. Mg # is the ilmenite-corrected Mg# (see text).

Sample Stratigraphic height (m)	GA430	GA429	GA270	GA244	GA247F	GA248	GA249	GA250
	138	146	158	165	178	198	199	223
SiO <sub>2</sub>	47.32	51.53	45.39	50.33	44.68	49.63	52.70	43.26
TiO <sub>2</sub>	2.21	1.98	5.26	1.23	3.30	2.88	2.08	5.35
Al <sub>2</sub> O <sub>3</sub>	14.37	19.29	14.42	17.25	15.54	14.84	18.61	11.02
FeO	13.37	7.48	14.30	10.25	14.21	13.31	8.09	18.20
MnO	0.26	0.13	0.21	0.19	0.31	0.26	0.16	0.26
MgO	8.86	4.60	6.16	8.00	6.34	4.40	3.63	8.78
CaO	7.05	9.02	9.13	7.83	8.80	7.34	8.37	8.69
Na <sub>2</sub> O	2.67	3.88	2.84	3.08	3.09	2.84	4.15	1.84
K <sub>2</sub> O	2.27	0.74	0.60	0.55	1.53	2.11	0.97	0.40
P <sub>2</sub> O <sub>5</sub>	0.14	0.52	0.15	0.14	0.68	0.93	0.31	0.25
LOI	dl	0.39	dl	0.14	0.67	na	0.91	dl
Ni	150	49	85	71	79	na	23	144
Rb	39	10	dl	6	50	na	16	10
Sr	315	566	380	491	301	na	453	272
Zr	60	84	80	42	182	na	172	114
Nb	5.8	7.5	9.0	2.1	14.4	na	11.0	11.9
Mg#	54.3	52.5	43.6	58.4	44.5	37.2	44.6	46.4
Mg #	-	53.1	47.8	61.0	52.4	41.6	50.8	57.4

Sample Stratigraphic height (m)	GA251	GA256	GA428	GA437	GA267	GA259	GA266
	224	286	321	369	388	392	446
SiO <sub>2</sub>	45.38	48.04	47.05	41.12	48.78	48.52	50.08
TiO <sub>2</sub>	4.34	2.31	3.17	6.94	1.39	1.26	1.96
Al <sub>2</sub> O <sub>3</sub>	15.19	15.18	16.62	10.81	16.50	17.08	17.26
FeO	13.97	12.82	12.81	19.90	9.44	10.39	10.27
MnO	0.21	0.17	0.18	0.26	0.19	0.19	0.18
MgO	6.00	5.99	5.91	6.38	8.19	7.00	5.63
CaO	9.64	10.06	9.39	6.94	10.97	8.56	8.05
Na <sub>2</sub> O	2.79	2.83	2.67	2.02	2.79	3.50	3.81
K <sub>2</sub> O	0.46	0.84	0.59	0.74	0.56	2.07	0.92
P <sub>2</sub> O <sub>5</sub>	0.52	0.37	0.20	0.22	0.18	0.31	0.68
LOI	na	1.37	0.36	0.02	0.90	0.86	1.16
Ni	na	154	72	34	92	101	53
Rb	na	21	dl	dl	11	69	21
Sr	na	407	466	274	219	239	326
Zr	na	94	83	174	88	102	187
Nb	na	4.0	5.9	15.8	6.3	11.0	15.5
Mg#	43.5	45.6	45.3	36.5	60.9	54.7	49.6
Mg #	63.3	54.1	52.2	45.8	63.5	54.7	53.4

The high Mg# values at GA244 and GA267 coincide with a drop in TiO<sub>2</sub>, FeO, Zr and Nb contents (Fig. 3.10). The increase of FeO and TiO<sub>2</sub> after their low at GA244 is followed by a decrease. Their minimum at GA267 is succeeded by a modest increase, whereas Zr and Nb concentrations become strongly elevated. The TiO<sub>2</sub> profile correlates well with the modal ilmenite variations in the gabbro (Fig. 3.11). The behaviour of Na<sub>2</sub>O, CaO, and P<sub>2</sub>O<sub>5</sub> is more ambiguous (Fig. 3.10). CaO reaches a small minimum at GA244 but a distinct maximum at GA267 after a strong decrease at GA437. For Na<sub>2</sub>O and P<sub>2</sub>O<sub>5</sub>, no peak at all is observed at GA244 and GA267 although P<sub>2</sub>O<sub>5</sub> contents strongly rise above GA244.

A third, less distinct, discontinuity occurs in the upper part of the basal zone (BZ) and starts with the increase of Mg# at c. 200 m, which is concurrent with low TiO<sub>2</sub>, FeO and Nb contents (Fig. 3.10). The Mg# however reaches its actual maximum at c. 225 m, which on its turn coincides with low Na<sub>2</sub>O and Zr contents. The P<sub>2</sub>O<sub>5</sub> contents (Fig. 3.10) remain low between beginning of the discontinuity at GA249 and its actual maximum at GA250.

In order to evaluate the effect of ilmenite on the Mg#, the Mg# has been recalculated after subtracting the amount of iron in ilmenite ( $= \{ \text{modal amount of ilmenite} * \text{density of ilmenite} / \text{density of the gabbro} \} * \{ \text{wt. \% FeO in ilmenite} / 100 \}$ ) from whole rock FeO. The shape of the Mg# profile does not significantly change. It results in slightly higher maxima for Mg# at c. 170 and 390 m. The increase in Mg#, that starts at c. 200 and ends at 225 m, becomes much more pronounced.

### 3.6 MAGMATIC EVOLUTION

The presence of igneous layering indicates that the Flostá Gabbro represents a solidified magma chamber. The shape of the Mg# profile is evidently not due to varying amounts of ilmenite. This implies that anomalies in the profiles of Mg# and probably other elements find their origin in the pre-crystallization stage. The Mg# profile (Fig. 3.10) indicates that, in addition to the first magma pulse from which the lowest part of the BZ crystallized, at least two more magma pulses were involved in the crystallization of the Flostá Gabbro. The two pulses are defined by distinct maxima for Mg# at 170 m in the lower part of the BZ and at 380 m in UZ. The new influxes are also manifest in the profiles for major and trace elements. Evidence from mineral data for the multiple injection of magmas is limited.

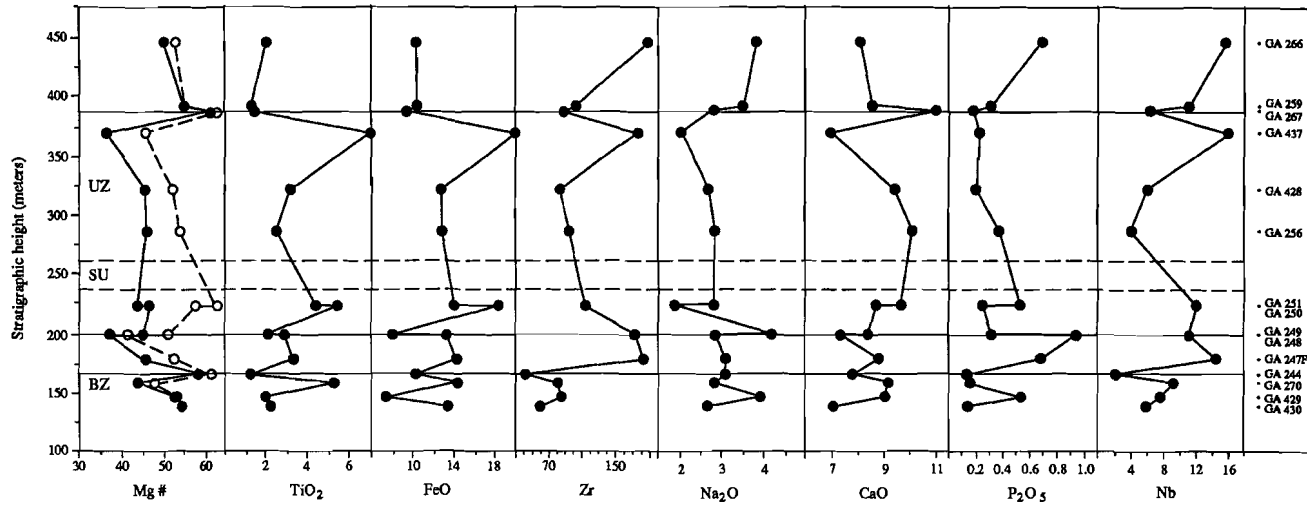


Figure 3.10 Whole rock chemical profiles of Mg#, TiO<sub>2</sub> (wt.%), FeO (wt.%), Zr (ppm), Na<sub>2</sub>O (wt.%), CaO (wt.%), P<sub>2</sub>O<sub>5</sub> (wt.%) and Nb (ppm) versus the stratigraphic height (meters).



When plotted versus stratigraphic height (Fig. 3.11), the anorthite content displays two maxima coinciding with the anomalies deduced from whole rock chemistry at 170 m and 380 m.

A third maximum, between 220 and 225 m in the upper part of the BZ, is not confined to one position in the sequence. The gradual increase of the Mg# from GA248 to GA251 may point to mixing of new magma with fractionated magma or with upward migration of intercumulus liquid (Irvine, 1980a). Assuming that fractionated liquid was also present during injection of the other pulses, the absence of such gradual increases at the other Mg# maxima might be explained in terms of more rapid, effective mixing of these two magmas.

Several processes have been proposed in literature to explain the kinds of layering as described above. Modally graded layers have been explained by current deposition (Wager and Brown, 1968; Irvine, 1987; Conrad and Naslund, 1989), rhythmic nucleation (Maaløe, 1978) and in-situ crystallization (McBirney and Noyes, 1979). Deposition by magmatic density currents has been invoked for grain-size graded layering (Irvine, 1980b, 1987). Crystal settling has been proposed to explain thick homogeneous layers (Wager and Brown, 1968).

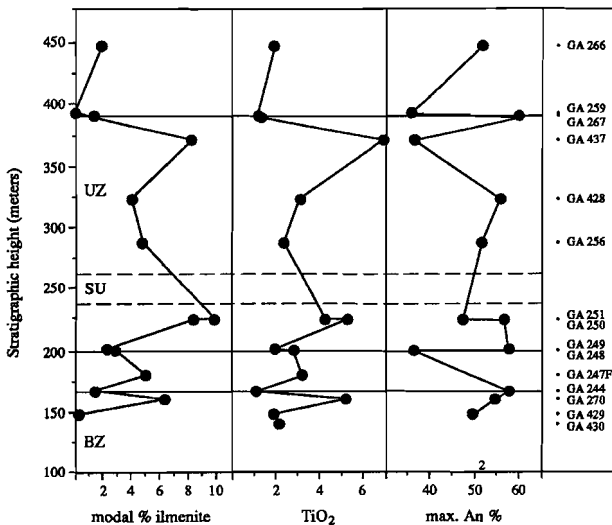


Figure 3.11 Modal percentage ilmenite, TiO<sub>2</sub> (wt%) and the anorthite (An%) content of plagioclase versus the stratigraphic height.

From the summary above, three main types of processes appear that may explain the formation of the observed types of layering: 1) current deposition; 2) crystal settling; 3) in-situ crystallization. The involvement of process 1) in the formation of at least part of the sequence is favoured by the homogeneous infill of troughs and subsequent discontinuous blanketing by a layer of medium-grained gabbro. This implies deposition from currents rather than in-situ crystallization or gravitational settling. It is also supported by the probable cross bedding and discordant contacts between layered units. Current activity may simply be the result of convection of the magma injected into the magma chamber. Convection may have been reinforced by influxes of new magma.

Mafic laminae as observed at a variety of stratigraphic levels in the Flosta Gabbro may be explained as density current deposits (Irvine, 1987). Mafic minerals crystallized in the magma or detached from the roof and margins will be picked up by an upward current and transported together with plagioclase, if the current energy is high enough to lift the relatively heavy mafic crystals. If however, this current energy is near the critical value at which the mafic minerals can no longer be transported, mafic crystals will tend to be redeposited earlier than the plagioclase, giving rise to the formation of mafic laminae by a kind of gravitational sorting. When the currents move over an uneven surface, the currents will be slowed down against the uphill side of the surface, thus depositing irregular bodies of mafic minerals, while the plagioclase remains floating. These deposits are represented by the mafic schlieren.

Process 2), crystal settling, is an unlikely mechanism to build the layering described above. Conditions in a small magma chamber like the Flosta Gabbro would not have remained sufficiently constant to make this process viable. The injection of new magma pulses into such a small magma chamber, that is meanwhile cooling at its margins, will most likely trigger convection.

In-situ crystallization, process 3), has been put forward to explain modal grading (McBirney and Noyes, 1979) as well as homogeneous packages with an internal chemical gradient. Modally graded layering is of subordinate importance in the BZ of the Flosta Gabbro. As the neighbouring layers have been deposited by currents, we favour this kind of deposition, involving gravitational sorting, for the modally graded layers too. In the UZ, relatively thick homogeneous medium-grained layers are intercalated with thinly layered units. It is not possible to put any constraints on the internally chemical variation within these homogeneous layers. The presence of grain-size grading favours deposition by density currents. This is supported by the presence of a few mafic laminae.

However, it is clear that the nature of current activity in the UZ differed from activity in the BZ.

The gabbro shows evidence for prograde metamorphism: first amphibolitization, and subsequently the development of a granulite assemblage. This indicates that the magma intruded under amphibolite facies or lower temperature conditions. Hence, the difference in temperature between the hot magma and its country rocks would have been several hundred degrees. This would have resulted in relatively rapid crystallization along the margins and the roof of the magma chamber, thus insulating the interior of the magma chamber. When the crystallized pile became gravitationally unstable, it slumped and resulted in formation of the SU.

The Flosta Gabbro is a roughly lensoid concordant body, and therefore its formation may be thought analogous to that of a sill. In the continental crust, the formation of sills at levels deeper than 45 km is impossible for a reasonable tensile stress (Francis, 1982). The feeder dikes to these sill-like bodies are generally situated near one of the lateral margins of the body and not near the middle of the base (Francis, 1982). An obvious feeder dike is lacking for the Flosta Gabbro. But 500 meter to the west, a small gabbroic dike occurs in the country rock. Its topographic position with regard to the Flosta Gabbro makes it possible that it represents a feeder dike. The similarity in Sm-Nd isotope systematics of this gabbroic dike and the Flosta Gabbro (de Haas et al., 1992b; Chapter IV of this thesis), suggests that they are genetically related.

### 3.7 LOWER CRUSTAL IMPLICATIONS

The Bamble Sector, like many other granulite facies terrains (cf. Harley, 1989), is generally considered to represent a slice of denuded lower continental crust, and as such provides a probe to investigate the processes of crustal accretion and stabilization. The scattered presence of small, magma chambers, a few hundred meters thick, like the Flosta Gabbro, will influence the rheological state and contribute to the heat and fluid budget of the lower crust (cf. Frost et al., 1989). Other gabbros in the Bamble Sector which possibly represent this kind of small magma chamber may be the Ubergsmoen, Selåsfjellet and Kverve gabbros (de Haas and Nijland, unpubl. data) and the Laget hyperite complex (Touret, 1968, 1969), all of them displaying modal and/or grain-size graded layering and other igneous structures (de Haas and Nijland, unpublished data).

Field relations suggest that these gabbros may be of the same age as the Flosta Gabbro.

Information about the tectonic environment in which these gabbros were emplaced, is provided by the observed metamorphic (Visser and Senior, 1990) and geochronological (Demaiffe and Michot, 1985) features of the area. These and other authors (Smalley and Field, 1985; Smalley et al., 1983b) propose a continental collision setting with associated magmatic addition for the Proterozoic of southern Norway.

Compressional stress acting upon a mass of basic magma ponding below the crust in a collisional setting may result in the separation of batches of magma which migrate upward through the fracture. Compressive stresses will induce fracturing if the fluid or magma pressure exceeds the lithostatic pressure (Spera, 1980). The lower crust normally shows a ductile behaviour (Kusznir and Park, 1986) but the presence of a pressurized fluid phase lowers the effective stress and enables brittle failure to ensue to greater depths. Countering compressional stress acting on the walls of the fracture inhibits the transfer of large amounts of magma. Injection of small batches of magma under a compressive regime may count for the multiple replenishment in, and occurrence of small gabbro bodies in the Bamble Sector. The restricted amount of magma injected in the crust explains why the magma chambers did not act as storage reservoirs for extensive basaltic volcanism as is observed for large extension-related intrusions. The restricted size of these gabbros is in marked contrast with voluminous Proterozoic layered intrusions like the Muskox Intrusion (LeCheminant and Heaman, 1989) and the Duluth complex (Miller and Weiblen, 1990) which are associated with extensional tectonics. These intrusions also have a much more primitive composition.

### **Acknowledgements**

Rob H. Verschure and Cees Maijer are thanked for their provoking discussions in the field. Blakstad Yrkesskole provided lodging during fieldwork, and the Grand Taket in Arendal inspiring day endings. C. Maijer, R. D. Schuiling, J. L. R. Touret and J. B. H. Jansen kindly read earlier versions of this chapter. Constructive reviews were provided by B. Robins, J. R. Wilson and R. Boyd.

## CHAPTER IV

### SM-ND AGE DETERMINATIONS OF SOME CORONITIC GABBROS AND THE NATURE OF THE PROTEROZOIC MANTLE BELOW BAMBLE.

#### 4.1 INTRODUCTION

Despite the many studies on the coronitic gabbros of the Bamble Sector, no reliable isotopic ages for the gabbros were available up to now, although emplacement of gabbroic rocks at c. 1.04 Ga has been suggested by O'Nions et al. (1969) on the basis of apparent K-Ar ages of Mg-rich amphiboles and phlogopites. Starmer (1985a) argued that the coronitic gabbros were emplaced during the Sveconorwegian Orogeny (1.25 - 0.9 Ga) under a tensional regime. Only three age determinations have been reported for gabbros from the Kongsberg and Telemark Sectors (**Table 4.1**).

Sm-Nd isotope studies have been performed in different parts of the SWSD, but previous to this study no Sm-Nd data were available for the Bamble Sector. Menuge (1985) reported a disputed Sm-Nd whole rock isochron age of  $1.19 \pm 0.04$  Ga ( $\epsilon_{Nd}(T) = +2.2 \pm 0.7$ ) for the Rjukan metavolcanics from the Telemark Sector. Åhäll and Daly (1989) dated amphibolites from the Östfold-Marstrand Belt (SLM in **Fig. 4.1**) at  $1.76 \pm 0.08$  Ga ( $\epsilon_{Nd}(T) = +4.3 \pm 0.9$ ). Mearns (1986) obtained an age of  $1.70 \pm 0.03$  Ga for a garnet lherzolite from the Western Gneiss Region (WGR in **Fig. 4.1**) with a similar initial  $\epsilon_{Nd}$  value of  $+4.7 \pm 0.7$ .

The initial  $\epsilon_{Nd}$  values of the amphibolites and garnet lherzolite indicate that the mantle source of the newly accreted crust of the Southwest Scandinavian Domain had a depleted signature, comparable to the depleted mantle of DePaolo (1981). Mearns et al. (1986) on the other hand postulate a less depleted mantle below Southwest Scandinavia during the Proterozoic. Low initial  $\epsilon_{Nd}$  values have also been reported for dolerites along the Protogine Zone, southern Sweden (Johansson and Johansson, 1991).

Sm-Nd isotope analyses for five gabbros from the Bamble Sector have been performed in order to constrain both the timing of their emplacement and the evolution of the mantle beneath this part of the Baltic Shield.

**Table 4.1** Previous age determinations of gabbros from the Kongsberg and Telemark Sectors. <sup>1</sup> Jacobsen and Heier (1978); <sup>2</sup> Munz and Morvik (1991); <sup>3</sup> Dahlgren et al. (1990).

Gabbro, <i>area</i>	Method	Age
Vinoren, <i>Kongsberg</i> <sup>1</sup>	Rb-Sr (WR)	1.18 ± 0.05 Ga Sr(I) = 0.7024 ± 1
Morud Gabbro, <i>Kongsberg</i> <sup>2</sup>	Sm-Nd (WR + min)	1.22 ± 0.02 Ga Nd(I) = 0.51112 ± 5
Hesjøbutind Gabbro, <i>Telemark</i> <sup>3</sup>	U-Pb zircon	1.15 Ga

## 4.2 GEOLOGY

Crustal accretion of the SWSD (Fig. 4.1) took place mainly between 1.75 and 1.5 Ga ago during the Gothian Orogeny (Gaál and Gorbatshev, 1987), but the exact timing for the individual crustal segments is not yet well constrained.  $T_{DM}$  model ages for charnockitic migmatites and granitic gneisses from the Rogaland/Vest-Agder Sector indicate a period of crustal accretion between 1.85 - 1.55 Ga ago (Menuge, 1988). Sm-Nd model ages of acidic gneisses and post-tectonic granites suggest a major episode of crustal accretion in the Telemark Sector between 1.6 and 1.5 Ga ago (Menuge, 1985). Skjernaa and Pedersen (1982) reported Rb-Sr reference ages of 1.71 and 1.85 Ga for augen gneisses from the Östfold area. Welin and Gorbatshev (1978b) obtained a Rb-Sr age of  $1.71 \pm 0.12$  Ga for the Tjörn Tonalite from the Östfold-Marstrand Belt. The  $1.76 \pm 0.08$  Ga Sm-Nd whole rock age of the Stora Le-Marstrand amphibolites (Åhäll and Daly, 1989) supplies clear proof of mafic magmatism at the onset of the Gothian Orogeny. Rb-Sr whole rock data suggest that the maximum age of the crust in the Kongsberg Sector is c. 1.6 Ga, although generation by remelting of much older crust cannot be ruled out (Jacobsen and Heier, 1978).

The timing of crustal accretion of the Bamble Sector is also poorly documented. Field et al. (1985) dated charnockitic orthogneisses around Arendal at 1.54 Ga (Rb-Sr), which they interpreted as the time of peak metamorphism. The low initial  $^{87}\text{Sr}/^{86}\text{Sr}$  ratios suggest a crustal history for the gneiss precursors of at most 50 Ma. O'Nions and Baadsgaard (1971) obtained a Rb-Sr age of 1.58 Ga (recalculated with  $\lambda\text{-}^{87}\text{Rb}$  value of  $1.42 \cdot 10^{-11}\text{a}^{-1}$ ) for the northern part of the Levang gneiss (Fig. 4.1).

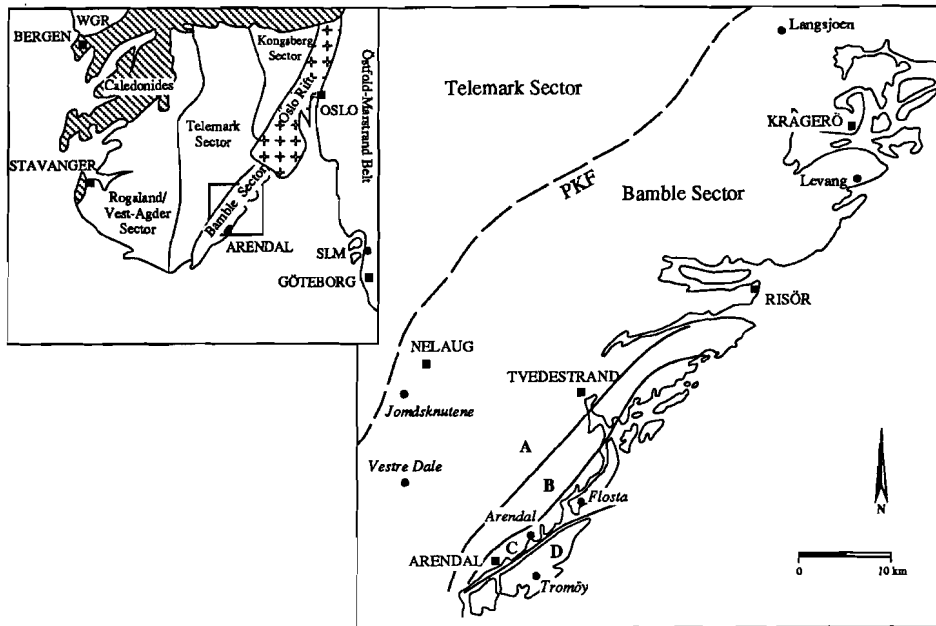


**Figure 4.1** Map of the Bamble area. Black circles mark the locations of the gabbros, the Levang gneiss and the Langsjoen charnockitic gneiss. Zoning after Smalley et al. (1983b). Inset shows the major geological divisions of the Southwest Scandinavian Domain; WGR: Western Gneiss Region, SLM: Stora Le-Marstrand amphibolites (modified after Verschure, 1985).

The oldest age recorded so far in the Bamble area has been reported by Field et al. (1985). They dated the Langsjoen charnockite (Fig. 4.1) at  $1.62 \pm 0.23$  Ga (Rb-Sr) and argued that an older basement already existed.

The five gabbros used for this dating study are distributed over the amphibolite-granulite facies transition zone near Arendal (Fig. 4.1). The Vestre Dale and the Jomåsknutene Gabbros are situated in mixed gneisses and quartzite complexes of the amphibolite facies terrain (zone A; Smalley et al., 1983b). The Flosta Gabbro and the Arendal Gabbro are surrounded by charnockitic to enderbitic gneisses in the granulite facies terrain of the Bamble Sector (zone C). The Tromøy Gabbro has been emplaced in enderbitic gneisses (zone D).

### 4.3 PETROGRAPHY

An extensive account on the petrology of the Vestre Dale Gabbro and the Flosta Gabbro has already been given in Chapters II and III. The Jomåsknutene Gabbro (co-ordinates: 32VMK 4752/785-4013/4962; Nelaug-sheet 1612 III, 1:50.000; Norges geografiske oppmåling 1967), in which different units can be discerned on the basis of grain size distributions (Dam, pers. com.), is the largest and most complex gabbro of all. Its primary magmatic mineralogy differs from that of the Vestre Dale Gabbro in that the Jomåsknutene Gabbro contains less olivine. Plagioclase is the dominant cumulus phase, locally up to 70 modal %. Clinopyroxene, magnetite and ilmenite are intercumulus phases. Clinopyroxene has a dark appearance due to exsolution of ilmenite. Apatite and zircon are common accessories. Like in the Vestre Dale Gabbro, coronitic microstructures have been developed between plagioclase and olivine and between plagioclase and opaque. A difference with the coronas in the Vestre Dale Gabbro is the regular presence of an outer rim of garnet. Part of the olivine has been replaced by orthopyroxene-magnetite symplectites. The major part of the Jomåsknutene Gabbro has been affected by amphibolitization and scapolitization. Sample selection of the Jomåsknutene Gabbro for this study has been confined to samples which at least retained their magmatic texture. The Jomåsknutene Gabbro also comprises an elongate body which can be traced for one kilometre in the gabbro parallel to the other units; it is only a few tens of meters wide. This hornblende is nearly entirely (> 90 modal %) made up by pargasitic hornblende and minor orthopyroxene and magnetite  $\pm$  olivine  $\pm$  green spinel  $\pm$  relics of plagioclase.

Plagioclase is the major constituent in both the Arendal Gabbro (co-ordinates: 32VMK 4891-4817; Arendal-sheet 1611 IV, 1:50.000; Norges geografiske oppmåling 1967) and the Tromøy Gabbro (co-ordinates: 32VMK 4896-4794; Arendal-sheet 1611 IV, 1:50.000; Norges geografiske oppmåling 1967). Orthopyroxene-magnetite symplectites and coronas of orthopyroxene and pargasite-spinel symplectites indicate the former presence of olivine. Polygonal clusters of pyroxene and hornblende are rimmed by garnet. Intercumulus clinopyroxene has exsolved orthopyroxene and ilmenite. Apatite, zircon, ilmenite and magnetite are accessory phases.



#### 4.4 ANALYTICAL METHODS

Sm-Nd isotope analyses were performed at the Isotope Geology Laboratory, Vrije Universiteit, Amsterdam. Whole rock powders were dissolved in a mixture of 4-6 ml HF (40%), 1 ml concentrated HNO<sub>3</sub> and 1 ml HClO<sub>4</sub> (1:1) at 160°C for 5 days in PFA screw-top beakers. After drying at 160°C the residues were redissolved in 1 ml HClO<sub>4</sub>. The samples were left on the hotplate for a few hours and were dried at 160°C. This process was repeated once. The residues were then taken up in 20 ml 6N HCl and left on the hotplate for one night prior to aliquotting. A mixed <sup>150</sup>Sm-<sup>148</sup>Nd spike was used for isotope dilution (Hebeda et al., 1988). After evaporation of the spiked and unspiked aliquots, the residues were taken up in 2 ml 2N HCl. The solutions were centrifuged for about 5 minutes at 4000 r.p.m. After separation of the REE using standard cation exchange chromatography, Nd and Sm were separated by HDEHP reversed phase columns.

Sm and Nd mass spectrometry analyses were made using a Finnigan MAT 261 mass spectrometer with a fixed multicollector array. The results are listed in Table 4.2. Total Nd blanks were less than 1 ng. The <sup>143</sup>Nd/<sup>144</sup>Nd ratios were normalized to <sup>146</sup>Nd/<sup>144</sup>Nd = 0.7219. Three analyses of the La Jolla standard gave <sup>143</sup>Nd/<sup>144</sup>Nd = 0.511853 ± 0.000005 (2σ). Quoted errors in <sup>143</sup>Nd/<sup>144</sup>Nd are within-run precision (1s). The precision of the <sup>143</sup>Nd/<sup>144</sup>Nd is estimated to be 0.001 %; the reproducibility of <sup>147</sup>Sm/<sup>144</sup>Nd ratios is 0.3%, based upon duplicate analyses. Sm and Nd concentrations have an uncertainty of c. 1.0 %.

#### 4.5 AGE CALCULATIONS

Isotopic data were regressed using the method of York (1969), with <sup>147</sup>Sm/<sup>144</sup>Nd data offset to optimize the initial ε<sub>Nd</sub> values (Fletcher and Rosman, 1982). The decay constant used was λ-<sup>147</sup>Sm = 6.54 \* 10<sup>-12</sup> a<sup>-1</sup>. All calculated isochron errors are 2s and multiplied by √MSWD if MSWD > 1. <sup>143</sup>Nd/<sup>144</sup>Nd ratios are expressed in ε units (see DePaolo and Wasserburg (1976) for ε notation).

Six samples of the *Vestre Dale Gabbro*, covering the compositional range of the cumulates show a good fit in a Sm-Nd evolution diagram. The samples define an isochron age of T = 1.11 ± 0.14 Ga with an initial ε<sub>Nd</sub> = +1.8 ± 0.5 (Fig. 4.2). The large isochron age is due to the small spread in the Sm/Nd ratio.

**Table 4.2** Sm-Nd isotope data of the Vestre Dale Gabbro ( $T = 1.11 \pm 0.14$  Ga), Jomåsknutene Gabbro ( $T = 1.77 \pm 0.19$  Ga), Flosta Gabbro ( $T = 1.64 \pm 0.23$  Ga), Tromøy Gabbro ( $T = 1.1$  Ga) and Arendal Gabbro ( $T = 1.1$  Ga).  $^{143}\text{Nd}/^{144}\text{Nd}(0)$  is measured ratio.

Sample		Sm (ppm)	Nd (ppm)	$^{147}\text{Sm}/^{144}\text{Nd}$	$^{143}\text{Nd}/^{144}\text{Nd}(0)$	$\epsilon_{\text{Nd}}(T)$
WT203	V	1.20	4.23	0.1707	$0.512543 \pm 7$	$+1.8 \pm 0.2$
WT209	V	2.61	9.38	0.1682	$0.512516 \pm 5$	$+1.7 \pm 0.2$
WT210	V	1.84	6.32	0.1760	$0.512576 \pm 12$	$+1.7 \pm 0.3$
WT216	V	3.32	11.41	0.1761	$0.512578 \pm 11$	$+1.8 \pm 0.3$
WT217	V	1.97	7.27	0.1640	$0.512496 \pm 4$	$+1.9 \pm 0.2$
WT225	V	2.11	7.89	0.1618	$0.512470 \pm 12$	$+1.7 \pm 0.2$
GA144	J	3.96	15.29	0.1564	$0.512463 \pm 7$	$+5.8 \pm 0.3$
GA146	J	3.78	11.65	0.1963	$0.512922 \pm 5$	$+5.7 \pm 0.3$
GA148	J	2.14	7.12	0.1815	$0.512750 \pm 5$	$+5.7 \pm 0.3$
GA155	J	3.93	11.57	0.2053	$0.512972 \pm 7$	$+4.6 \pm 0.3$
GA158	J	2.74	8.54	0.1941	$0.512911 \pm 6$	$+5.9 \pm 0.3$
GA456	J	5.66	21.80	0.1569	$0.512428 \pm 5$	$+5.0 \pm 0.3$
GA244	F	1.61	7.09	0.1370	$0.512304 \pm 7$	$+6.1 \pm 0.3$
GA254	F	4.58	18.24	0.1518	$0.512410 \pm 9$	$+5.0 \pm 0.3$
GA256	F	4.82	20.19	0.1445	$0.512359 \pm 10$	$+5.6 \pm 0.3$
GA267	F	3.37	12.36	0.1646	$0.512587 \pm 16$	$+5.8 \pm 0.3$
GA439	F	4.92	16.75	0.1774	$0.512727 \pm 9$	$+5.8 \pm 0.3$
GL61	T	3.80	12.20	0.1883	$0.512847 \pm 6$	$+5.3 \pm 0.3$
GL63	T	3.87	12.40	0.1889	$0.512843 \pm 9$	$+5.1 \pm 0.3$
GL64	T	4.52	14.58	0.1876	$0.512840 \pm 8$	$+5.2 \pm 0.3$
GL71	A	4.94	15.28	0.1957	$0.512931 \pm 4$	$+5.9 \pm 0.3$
GL75	A	5.19	16.12	0.1948	$0.512933 \pm 6$	$+6.0 \pm 0.3$

The six samples of the *Jomåskrutene Gabbro* were collected along a traverse through the gabbro, perpendicular to its layering. They comprise two coarse-grained gabbros (GA144 and 146) and one hornblendite (GA148) from the western part of the intrusion, and a coarse-grained gabbro (GA155), a medium-grained, coronitic gabbro (GA158) and a sample from the fine-grained gabbroic dyke (GA456) from the eastern part. The variation in the  $^{147}\text{Sm}/^{144}\text{Nd}$  ratios is larger than for the Vestre Dale gabbro. The six samples are isochronous and yield  $T = 1.77 \pm 0.19$  Ga with an initial  $\epsilon_{\text{Nd}} = +5.4 \pm 0.6$  (Fig. 4.3).

The whole rock isochron of the *Flosta Gabbro* has been calculated from four gabbro samples, which crystallized from different magma pulses, and a sample of the gabbroic dyke (GA439) (De Haas et al., 1992c; Chapter III of this thesis). The whole rock isochron defines an age of  $T = 1.64 \pm 0.23$  Ga for the Flosta Gabbro, with an initial  $\epsilon_{\text{Nd}} = +5.7 \pm 1.3$  (Fig. 4.4).

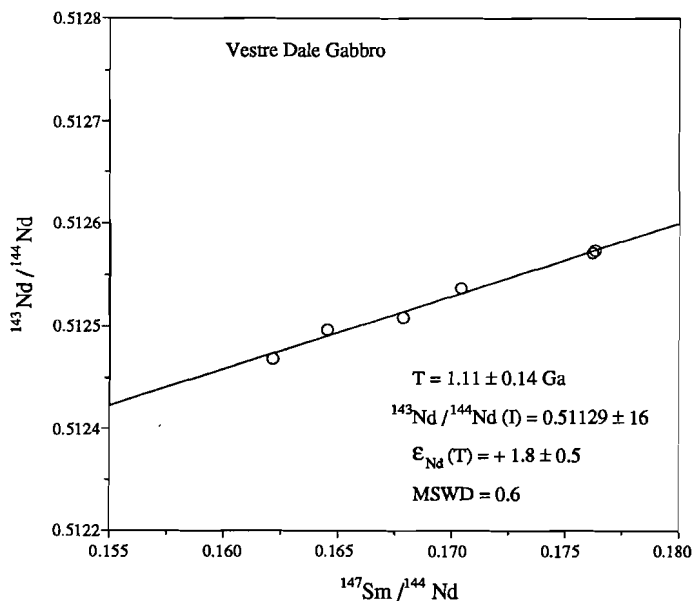


Figure 4.2 Sm-Nd isochron diagram for the Vestre Dale Gabbro.

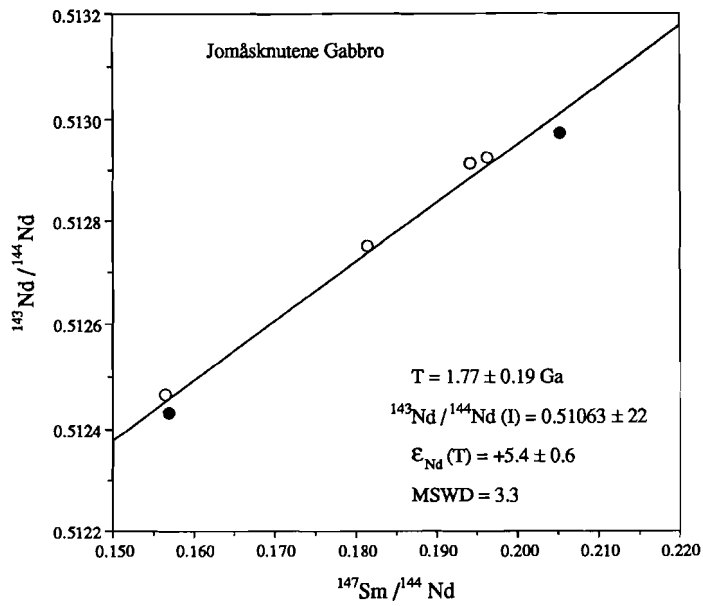


Figure 4.3 Sm-Nd isochron diagram for the Jomåsknutene Gabbro; GA155 and GA456 are indicated by filled symbols.

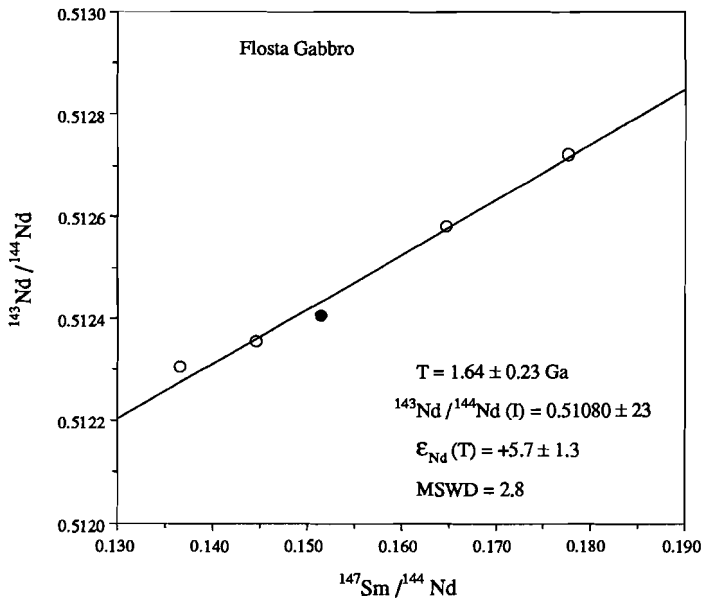


Figure 4.4 Sm-Nd isochron diagram for the Flosta Gabbro; GA254 is indicated by a filled symbol.

Due to the small variations observed in major and trace element chemistry, only two samples from the *Arendal Gabbro* and three from the *Tromøy Gabbro* have been analyzed. The variation in their  $^{147}\text{Sm}/^{144}\text{Nd}$  and  $^{143}\text{Nd}/^{144}\text{Nd}$  ratios is negligible. The  $^{147}\text{Sm}/^{144}\text{Nd}$  ratios are slightly lower than that of present-day CHUR. The Arendal and the Tromøy Gabbros both truncate the regional main foliation and were metamorphosed and deformed along their margins. These gabbros are therefore considered to be post-Gothian but predating the main phase of Sveconorwegian metamorphism. For this reason an age of 1.1 Ga has been assigned to these gabbros. The Arendal Gabbro has  $\epsilon_{\text{Nd}}(1.1 \text{ Ga})$  values of  $+5.9 \pm 0.3$  and  $+6.0 \pm 0.3$ ;  $\epsilon_{\text{Nd}}(1.1 \text{ Ga})$  values for the Tromøy Gabbro range from  $+5.1 \pm 0.3$  to  $+5.3 \pm 0.3$ .

## 4.6 DISCUSSION

### 4.6.1 Interpretation of the isochron ages

The different cumulates of the Vestre Dale Gabbro crystallized from one, tholeiitic, parental magma. (de Haas et al., 1992a; Chapter II of this thesis). All samples have the same  $\epsilon_{\text{Nd}}(1.11 \text{ Ga})$  within analytical error. The Sm-Nd age correlates, within the error limits, with a seven-point Rb-Sr errorchron age for the Vestre Dale Gabbro of  $1.26 \pm 0.07 \text{ Ga}$  (de Haas et al., 1992d; Chapter V of this thesis). Therefore it is concluded that the age of  $1.11 \pm 0.14 \text{ Ga}$  represents the time of crystallization.

The isochron age obtained from the Jomåsknutene Gabbro should be regarded with caution, since field investigations revealed that this gabbro crystallized from more than one magma pulse. Four samples have  $\epsilon_{\text{Nd}}(1.77 \text{ Ga})$  values ranging from  $+5.7 \pm 0.3$  to  $+5.9 \pm 0.3$ , but GA456, the fine-grained gabbroic dyke, and gabbro GA155 have an  $\epsilon_{\text{Nd}}(1.77 \text{ Ga})$  of  $+5.0 \pm 0.3$  and  $+4.6 \pm 0.3$  respectively. The high Nd concentration of GA456, more than 40% higher than that of GA144 (Table 4.2), suggests that crustal assimilation may have reduced its initial  $^{143}\text{Nd}/^{144}\text{Nd}$  ratio. The low initial ratio of GA155 might be related to scapolitization. GA146 however has also partly been scapolitized, but its initial ratio falls within the range of the three other samples. GA155 has, in addition, much lower bulk  $\text{K}_2\text{O}$  and Rb contents than GA456 (Appendix 1, Chapter VI of this thesis), so crustal assimilation is not obvious. Alternatively, this unit may have crystallized from a less depleted magma. Recalculation of the isochron, after discarding these two samples from the data set (Fig. 4.3), yields the same age but lowers the error:

1.77 ± 0.15 Ga. It significantly lowers the MSWD (0.2), and the initial  $\epsilon_{Nd}$  value becomes slightly higher: +5.7 ± 0.4. The absence of a correlation between 1/Nd and  $^{143}Nd/^{144}Nd$  excludes the possibility that the linear correlation represents mixing between two components. The isochron age of 1.77 ± 0.19 Ga is therefore considered as the crystallization age of the gabbro.

The good fit between the four samples of the Flosta Gabbro and the gabbroic dyke indicates that the different magmas had a similar isotopic composition, possibly with exception of GA254 (Table 4.2). The increase in the  $^{147}Sm/^{144}Nd$  ratios of the gabbro samples and the dyke with their stratigraphic position (see Table 4.2 and Table 3.2), assuming that the gabbroic dyke indeed acted as a feeder dyke, and as such crystallized from the latest magma pulse, suggests that the succeeding magma pulses were generated during progressive melt extraction of the source, which enhanced its Sm/Nd ratio. The preservation of the primary isotopic fractionation trend in the intrusion indicates that emplacement and crystallization occurred almost immediately after extraction. The isochron age of 1.64 ± 0.23 Ga is therefore interpreted as a crystallization age. The reason for the low initial  $\epsilon_{Nd}$  value of GA254 is not understood as both the petrography and chemistry are similar to the other samples. Omitting GA254 (Fig. 4.4) does not result in a significantly different age, but lowers the error: 1.62 ± 0.14 Ga (MSWD = 0.9). The initial  $\epsilon_{Nd}$  remains the same, but the error is reduced to +5.7 ± 0.8.

#### 4.6.2 Age correlations

The ages of the Jomåsknutene and Flosta Gabbros have major implications for the crustal evolution of the Bamble Sector. Firstly, intrusion of the coronitic gabbros is not solely restricted to the Sveconorwegian Orogeny. Secondly, the ages of the Jomåsknutene and the Flosta Gabbros are among the oldest recorded so far in the Bamble Sector. Both ages are within error of the age of the Langsjoen charnockitic gneiss (Fig. 4.1), for which a Rb-Sr whole rock age of 1.62 ± 0.23 Ga has been obtained (Field et al., 1985).

The age of the Jomåsknutene Gabbro is comparable with the age of the Stora Le-Marstrand (SLM) amphibolites from the Östfold-Marstrand Belt (1.76 ± 0.08 Ga; Åhäll and Daly, 1989) and the Almklovsdalen garnet lherzolite from the Western Gneiss Region, dated at 1.70 ± 0.03 Ga (Mearns, 1986). No similar ages have been reported for mafic rocks from the Kongsberg and Telemark Sectors but Munz and Morvik (1991)

and Dahlgren et al. (1990) provided evidence for Sveconorwegian mafic magmatism in these sectors. The ages of two gabbros from the Telemark and Kongsberg Sectors (Table 4.1) fall within the error limits of the age of the Vestre Dale Gabbro. The age of the Vestre Dale Gabbro also correlates well with the age of the Rjukan volcanics of the Telemark Sector, dated at  $1.19 \pm 0.04$  Ga (Menuge, 1985). However, it cannot be ruled out that these rocks are a product of Gothian magmatism (Verschure, 1985).

Correlations between the Southwest Scandinavian Domain and the Grenville Province in North America have been demonstrated in many studies (e.g. Gower, 1985). The U-Pb baddeleyite age of 1.17 Ga of a coronitic metagabbro from the southwestern Grenville Province (Davidson and van Breemen, 1988) and 1.16 Ga zircon and baddeleyite ages for gabbroic rocks of the Lac St.-Jean anorthositic complex, obtained by Higgins and Van Breemen (1989), are very similar to the age of the Vestre Dale Gabbro.

#### **4.6.3 Depletion and evolution of the sub-Bamble mantle**

The positive initial  $\epsilon_{Nd}$  values of the five gabbros indicate that these gabbros were derived from a depleted mantle (DM) source. The initial  $\epsilon_{Nd}$  values of the Jomåsknutene and Flosta Gabbros plot close to the DM curve of DePaolo (1981), as do initial values of other Proterozoic mafic rocks from the Baltic Shield, Greenland and North America (Fig. 4.5).  $\epsilon_{Nd}(1.1 \text{ Ga})$  values of the Arendal and Tromøy Gabbros plot, respectively, slightly above and below the DM curve of DePaolo (1981). These gabbros have nearly chondritic  $^{147}\text{Sm}/^{144}\text{Nd}$  ratios and their  $^{143}\text{Nd}/^{144}\text{Nd}$  ratios therefore show little variation with time. Calculated  $\epsilon_{Nd}(1.77 \text{ Ga})$  values fall in the range of the initial value of the Jomåsknutene Gabbro (Fig. 4.5). The  $\epsilon_{Nd}(1.11 \text{ Ga})$  of the younger Vestre Dale Gabbro is much lower than the  $\epsilon_{Nd}(1.1 \text{ Ga})$  values of the Arendal and Tromøy Gabbros. It is similar to the  $\epsilon_{Nd}(1.19 \text{ Ga})$  value of  $+2.2 \pm 0.7$  for the Rjukan volcanics from the Telemark Sector.

The initial  $\epsilon_{Nd}$  value of the Vestre Dale Gabbro plots close to the Southwest Scandinavian depleted-mantle curve of Mearns et al. (1986) (Fig. 4.5), which assumes an undepleted mantle reservoir up to 1.74 Ga. The postulated curve was actually for the Western Gneiss Region, an area which has possibly been transported over considerable distances eastward, and, therefore, may have a completely different history than the Southwest Scandinavian Domain. However, this curve also applies to rocks from the Oslo Rift region, the Fen Complex and the Central Scandinavian Dolerite Group.

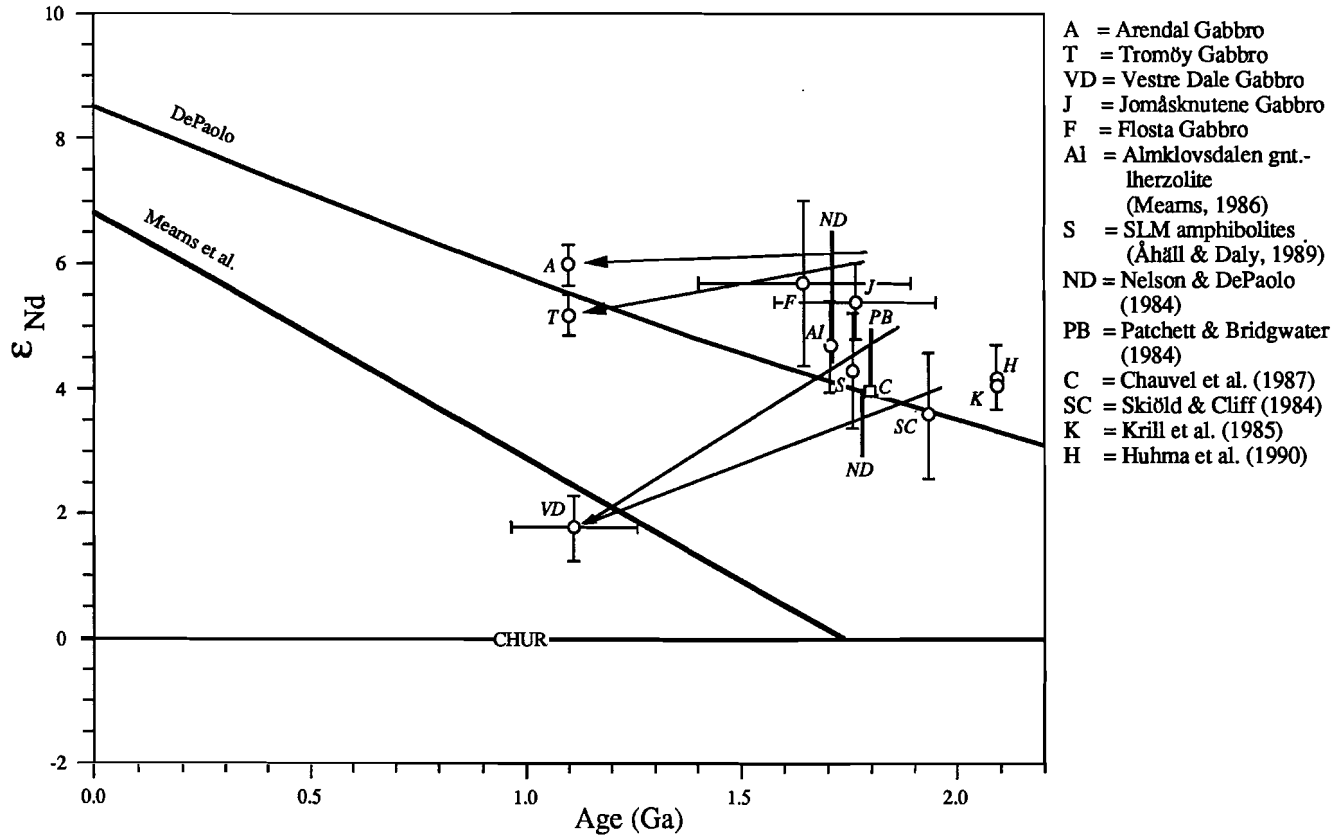


Figure 4.5 Sm-Nd evolution diagram, showing  $\epsilon_{Nd}$  versus age for the Bamble gabbros. Initial ratios of other Proterozoic basic rocks have been plotted for comparison. The initial ratios are, when possible, indicated with  $2\sigma$  error bars; horizontal bars indicate the error in the ages of the Vestre Dale Gabbro, the Jomåsknutene Gabbro and the Flosta Gabbro. Arrows indicate the suggested evolution of the mantle sources of the basic magmas.



Moreover, the Nd mantle signature would become less depleted further towards the south and west (Mearns, pers. com. 1990). Low initial  $\epsilon_{Nd}$  values have also been observed for the Ölme dolerite from Värmland ( $\epsilon_{Nd}(1.51 \text{ Ga}) = +1.7$ ), and dolerite dykes from the Protogine Zone ( $\epsilon_{Nd}(1.18 \text{ Ga}) = -2$  and  $\epsilon_{Nd}(0.93 \text{ Ga}) = 0$ ) in southern Sweden (Johansson and Johansson, 1990).

At first sight, the Nd isotope data are not unambiguous with regard to the evolution of Nd in the mantle below Bamble. Nd isotope data of the Jomåsknutene and Flosta Gabbros favour a depleted mantle reservoir with an  $\epsilon_{Nd}$  of about +5.5 at c. 1.7 Ga, similar to that of other Proterozoic mafic rocks. Regional support for such depleted mantle reservoir is also provided by Menuge (1985, 1988) who concluded that the Telemark Sector and Rogaland/Vest-Agder accreted from a depleted mantle source with an  $\epsilon_{Nd}(1.50 \text{ Ga})$  value of +5.5. The low initial  $\epsilon_{Nd}$  value of the Vestre Dale Gabbro, on the other hand, suggests a mantle evolution like that postulated by Mearns et al. (1986).  $T_{DM}$  model ages for the Vestre Dale Gabbro, calculated relative to the depleted mantle curve of DePaolo (1981), however, suggest separation of its source from a depleted mantle reservoir between 1.69 and 1.88 Ga (see also Fig. 4.5). Afterwards this source evolved with a  $^{147}\text{Sm}/^{144}\text{Nd}$  ratio lower than CHUR, resulting in a relatively low  $\epsilon_{Nd}(1.11 \text{ Ga})$ . The reason for this low  $\epsilon_{Nd}$  value of the Vestre Dale Gabbro on the one hand and the high  $\epsilon_{Nd}$  of the other gabbros on the other hand, will be discussed in detail in Chapter VI of this thesis together with trace element data.

#### 4.7 CONCLUSIONS

This study demonstrates that two periods of basic magmatism can be distinguished in the Bamble Sector, coeval with the Gothian and Sveconorwegian Orogenies. Early basic magmatism at c. 1.7 Ga ago can be correlated with basic magmatic activity in the Östfold-Marstrand Belt, whereas late basic magmatism at 1.1 Ga can be correlated with basic igneous activity in the Kongsberg and Telemark Sectors. The 1.11 Ga age of the Vestre Dale Gabbro is similar to ages of some Grenvillian gabbros. The initial  $\epsilon_{Nd}$  values of the Jomåsknutene and Flosta Gabbros reveal that the mantle below Bamble was depleted, with  $\epsilon_{Nd}(1.7 \text{ Ga})$  of about +5.5, which is in marked contrast with the Nd isotope evolution curve for the Southwest Scandinavian mantle, postulated by Mearns et al. (1986).

**Acknowledgements**

This chapter benefitted from critical comments and valuable suggestions by T.G. Nijland, J.L.R. Touret, J.B.H. Jansen, J.F. Menuge and R. Gorbatshev. Dr. E.W. Mearns and Dr. L. Johannson are thanked for their kindness to share their data. P. Remkes and J.C. van Belle are kindly thanked for their assistance in the laboratory. F. Benavente performed part of the isotope analyses.

## CHAPTER V

### RB-SR ISOTOPE SYSTEMATICS OF THE VESTRE DALE GABBRO AND ITS COUNTRY ROCKS.

#### 5.1 INTRODUCTION

The Mid-Proterozoic Bamble Sector forms part of the Southwest Scandinavian Domain (Gaál and Gorbatshev, 1987). It is separated from the Telemark Sector in the northwest by the Porsgrunn-Kristiansand Fault (PKF) (Fig. 2.1). In the northeast the Bamble Sector is covered by Cambro-Ordovician sediments from the Oslo Rift Region. The geology of the Bamble Sector has been influenced by two orogenic phases: the Gothian Orogeny between 1.75 and 1.5 Ga and the Sveconorwegian Orogeny (1.25 - 0.9 Ga). The Gothian Orogeny was accompanied by amphibolite-granulite facies metamorphism. The nature of the Sveconorwegian Orogeny is still controversial. Some authors (*e.g.* Field et al., 1985; Brickwood and Craig, 1987) have claimed that there has been no Sveconorwegian high-grade reworking in the Bamble Sector, but recent work (*e.g.* Kullerud and Dahlgren, 1990; Nijland and Senior, 1991; de Haas et al., 1992a; Chapter II of this thesis) has demonstrated that a high-grade event during the Sveconorwegian Orogeny is likely.

The Vestre Dale Gabbro (Fig. 2.1) is one of the many coronitic gabbros in the Bamble Sector (*e.g.* Brøgger, 1934a; Frodesen, 1968a; Starmer, 1969; Brickwood and Craig, 1987). Until recently, it was assumed that intrusion of the coronitic gabbros was restricted to the Sveconorwegian Orogeny. However, de Haas et al. (1992b; Chapter IV of this thesis), studied the whole-rock Sm-Nd systematics of several gabbros, and demonstrated that some of them intruded at the onset of the Gothian Orogeny, *e.g.* the Jomåsknutene Gabbro which has been dated at  $1.77 \pm 0.19$  Ga.

The Vestre Dale Gabbro, which was first described by Theulings et al. (1986), is a lens-shaped body with troctolitic and olivine gabbros in the core and olivine-free ferroic gabbro along the margins (Fig. 2.2) (de Haas et al., 1992a; Chapter II of this thesis). The gabbro has been emplaced in migmatites whose foliation generally wraps around the gabbro. Near the entrance of the Vestre Dale quarry, an agmatitic zone forms the contact: dark, angular to subrounded gabbroic blocks float in a leucocratic matrix (Fig. 2.3). The development of such agmatitic structures in combination with the absence of chilled margins and the absence of modally and grain-size graded layering, led de Haas et al. (1992a; Chapter II of this thesis) to propose that the Vestre Dale Gabbro was emplaced as a crystal mush. Sm-Nd whole-rock dating of the Vestre Dale

Gabbro yielded an age of  $1.11 \pm 0.14$  Ga with an  $\epsilon_{\text{Nd}}(T)$  of  $+1.8 \pm 0.5$ . (de Haas et al., 1992b; Chapter IV of this thesis). The country-rock gneisses and the leucocratic matrix have not yet been dated.

In this chapter whole rock Rb-Sr data of the Vestre Dale Gabbro, the leucocratic matrix and the migmatites are presented. The leucocratic matrix and migmatites were sampled near the entrance of the quarry, all within a distance of 4 metres from the contact. In addition, Rb-Sr and K-Ar analyses on biotites and muscovites from three migmatites and from one sample from the leucocratic matrix are presented.

## 5.2 PETROGRAPHY

The petrography of the Vestre Dale Gabbro has been described in Chapter II of this thesis. The migmatites mainly consist of perthitic K-feldspar, quartz and, in lesser amount, plagioclase and biotite. Muscovite orientated parallel to the main foliation of the biotite is interpreted as primary. Plagioclase has largely been replaced by sericite. Poikiloblastic muscovite has grown at the expense of K-feldspar. In most samples biotite has partly been altered to chlorite; locally rims of muscovite have been developed. Prehnite, epidote and calcite locally interleave the biotite (cf. Field and Rodwell, 1968). Zircon is present as small inclusions in the biotite. In the leucocratic matrix of the agmatite, plagioclase is much more abundant; K-feldspar, quartz and biotite only occur sporadically. Opaque minerals, apatite, zircon and zoned allanite are accessory phases. Alteration products include zoned chlorite, muscovite, rutile, and titanite. Interleaves of prehnite in the biotite are more abundant than in biotites from the migmatites and are often accompanied by clinozoisite. The samples have a granular texture.

## 5.3 RESULTS

The analyses were performed at the Isotope Geology Laboratory, Vrije Universiteit, Amsterdam. Whole rock Rb and Sr contents were measured by XRF spectrometry on pressed-powder pellets using a Philips PW 1450/AHP automatic spectrometer. Rb and Sr contents of the biotite and muscovite were measured by mass-spectrometric isotope dilution. The analytical procedures for Rb-Sr isotope analyses are described in Chapter II of this thesis. Whole rock and mineral Rb-Sr data are listed in Tables 5.1a-c and 5.2a-b. The age calculations are based upon  $\lambda^{87}\text{Rb} = 1.42 \cdot 10^{-11} \text{a}^{-1}$ . All calculated errors

are  $2\sigma$  and multiplied by  $\sqrt{\text{MSWD}}$  if  $\text{MSWD} > 1$ . Isochron line-fits were made using the method of York (1969).

The potassium contents of the biotite and muscovite were determined by flame photometry with a lithium internal standard and caesium chloride-aluminium nitrate buffer. Argon was extracted in a bakeable glass vacuum apparatus and analyzed by isotope dilution techniques in a Varian GD-150 mass-spectrometer; the measurements were made by the static method. The analytical accuracy is believed to be within 1% for potassium and 2% for radiogenic argon. The decay constants used for K-Ar age calculations are  $\lambda_\alpha = 0.581 \cdot 10^{-10} \text{a}^{-1}$  and  $\lambda_\beta = 4.962 \cdot 10^{-10} \text{a}^{-1}$ . K-Ar data of the biotites and muscovites are listed in **Tables 5.3a-b**.

Isochron calculations yielded the following results:

1) Seven samples of the **Vestre Dale Gabbro**, ranging in composition from olivine-rich gabbro to ferroic gabbro define an errorchron ( $\text{MSWD} = 10.1$ ) with an age of  $1.26 \pm 0.07$  Ga and an initial  $^{87}\text{Sr}/^{86}\text{Sr}$  ratio of  $0.70309 \pm 0.00008$  (**Fig. 5.1**).

2) Eight samples from the **leucocratic matrix** define an errorchron ( $\text{MSWD} = 29.3$ ) with an age of  $1.28 \pm 0.09$  Ga and an initial  $^{87}\text{Sr}/^{86}\text{Sr}$  ratio of  $0.70517 \pm 0.00104$  (**Fig. 5.2**).

3) Regression of eight **migmatites** yields an errorchron age of  $1.50 \pm 0.19$  Ga. The extremely high  $\text{MSWD}$  ( $= 151$ ) and the very low  $^{87}\text{Sr}/^{86}\text{Sr(I)}$  ratio of  $0.69336 \pm 0.01651$ , make the errorchron age meaningless.

4) **Biotites** from three migmatitic gneisses (**Fig. 5.3**) yield an isochron age of  $0.90 \pm 0.05$  Ga ( $\text{MSWD} = 0.0$ ). **Muscovites** from these samples are also isochronous (**Fig. 5.4**), and yield a slightly older age of  $0.95 \pm 0.03$  GA ( $\text{MSWD} = 0.5$ ). The slope of the line between a sample from the leucocratic matrix (86BAM 47) and its biotite corresponds to an age of  $0.88 \pm 0.01$  Ga (**Fig. 5.3**).

5) K-Ar ages of the **biotites** from the migmatites range between 0.85 and 0.90 Ga; **biotites** from leucocratic matrix sample 86BAM 47 yield a K-Ar age of 0.88 Ga (**Table 5.3a**). K-Ar ages of the **muscovites** from the migmatites range between 0.87 and 0.89 Ga (**Table 5.3b**).

**Table 5.1a** Whole rock Rb-Sr isotope analyses of the Vestre Dale Gabbro.

Sample	Rb (ppm)	Sr (ppm)	$^{87}\text{Rb}/^{86}\text{Sr}$	$^{87}\text{Sr}/^{86}\text{Sr}$
WT203/86BAM 63	3	233	0.0375	0.703712
WT209/86BAM 68	8	307	0.0743	0.704486
WT214/86BAM 71	6	217	0.0814	0.704584
WT216/86BAM 72	19	288	0.1905	0.706533
WT217/86BAM 73	6	194	0.0864	0.704599
WT220/86BAM 76	4	324	0.0383	0.703829
WT225/86BAM 79	6	214	0.0839	0.704628

**Table 5.1b** Whole rock Rb-Sr isotope analyses of the leucocratic matrix.

Sample	Rb (ppm)	Sr (ppm)	$^{87}\text{Rb}/^{86}\text{Sr}$	$^{87}\text{Sr}/^{86}\text{Sr}$
86BAM 45	93	271	0.9983	0.723224
86BAM 46	64	332	0.5551	0.715616
86BAM 47	89	286	0.9027	0.720858
86BAM 48	75	288	0.7601	0.719135
86BAM 49	73	328	0.6417	0.716939
86BAM 50	105	251	1.212	0.727505
86BAM 51	88	245	1.042	0.724607
86BAM 52	111	234	1.374	0.731002

**Table 5.1c** Whole rock Rb-Sr isotope analyses of the migmatites.

Sample	Rb (ppm)	Sr (ppm)	$^{87}\text{Rb}/^{86}\text{Sr}$	$^{87}\text{Sr}/^{86}\text{Sr}$
86BAM 37	245	110	6.549	0.833087
86BAM 38	209	99	6.192	0.823878
86BAM 39	162	103	4.593	0.795181
86BAM 40	127	96	3.854	0.776940
86BAM 41	258	116	6.522	0.835809
86BAM 42	210	53	11.71	0.956105
86BAM 43	166	47	10.10	0.922610
86BAM 44	300	88	9.972	0.880593

**Table 5.2a** Rb-Sr isotope analyses of three biotites from the migmatites and one from the leucocratic matrix (sample 86BAM 47).

Sample	Rb (ppm)	Sr (ppm)	$^{87}\text{Rb}/^{86}\text{Sr}$	$^{87}\text{Sr}/^{86}\text{Sr}$
86BAM 37	728	7.4	438.43	6.2443
86BAM 40	630	5.7	527.93	7.4025
86BAM 42	773	4.0	1849.75	24.3976
86BAM 47	514	10	177.58	2.9539

**Table 5.2b** Rb-Sr isotope analyses of muscovites from the migmatites.

Sample	Rb (ppm)	Sr (ppm)	$^{87}\text{Rb}/^{86}\text{Sr}$	$^{87}\text{Sr}/^{86}\text{Sr}$
86BAM 37	433	6.8	241.68	3.9554
86BAM 40	316	19	50.33	1.4022
86BAM 42	414	5.3	325.56	5.1675

**Table 5.3a** K-Ar data and ages of three biotites from the migmatites and one from the leucocratic matrix (sample 86BAM 47).

Sample	K (wt.%)	Radiogenic $^{40}\text{Ar}$ (ppm wt.)	Calculated age (Ga)
86BAM 37	7.74	0.0349	0.90
86BAM 40	7.33	0.0326	0.85
86BAM 42	8.05	0.0357	0.89
86BAM 47	7.17	0.0317	0.88

**Table 5.3b** K-Ar data and ages of muscovites from the migmatites.

Sample	K (wt.%)	Radiogenic $^{40}\text{Ar}$ (ppm wt.)	Calculated age (Ga)
86BAM 37	9.00	0.0405	0.89
86BAM 40	8.73	0.0392	0.89
86BAM 42	8.99	0.0389	0.87

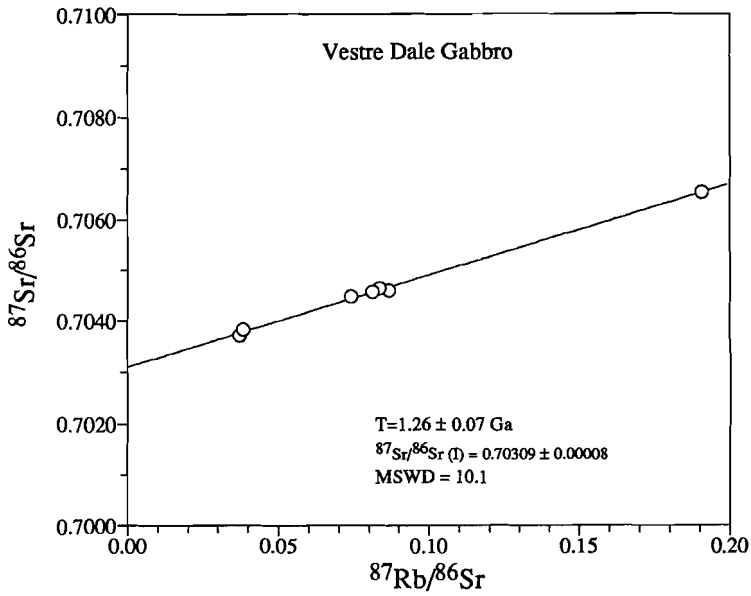


Figure 5.1 Rb-Sr errorchron of the Vestre Dale Gabbro.

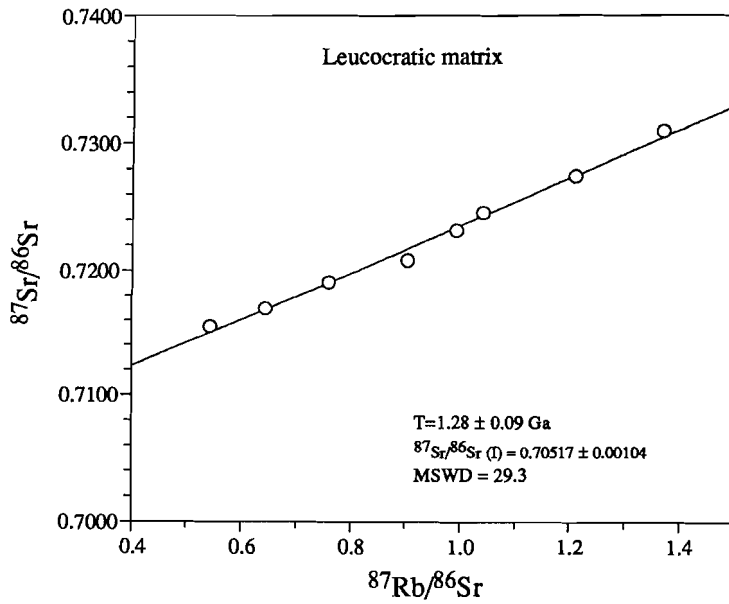


Figure 5.2 Rb-Sr errorchron of the leucocratic matrix.



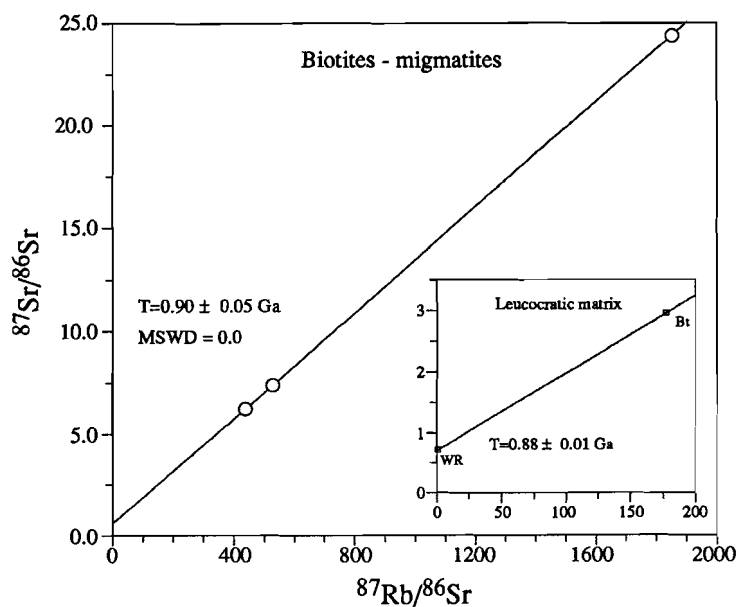


Figure 5.3 Rb-Sr isochron diagram of biotites from three migmatitic gneiss samples. Inset shows a whole rock - biotite isochron diagram of leucocratic matrix sample 86BAM 47.

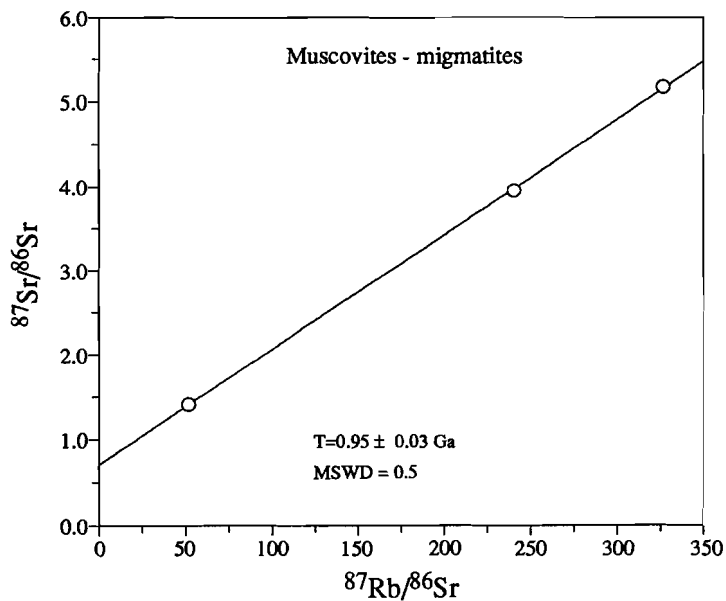


Figure 5.4 Rb-Sr isochron diagram of muscovites from the same samples as in Figure 5.3.

## 5.4 DISCUSSION AND CONCLUSIONS

The errorchron age of  $1.26 \pm 0.07$  Ga of the Vestre Dale Gabbro corresponds, within the error limits, with the Sm-Nd whole-rock age of  $1.11 \pm 0.14$  Ga (de Haas et al., 1992b; Chapter IV of this thesis). The errorchron age of the leucocratic matrix is also comparable to the age of the gabbro. The errorchron age of the gabbro also compares reasonably well to whole rock ages of coronitic gabbros from the Kongsberg Sector, which are supposed to be contemporaneous with the coronitic gabbros from Bamble (Starmer, 1985a, 1991). Jacobsen and Heier (1978) obtained a Rb-Sr whole-rock isochron age for the Vinoren Gabbro of  $1.18 \pm 0.05$  Ga with an  $^{87}\text{Sr}/^{86}\text{Sr}(I) = 0.7024 \pm 0.0001$ . Munz and Morvik (1991) reported an internal Sm-Nd isochron age of  $1.22 \pm 0.02$  Ga for a sample from the Morud Gabbro, Modum Complex. The fair agreement between the Sm-Nd whole-rock age of the Vestre Dale Gabbro and its Rb-Sr errorchron age may be taken as evidence of the absence of any serious influence of the main phase of the Sveconorwegian Orogeny (1.1 - 0.9 Ga) on the Rb-Sr system, at least on hand-specimen scale. Munz and Morvik (1991) demonstrated that the Sveconorwegian Orogeny reset the Rb-Sr system of the Morud Gabbro on a mineral scale. A Rb-Sr whole-rock-plagioclase-clinopyroxene isochron yielded an age of  $0.87 \pm 0.02$  Ga.

The emplacement of the Vestre Dale Gabbro at 1.11 Ga will inevitably have affected the Rb-Sr isotope system of the migmatites near the gabbro. The errorchron age of the migmatites is meaningless, regarding the extremely high MSWD and very low initial  $^{87}\text{Sr}/^{86}\text{Sr}$  ratio (though with a large error). Complete re-equilibration of the Rb-Sr isotopic system in the migmatitic gneisses at 1.11 Ga, would have resulted in a horizontal line in the  $^{87}\text{Rb}/^{86}\text{Sr}$  vs.  $^{87}\text{Sr}/^{86}\text{Sr}$  diagram at  $T = 1.11 \pm 0.14$  Ga. From **Figure 5.5** it appears that samples 86BAM 37, 38, 39, 40, 41 and 44 enclose a rather narrow range of  $^{87}\text{Sr}/^{86}\text{Sr}$  at  $T = 1.11 \pm 0.14$  Ga, but that complete re-equilibration was not attained. With these samples, an errorchron (MSWD = 103) can be constructed, which yields a lower age,  $1.31 \pm 0.19$  Ga, and an initial  $^{87}\text{Sr}/^{86}\text{Sr}$  ratio of  $0.7070 \pm 0.0152$ . Samples 86BAM 42 and 43 show no sign of equilibration with these samples. Possibly, they were taken outside the range of homogenization.

The Rb-Sr ages of the biotites and the muscovites and their K-Ar ages, which are generally lower, are all substantially lower than the whole rock ages. These mineral ages are related to Sveconorwegian cooling. The K-Ar ages are lower than the K-Ar ages of micas, reported by O'Nions et al. (1969). Most of their biotite K-Ar ages range between 0.93 and 1.06 Ga. It should however be realized that the data of

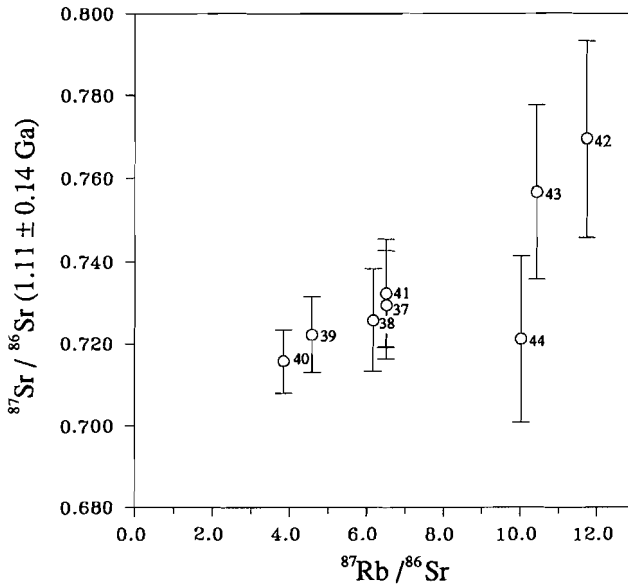


Figure 5.5  $^{87}\text{Rb}/^{86}\text{Sr}$  versus  $^{87}\text{Sr}/^{86}\text{Sr}$  diagram for eight migmatites at  $T = 1.11 \pm 0.14$  Ga.

O'Nions et al. (1969) refer to the northeastern part of the Bamble Sector. Our K-Ar ages fit better with K-Ar biotite ages from the Arendal-Flaten area (Kulp and Neumann 1961; recalculated with present-day used decay constants), and with biotites from Rogaland (Verschure et al., 1980). These observations are in accordance with the idea of westward younging in the Sveconorwegian province (e.g. Gaál and Gorbatshev, 1987; Falkum, 1990).

### Acknowledgements

P.J. Valbracht, T.G. Nijland, D. Visser, J.L.R. Touret and R.D. Schuling are thanked for their critical comments which improved an earlier version of this chapter.

## CHAPTER VI

### IDENTIFICATION OF THE SOURCE AND PETROGENESIS OF THE CORONITIC GABBROS FROM THE ARENDAL-NELAUG AREA.

#### 6.1 INTRODUCTION

Despite the many studies on the Bamble coronitic gabbros (*e.g.* Brøgger, 1934a; Frodesen, 1968a,b, 1973; Starmer, 1969, Brickwood and Craig, 1987), hardly any attention has been paid to their source and petrogenesis. Attention in these studies was mainly focused on the description and the origin of the coronitic microstructures (Frodesen, 1968a; Starmer, 1969; Joesten, 1986) and the mineral chemistry of the hyperites (Brickwood and Craig, 1987). Frodesen (1973) was the first to present trace element data (excluding the REE) of a coronitic gabbro. This study concentrated on the behaviour of the trace elements during magmatic differentiation, regional metamorphism and scapolitization. Later studies by Elliott (1973) and Field and Elliott (1974) focused on the chemistry of gabbro/amphibolite transitions. It was not until recently that more chemical, and in addition isotopic, data for the Bamble hyperites became available (de Haas et al. 1992a,b; Chapters II and IV of this thesis). In de Haas et al. (1992a; Chapter II of this thesis) the tholeiitic signature of one of the hyperites, the Vestre Dale Gabbro, was confirmed. Furthermore it was demonstrated that this gabbro had not crystallized from a primary mantle-derived magma, but from a magma which had already been subjected to some degree of fractionation. From the Sm-Nd isotope study on five coronitic gabbros it was concluded that the gabbros had been derived from a depleted mantle reservoir, but the range in initial  $^{148}\text{Nd}/^{144}\text{Nd}$  ratios indicated that this depleted mantle reservoir was, at least isotopically, heterogeneous. The Gothian Jomåsknutene ( $1.77 \pm 0.19$  Ga) and Flosta ( $1.64 \pm 0.23$  Ga) Gabbros have highly positive  $\epsilon_{\text{Nd}}(\text{T})$  values,  $+5.4 \pm 0.6$  and  $+5.7 \pm 1.3$  respectively, like the Sveconorwegian Arendal,  $\epsilon_{\text{Nd}}(1.1 \text{ Ga}) = +5.9 \pm 0.3$ , and Tromøy,  $\epsilon_{\text{Nd}}(1.1) = +5.3 \pm 0.3$  Ga, Gabbros. The 1.11 Ga Vestre Dale Gabbro, on the other hand, has a much lower initial  $\epsilon_{\text{Nd}}(\text{T})$  value:  $+1.8 \pm 0.5$  (de Haas et al., 1992b; Chapter IV of this thesis).

In this chapter, further constraints are placed on the composition of the Proterozoic mantle below Bamble and on the petrogenesis of the gabbros. Special attention will be paid to incompatible trace elements, and especially ratios of these elements, since these provide the best fingerprint of the source of a magma. In addition, the trace element chemistry may yield information about the prevailing tectonic regime during which the gabbros were emplaced. The trace element chemistry of the gabbros,

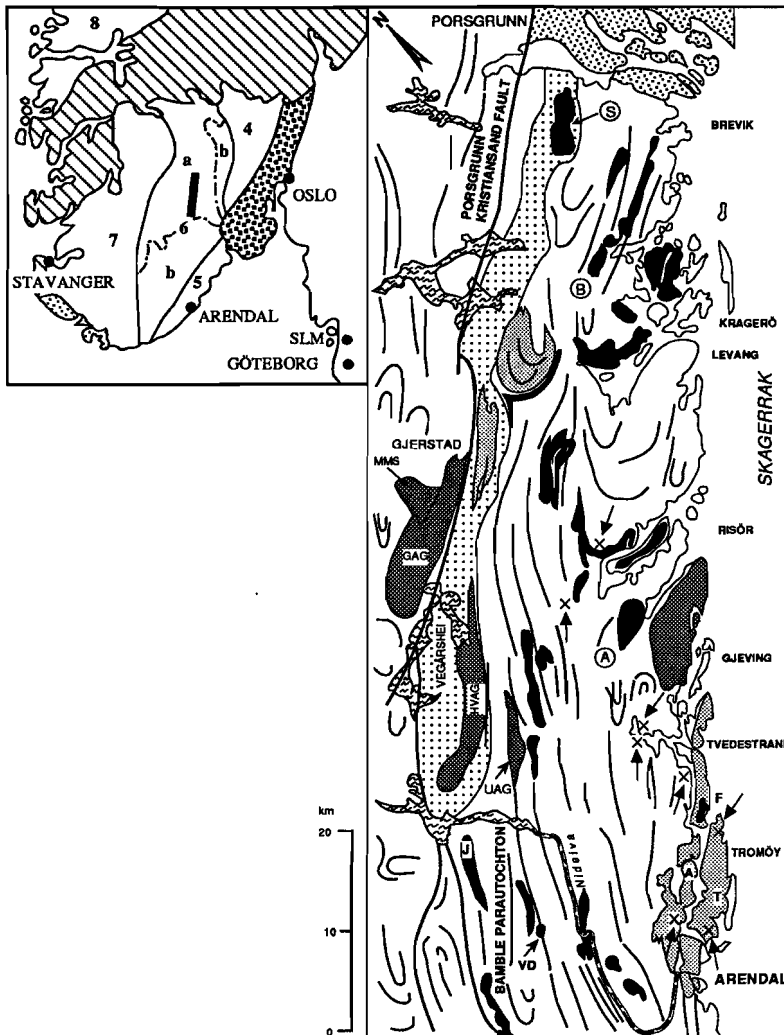


**Figure 6.1** Map of the Bamble Sector and SWSD with the location of the various basic rocks, used in this study. S: Skogen; B: Bjordam; A: Averid. Crosses mark the location of the metabasites of Smalley et al. (1983b). Black area in the Telemark Sector indicates the sample area of the Telemark supracrustals of Atkin and Brewer (1990). See **Figure 1.1** for legend.

and that of their source(s), will be compared to the trace element chemistry of basic rocks from other parts of the SWSD, like the Arendal metabasites (Smalley et al., 1983b), the volcanics from the Telemark Supracrustal Suite (Atkin and Brewer, 1990), the Rogaland anorthositic suite (e.g. Duchesne et al., 1985a) and the Stora Le-Marstrand amphibolites (Åhäll and Daly, 1989) (**Fig. 6.1**).

## **6.2 PETROGRAPHY**

The samples for this study are from the Vestre Dale, Jomåsknutene, Flosta, Arendal and Tromøy Gabbros, of which the petrology has been described Chapters II, III and IV of this thesis, and the Åmdal Gabbro (co-ordinates: 32VMK 4765-64985; Nelaug-sheet 1612 III, 1:50.000; Norges geografiske oppmåling 1967). This Mg-rich gabbro has intruded the core of the Jomåsknutene Gabbro, near Åmdal. Intercumulus spaces between the olivine-orthopyroxene cumulates are in this gabbro filled by a pargasitic amphibole. The green hercynitic spinel has a metamorphic origin. Spinel clusters appear to define a ghost-texture of plagioclase. No relics of plagioclase have been observed. Isotope data for the Åmdal Gabbro have not been obtained yet.

## **6.3 CHEMICAL CORRELATIONS BETWEEN THE GABBROS**

Before trying to identify the source of the gabbros, it is important to know to what extent the individual gabbros are compositionally related to each other. Therefore the chemical variations among the gabbros will be considered from Harker diagrams, REE patterns and other incompatible trace element plots. Variations will be compared with variations in the Vestre Dale Gabbro at first, since the geochemical evolution of this gabbro has been well established. Whole rock data of 27 selected samples are listed in **Appendix 1**. Trace element ratios of these samples are presented in **Table 6.1**. Whole rock analyses (and trace element ratios) of samples, of which no REE data have been obtained, are listed in **Appendix 2**.

### **6.3.1 Harker diagrams**

Harker diagrams for  $\text{TiO}_2$ ,  $\text{P}_2\text{O}_5$ , Zr and Ni versus the Mg# as differentiation index are presented in **Figure 6.2**. Samples of the Åmdal Gabbro, which shows hardly any differentiation, always plot close to the troctolitic and the olivine-rich gabbros of the Vestre Dale Gabbro. The Tromøy, the Jomåsknutene and Flosta Gabbros are clearly more evolved and compare better to the olivine-poor and ferroic gabbros of the Vestre Dale Gabbro in terms of Mg# (de Haas et al., 1992a; Chapter II of this thesis); the Arendal Gabbro and the most evolved samples of the Jomåsknutene and Flosta Gabbros have Mg# lower than 45.

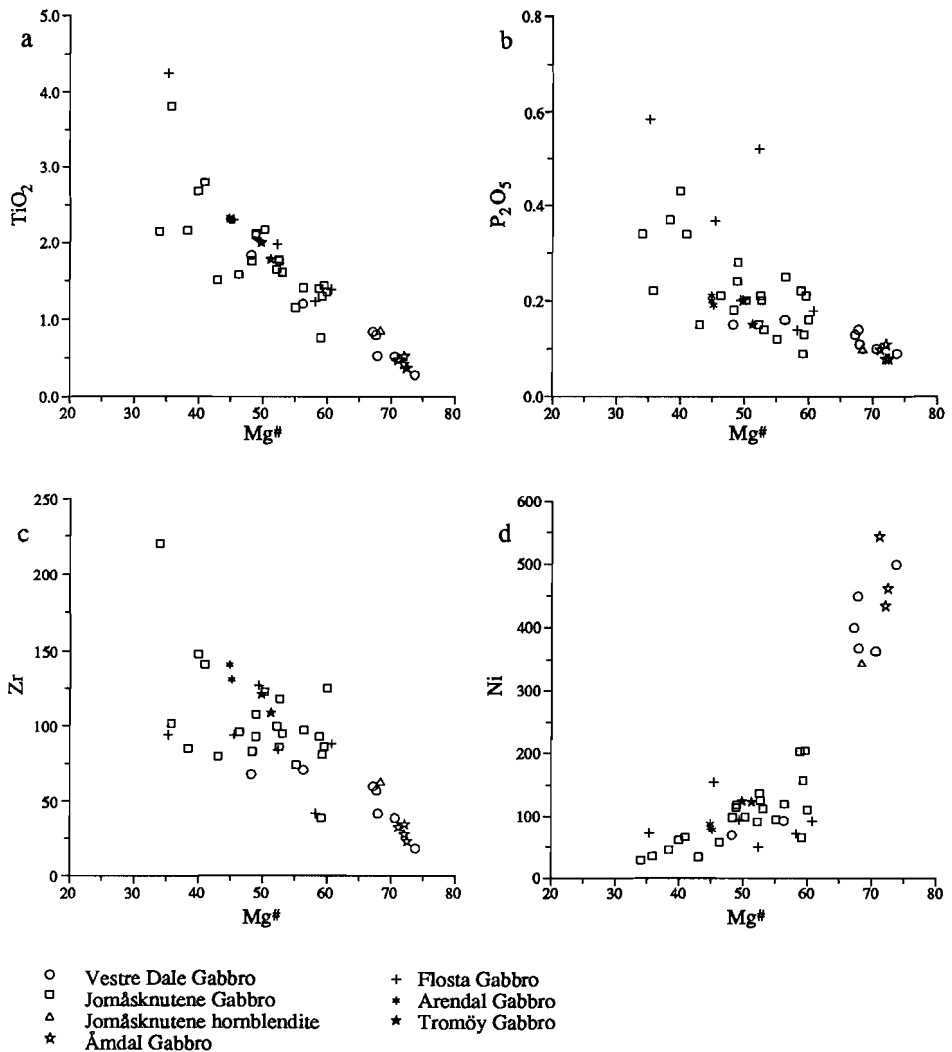


**Figure 6.2** Whole rock variation diagrams with Mg# as differentiation index. TiO<sub>2</sub> and P<sub>2</sub>O<sub>5</sub> in wt.%; Zr and Ni in ppm.

TiO<sub>2</sub>, Zr and P<sub>2</sub>O<sub>5</sub> trends of the Jomåsknutene and the Flosta Gabbros are in a broad sense similar to the trends shown by the Vestre Dale Gabbro for these elements (Fig. 6.2a-c). The TiO<sub>2</sub> enrichment trend, defined by most samples of these two gabbros and by the Arendal and Tromøy Gabbros, is a continuation of the trend displayed by the Vestre Dale Gabbro. GA146 (Jomåsknutene Gabbro) and GA254 (Flosta Gabbro) contain cumulus ilmenite and plot therefore above the trend. A similar enrichment is,

despite the larger variation, observed for  $P_2O_5$  and Zr. The Åmdal, Jomåsknutene, Arendal and Tromøy Gabbros define a fractionation trend for Ni compatible with the Ni trend of the Vestre Dale Gabbro (Fig. 6.2d). The Flosta samples plot slightly off this trend. The good fit between the trends of Ni and  $TiO_2$ , and to a lesser degree of  $P_2O_5$  and Zr, suggests a close genetic relationship between the parental magmas of the individual intrusions.

### 6.3.2 REE patterns

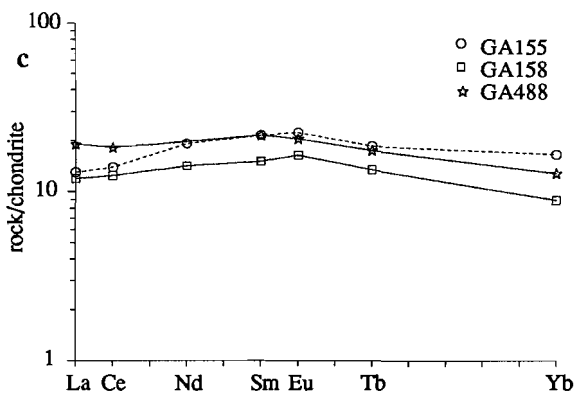
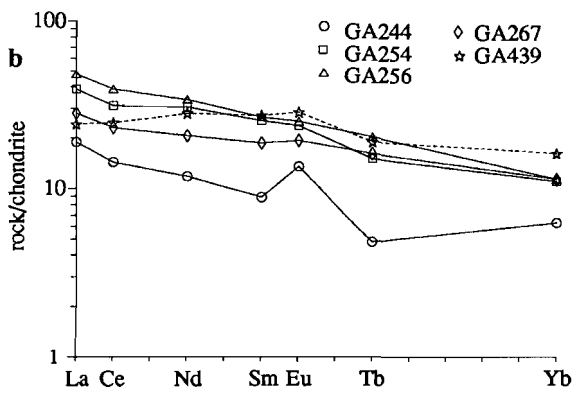
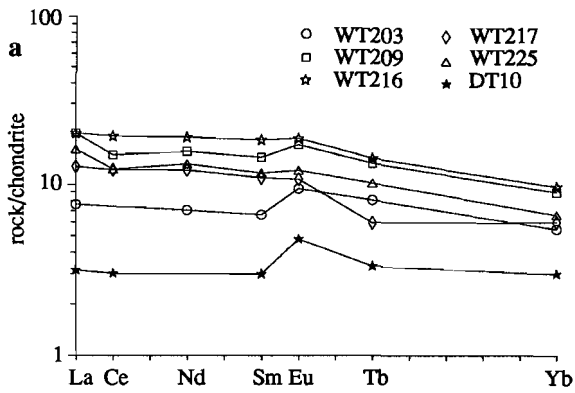
A distinction can be made between LREE enriched and LREE depleted gabbros (Fig. 6.3a-g). The Vestre Dale and Flosta Gabbros are LREE enriched; the Arendal, Tromøy and Åmdal Gabbros and the gabbroic dyke near the Flosta Gabbro (sample GA439) are LREE depleted. The Jomåsknutene Gabbro comprises both LREE enriched and LREE depleted samples.

The REE patterns of the Vestre Dale Gabbro are rather flat (Fig. 6.3a) with  $(La/Yb)_N$  ratios between 1.05 (DT10) to 2.42 (WT225). The vertical spreading of the patterns is the result of magmatic differentiation (de Haas et al., 1992a; Chapter II of this thesis).  $(La/Sm)_N$  ratios range from 1.06 to 1.38. The Flosta Gabbro has more fractionated patterns than the Vestre Dale Gabbro (Fig. 6.3b); in fact, the Flosta Gabbro has the most fractionated patterns of all studied intrusions with  $(La/Yb)_N$  ratios between 2.47 and 4.22.  $(La/Sm)_N$  ratios range between 1.51 and 2.13. As is the case with the Vestre Dale Gabbro, a correlation exists between the degree of fractionation, expressed by the Mg#, and the REE abundances. GA244 is the only sample with a positive Eu anomaly.

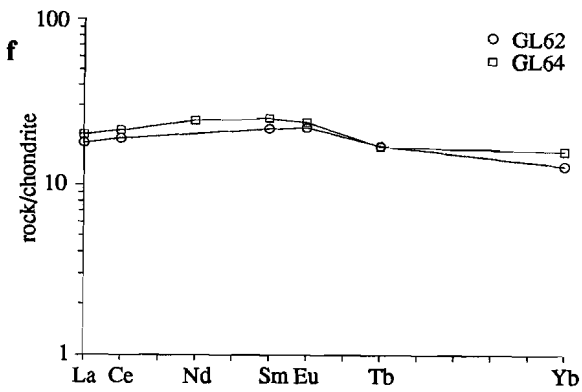
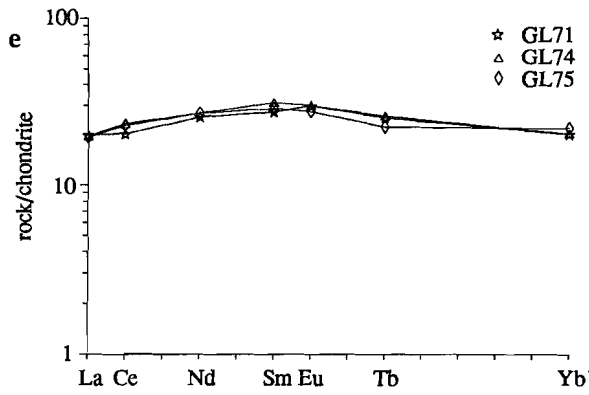
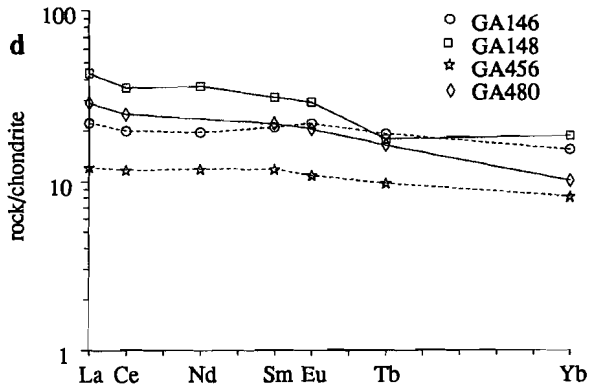
$(La/Sm)_N$  ratios of the LREE enriched samples of the Jomåsknutene Gabbro (Fig. 6.3c) are similar to  $(La/Sm)_N$  ratios of the Vestre Dale Gabbro. GA456 and GA480 have more fractionated patterns than GA146 and hornblendite GA148. GA146 is the only sample with a, small, positive Eu anomaly.

The Tromøy and Arendal Gabbros (Fig. 6.3e-f), the LREE depleted samples of the Jomåsknutene Gabbro (Fig. 6.3d) and the gabbroic dyke near the Flosta Gabbro (Fig. 6.3b), have inverted V-shaped patterns with  $(La/Sm)_N$  ratios between 0.60 and 0.89. They show modest LREE fractionation relative to the HREE with  $(La/Yb)_N$  ratios of 1.00 and 1.50, except for GA155 of the Jomåsknutene Gabbro which has a  $(La/Yb)_N$  ratio of 0.79. Eu anomalies are absent.





*Identification of the source and petrogenesis*



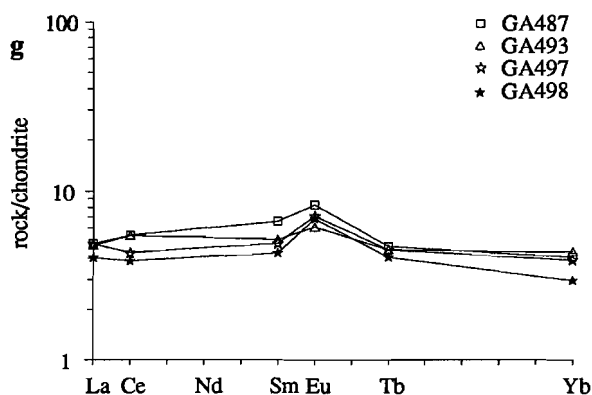


**Figure 6.3** Chondrite-normalized REE patterns: a) the Vestre Dale Gabbro; b) Flostå Gabbro; c) LREE enriched samples of the Jomåsknutene Gabbro; d) LREE depleted samples of the Jomåsknutene Gabbro; e) Tromøy Gabbro; f) Arendal Gabbro; g) Åmdal Gabbro. Normalization after Haskin et al. (1968).

The **Åmdal Gabbro** has, like the troctolitic and olivine-rich gabbros of the Vestre Dale Gabbro, low REE contents (**Fig. 6.3g**). They display, in contrast to most other gabbros, pronounced positive Eu anomalies. These anomalies provide additional evidence for the former presence of plagioclase in these rocks. The Åmdal Gabbro is characterized by rather flat patterns with  $(La/Yb)_N$  ratios between 1.09 and 1.24;  $(La/Sm)_N$  ratios fall in the range between 0.74 and 0.99.

$(Tb/Yb)_N$  ratios of most gabbros (**Table 6.1**) are rather low, i.e. close to 1. This indicates that the generation of the magmas was not accompanied with significant HREE fractionation. This suggests that the parental magmas were generated in the spinel stability field rather than in the garnet stability field (cf. Weaver and Tarney, 1981).

### 6.3.3 Incompatible trace element plots

More information regarding the compositional relations between the gabbros is provided by incompatible trace element plots with Zr on the x-axis (**Fig. 4a-e**). Like the REE, these elements are, in principle, hardly involved in the crystallization of basic magmas. Their absolute concentrations in the magma will increase during crystallization but the ratios between these elements remain constant. Nonetheless one should handle these ratios with care, especially in the case of the more differentiated samples.

*Identification of the source and petrogenesis*

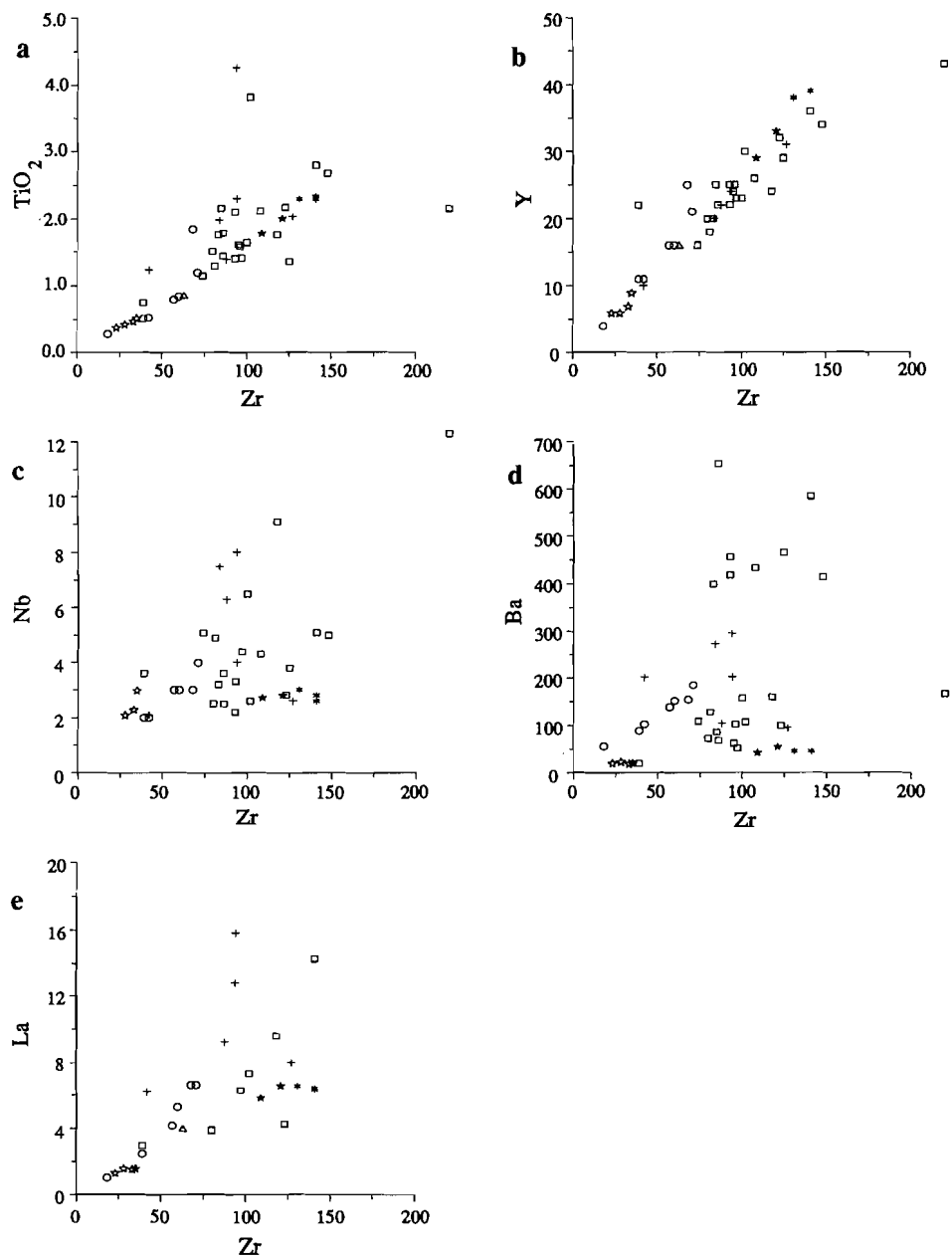


**Figure 6.4a-e** Incompatible trace element plots with Zr on the x-axis. TiO<sub>2</sub> in wt.%; Zr, Y, Nb, Ba and La in ppm. Symbols as in Fig. 6.2.

Continued enrichment of an incompatible element, like Zr or  $\text{TiO}_2$ , may finally result in oversaturation, followed by cumulus crystallization of ilmenite or zircon, so that these elements do not reflect the proportions of the magma anymore. This is well demonstrated in the Zr-TiO<sub>2</sub> plot (Fig. 6.4a). Ti/Zr ratios are rather uniform, averaging at 95, but samples of the Vestre Dale, Jomåsknutene, and Flosta Gabbros with more than 1.7 wt.%  $\text{TiO}_2$  have clearly higher Ti/Zr ratios.

Zr/Y ratios for most gabbros fall in the range between 3.4 and 4.4 (Fig. 6.4b; Table 6.1 and Appendix 2). Zr/Nb and Ba/Zr ratios (Fig. 6.4b; Table 6.1 and Appendix 2) are highly variable and appear to vary with the degree of LREE enrichment. Zr/Nb and Ba/Zr ratios of the LREE enriched Vestre Dale, Flosta and Jomåsknutene Gabbros range between 12 and 28 and between 1.1 and 4.8 respectively (Table 6.1 and Appendix 2). Zr/Nb and Ba/Zr ratios of the LREE depleted gabbros are higher (44 - 54) and lower (0.3 - 0.9) respectively. Zr/Nb ratios of the depleted Åmdal Gabbro, 12 - 14, however, better compare to the Zr/Nb ratios of the LREE enriched gabbros. Eight samples of the Jomåsknutene Gabbro, amongst which the LREE enriched sample GA456, have much higher Ba concentrations (between 414 and 654 ppm) than other samples of this, and the other gabbros, with similar Zr contents (Fig. 6.4d). Consequently, their Ba/Zr ratios are much higher, between 2.8 and 7.6 (see also Appendix 2). The Zr-La plot (Fig. 6.4e) shows less variation, although a distinction can be made between LREE enriched gabbros (Zr/La ratios between 5.9 and 15.6) and LREE depleted gabbros (Zr/La ratios between 15.9 and 28.7; Table 6.1).

The LREE enrichment is also accompanied by a decrease of the K/Ba ratios: K/Ba ratios for LREE depleted gabbros range between 45 and 60, whereas most LREE enriched gabbros have K/Ba ratios between 22 and 28 (Table 6.2). K/Rb ratios, on the other hand, remain remarkably constant: the Vestre Dale Gabbro has a mean K/Rb ratio of 444, whereas K/Rb ratios for the Arendal and the Tromøy Gabbros are 439 and 495 respectively.

**Table 6.1** Trace element ratios of the 27 selected samples (ratios of the other samples are listed in Appendix 2)

Sample	Ti/Zr	Zr/Y	Zr/Nb	Zr/La	Ba/Zr	(La/Sm) <sub>N</sub>	(La/Yb) <sub>N</sub>	(Tb/Yb) <sub>N</sub>
WT203 (V)	80	3.6	19.5	15.5	2.3	1.15	1.39	1.47
WT209 (V)	101	3.4	17.8	10.7	2.6	1.39	2.22	1.47
WT216 (V)	162	2.7	22.7	10.2	2.3	1.10	2.07	1.46
WT217 (V)	84	3.6	19.0	13.6	2.4	1.17	2.10	0.98
WT225 (V)	84	3.8	20.0	11.3	2.5	1.38	2.42	1.53
DT10 (V)	93	4.5	-	-	3.1	1.06	1.05	1.11
GA146 (J)	225	3.4	39.2	13.9	1.1	1.06	1.44	1.24
GA148 (J)	82	3.9	-	15.6	-	1.03	1.51	1.20
GA155 (J)	106	3.8	43.9	28.7	0.8	0.60	0.79	1.13
GA158 (J)	113	4.0	32.0	20.4	0.9	0.79	1.34	1.51
GA456 (J)	119	3.9	27.7	9.9	4.1	1.39	2.33	0.96
GA480 (J)	89	4.9	13.0	12.3	1.4	1.33	2.88	1.62
GA488 (J)	87	4.2	22.1	15.4	0.6	0.88	1.50	1.37
GA487 (Å)	91	3.9	11.7	21.7	0.6	0.74	1.20	1.16
GA493 (Å)	87	4.7	14.4	21.0	0.6	0.92	1.09	1.03
GA497 (Å)	92	4.7	13.3	17.5	0.9	0.99	1.24	1.15
GA498 (Å)	99	3.8	-	17.3	0.9	0.94	1.37	1.37
GA244 (F)	176	4.2	20.0	6.7	4.8	2.13	3.00	0.76
GA254 (F)	271	3.9	11.8	7.3	2.1	1.54	3.53	1.36
GA256 (F)	147	3.9	23.5	5.9	3.1	1.80	4.22	1.78
GA267 (F)	94	4.0	14.0	9.5	1.2	1.51	2.47	1.42
GA439 (F)	96	4.1	48.9	15.9	0.7	0.89	1.50	1.17
GL62 (T)	98	3.8	40.4	18.6	0.4	0.83	1.38	1.31
GL64 (T)	99	3.7	43.2	18.4	0.5	0.80	1.26	1.06
GL71 (A)	105	3.5	43.7	20.0	0.3	0.73	1.00	1.26
GL74 (A)	99	3.6	54.2	21.9	0.3	0.63	0.98	1.29
GL75 (A)	98	3.6	50.4	22.2	0.3	0.67	0.89	1.02

## 6.4 PETROGENESIS

### 6.4.1 Parental magma composition

The fractionation trends indicate that all studied gabbros have a tholeiitic signature. Fractionation trends indicate that at least part of the chemical variation, observed within as well as between the different intrusions, may be ascribed to fractionation processes: samples with a high Mg# have lower Zr, TiO<sub>2</sub>, P<sub>2</sub>O<sub>5</sub>, and REE and higher Ni contents than the more evolved samples. The fractionation trends and the similar Ti/Zr and Zr/Y ratios suggest a close genetical relationship between the gabbros. The variable Zr/Nb, Ba/Zr and Zr/La ratios and the range in (La/Sm)<sub>N</sub> ratios, however, demonstrate that compositional differences between the parental magmas did exist.

The absence of parental magma compositions hampers attempts to model the petrogenesis of the gabbros. Nevertheless, several constraints can be placed on their origin. Forsterite contents of olivine from the troctolitic gabbros of the Vestre Dale Gabbro ( $Fo_{74}$ ) and from the Åmdal Gabbro ( $Fo_{69-60}$ ) are too low to have been in equilibrium with primary, mantle-derived, melt, i.e. melts whose composition has been unmodified by differentiation processes after segregation from their mantle source (see also Chapter II of this thesis). Other gabbros are more evolved, so it is unlikely that they crystallized from primary, mantle-derived melts either. Forsterite contents of olivine in ultrabasic bodies related to other gabbros in the Nelaug-Arendal area do not exceed  $Fo_{78}$  (Krijgsman, 1991).

Table 6.2 K/Rb and K/Ba ratios of the gabbros.

Gabbro	K/Rb	K/Ba
Vestre Dale	444 ± 82	22 ± 7
Flosta	518 ± 176	28 ± 9
Jomåsknutene <sup>1</sup>	360 ± 76	27 ± 7
Jomåsknutene <sup>2</sup>	-	45 ± 14
Åmdal	-	60 ± 5
Tromøy	495	47
Arendal	439	53

<sup>1</sup> LREE enriched samples

<sup>2</sup> LREE depleted samples

Another direct manifestation of mantle-related magmatism may be a basic dyke with a lateral extension of 500 meters, near Solheimsvann, 5.5 km east of the Vestre Dale Gabbro (Theulings, 1988). Although much of the dyke has been amphibolitized, an original magmatic assemblage of olivine, clinopyroxene and spinel is still recognizable. Spinel, which often occurs as inclusions in olivine, has more than 5 wt.%  $Cr_2O_3$ . But as in other ultramafic bodies, olivine is relatively Mg-poor:  $Fo_{75}$  (Krijgsman, 1991).

The absence of more Mg-rich olivines could mean that either the melting conditions were such that the mantle was not able to generate more Mg-rich melts or that the parental magmas had already fractionated a certain amount of olivine elsewhere. Indeed, Klopprogge (1987) reported the occurrence of a dunite body at Nelaugtjern, one kilometre west of the Jomåsknutene Gabbro (Table 6.3). The mantle-like composition of the olivine in this dunite,  $Fo_{88}$ , suggests fractionation of a primary, mantle-derived melt, in a crustal magma chamber. However, this concerns only a single, and small (10 m<sup>2</sup>), occurrence within tonalitic to granodioritic gneisses; no other

occurrences of dunite-like bodies have been reported from the Nelaug-Arendal area so far.

**Table 6.3** Major element chemistry of the olivine and the dunite body from Nelaugtjern (data from Krijgsman, 1991).

	Whole rock	Olivine
SiO <sub>2</sub>	42.57	40.31
TiO <sub>2</sub>	0.03	-
Al <sub>2</sub> O <sub>3</sub>	1.63	-
FeO	8.23	12.03
MnO	0.09	0.11
MgO	41.39	47.02
NiO	-	0.20
CaO	2.10	0.00
Na <sub>2</sub> O	0.05	-
K <sub>2</sub> O	0.00	-
P <sub>2</sub> O <sub>5</sub>	0.00	-
LOI	9.91	-

If a primary melt was involved in the genesis of the gabbros, olivine fractionation may also have occurred before emplacement in the crust. The high density of such a primary melt, which is likely to be picritic (Cox, 1980), relative to the density of lower continental crust, inhibits its rising into the continental crust. Fractionation of olivine, which lowers the density of the picritic melt, enables its transmission into the crust (Cox, 1980). Geophysical evidence for a mafic lowermost crust below the Bamble Sector has been obscured by Oslo Rift magmatism (cf. Ramberg et al., 1977).

Assuming that the gabbros crystallized from a magma which had already fractionated olivine, regardless where, then the shape of REE pattern of this parental magma should resemble that of the primary magma, since partition coefficients of olivine for the REE are low, i.e. lower than 0.01 (e.g. McKay, 1989). The REE pattern of the parental magma of the Vestre Dale Gabbro can be estimated, using a simple mass balance equation of the form:

$$PM_{REE} * (\text{bulk } K_D * M_{cum} + M_{TL}) = cum_{REE}$$

where  $PM_{REE}$  is the REE content in the parental magma,  $\text{bulk } K_D$  the bulk distribution coefficient for the cumulus mineralogy of the gabbro,  $M_{cum}$  and  $M_{TL}$  the weight fractions of the cumulate phases and the trapped liquid respectively and  $cum_{REE}$  the REE content of the gabbro (cf. Barrie et al., 1991). Application of this equation to sample DT10, a



troctolitic gabbro of the Vestre Dale Gabbro with approximately 70 wt.% cumulus olivine, 20 wt.% cumulus plagioclase and 10 wt.% trapped liquid, results in the pattern depicted in **Figure 6.5**, assuming a  $D_{Eu}^{plag/liq}$  value of 0.5 (Allègre et al., 1977). The shape of the pattern for the parental magma does not significantly differ from that of DT10, except for the negative Eu anomaly ( $Eu/Eu^* = 0.8$ ). Sun and Nesbitt (1978) suggested the possibility that the Eu anomaly represents a source characteristic, but even then these authors regard plagioclase extraction as the ultimate cause, since plagioclase is the only mineral capable to separate Eu from the other REE. Thus, the assumption that a parental magma for the Vestre Dale Gabbro was derived from a primary, mantle-derived magma simply by fractionation of olivine is obviously too simplistic. The parental magma of the Vestre Dale Gabbro must, besides olivine, also have fractionated an amount of plagioclase.

Mass balance calculations have been performed, in order to get an idea of the amounts of plagioclase and olivine which must have been fractionated before crystallization of the Vestre Dale Gabbro started. The calculations are based upon the assumptions that 1) the parental magma had a picritic precursor, 2) the Fe/Mg ratio of the resulting basaltic magma is such that it is in equilibrium with the most Fo-rich olivine in the Vestre Dale Gabbro (i.e. Fo<sub>75</sub> in sample DT10), and 3) the picritic precursor did not have an Eu anomaly. With the results of the calculations and the REE contents of the parental magma of the Vestre Dale Gabbro, the Eu/Sm ratio of the picritic magma is calculated with the equation for Rayleigh fractionation. This ratio should be similar to the  $Eu^*/Sm$  ratio of the parental magma ( $Eu^*$  is interpolated from adjacent trivalent REE, in this case Sm and Tb).

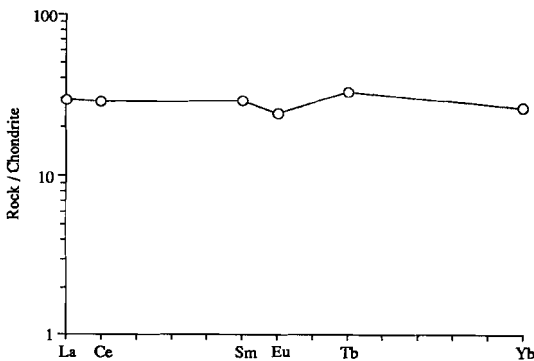


**Figure 6.5** Calculated REE patterns for the parental magma for the Vestre Dale Gabbro, calculated with a  $D_{Eu}^{plag/liq}$  value of 0.5 (Allègre et al., 1977).

The calculations have been performed with a picrite from the Nuanetsi picrites (sample N296; Ellam and Cox, 1989). For the basaltic end-member a basalt of the Vemork Formation from the adjacent Telemark Sector has been selected (sample RV45; Atkin and Brewer, 1990). The Vemork Formation forms part of the Rjukan Group of the Telemark supracrustals, which Atkin and Brewer (1990) regard as the extrusive counterparts of the mafic intrusions in the Bamble (and Kongsberg) Sector. The Mg# of the basalt RV45, 51.7, approximates the Mg# value of 47 derived for the parental magma of the Vestre Dale Gabbro (see Chapter II of this thesis). It appears that generation of this basaltic magma from the picrite requires subtraction of 24 % olivine ( $Fo_{88}$ ) and 19 % plagioclase ( $An_{86}$ ). The calculated Eu/Sm of the picritic precursor, 0.36, reasonably agrees with a Eu/Sm ratio of 0.39 for the parental magma. The weight fractions of olivine and plagioclase and the amount of magma remaining after fractionation, 57 %, can be used in Rayleigh fractionation calculations for any element. For example, fractionation of olivine and plagioclase in the calculated ratio results in a decrease in the Ni concentration from 478 ppm in the picrite to 70 ppm in the basalt (calculated with  $D_{Ni}^{ol/mq} = 8$ ; Irving, 1978); this is only slightly lower than the Ni concentration of the Vemork basalt, i.e. 79 ppm.

Despite the simplicity of the model and the uncertainty in the distribution coefficients, the calculations demonstrate that the generation of a basaltic magma from a picritic magma requires the fractionation of a fairly large amount of olivine and plagioclase. As mentioned before, part of the olivine has probably been fractionated below the crust-mantle boundary. Plagioclase however is not a stable phase in the subcontinental lithosphere (Jaques and Green, 1980). The occurrence of plagioclase lherzolites is confined to a depth less than 30 km. Seismic reflection and refraction profiling revealed that the Moho discontinuity below South Norway is presently situated at a depth of c. 32 km (Kinck et al., 1991). From this, together with a recrystallization pressure of 7 kbar for the Bamble Sector, a Proterozoic crustal thickness of c. 55 km can be inferred (see also Demaiffe and Michot, 1985). Therefore, fractionation should, at least partly, have taken place in a crustal magma chamber. Here, plagioclase crystallized together with olivine, giving rise to more primitive cumulates than observed in the Vestre Dale Gabbro. On the other hand, the existence of more primitive olivine-plagioclase cumulates directly related to the studied gabbros cannot be excluded; they may just not be exposed.

#### 6.4.2 LILE and LREE enrichments

A remarkable feature among the various REE patterns concerns the variation in  $(La/Sm)_N$  ratios. The Åmdal Gabbro crystallized from a LREE depleted magma with a  $(La/Sm)_N$  ratio of 0.9, whereas the parental magma of the Vestre Dale Gabbro was slightly LREE enriched with a  $(La/Sm)_N$  of c. 1.1.  $(La/Sm)_N$  values of the more evolved Flosta Gabbro provide evidence for even more LREE enriched magmas. The Arendal Gabbro, on the other hand, crystallized from a more depleted magma than the Åmdal Gabbro.

LREE enrichment is a common feature among continental tholeiites (Dupuy and Dostal, 1984). The high degrees of partial melting involved in the generation of tholeiitic magmas (20-30 %; Jaques and Green, 1980), exclude the possibility that the LREE enriched magmas are the result of small degrees of partial melting; high degrees of partial melting will not allow the REE to be fractionated from each other. The concurrent variation in the Zr/Nb ratio (with exception of the Åmdal Gabbro), which is known to be hardly affected by variation of source melting conditions (Pearce and Norry, 1979), also argues against variable degrees of partial melting as a mechanism to explain the observed enrichments. This leaves crustal contamination and derivation of the gabbros from a variably enriched mantle source, or a combination of both, as the possible causes for the observed enrichments. The Arendal and Tromøy Gabbros would, in this respect, be derived from the least enriched source (LREE depleted, high Zr/Nb and low Ba/Zr) and the Flosta Gabbro from the most enriched source (LREE enriched, low Zr/Nb and high Ba/Zr).

Several objections can be raised against crustal contamination as the principal source for the enrichments. Field evidence for crustal contamination is lacking; country rock xenoliths have not been observed in the gabbros studied. The occurrence of LREE enriched as well as LREE depleted samples in one gabbro (the Jomåsknutene Gabbro) makes it unlikely that the enrichments are due to contamination of the magma during its way up through the continental crust. Variable contamination by crustal-derived material before ascending through the continental crust is neither a viable option: whereas LREE enrichment is accompanied by an increase in K/Ba ratios, the K/Rb ratios remain remarkably constant (Table 6.2). It would be expected that, if the variation in K/Ba ratios was caused by variable contamination, a similar variation in K/Rb should be observed. Another major objection against crustal contamination concerns the major element chemistry of the gabbros. Equivalent enrichment of the mantle source in the major elements would subsequently yield andesitic rather than tholeiitic melts. This does

not mean that the source and/or the parental magmas have not been contaminated by crustal material at all, but it did not contribute to the overall pattern of LREE and LILE (Large-Ion Lithophile Elements: Ba, K, Rb, Th) enrichments. The LILE and LREE enrichment therefore appears to be a source-inherited characteristic. Derivation of the parental magmas from a variable enriched mantle source appears to be the best appropriate explanation for the observed enrichments. In a comparable way, Smalley et al. (1983b) explained the variable LILE and LREE enrichments in the Arendal metabasites.

### **6.4.3 Sr and Nd isotopes**

The effects of variable LILE and LREE enrichments of the mantle below Bamble are also expected to be reflected in the isotopic compositions of the gabbros. Sm-Nd isotopic systematics of the Jomåsknutene and the Flosta Gabbros revealed that the Mid-Proterozoic mantle below Bamble had a depleted composition with respect to the CHondritic Uniform Reservoir (CHUR) (de Haas et al., 1992b; Chapter IV of this thesis). This means that in terms of Sm/Nd and Rb/Sr ratios, the mantle evolved with a  $^{147}\text{Sm}/^{144}\text{Nd}$  and  $^{87}\text{Rb}/^{86}\text{Sr}$  ratio higher respectively lower than CHUR. LREE and LILE enrichment will lower the Sm/Nd ratio and enhance the Rb/Sr ratio. An enriched source will therefore, in the course of the time, develop towards higher  $^{87}\text{Sr}/^{86}\text{Sr}$  and lower  $^{143}\text{Nd}/^{144}\text{Nd}$  ratios. Indeed, the  $\epsilon_{\text{Nd}}$  value and  $^{87}\text{Sr}/^{86}\text{Sr}$  ratio of the LREE enriched Vestre Dale Gabbro at  $T = 1.11$  Ga are lower respectively higher than  $\epsilon_{\text{Nd}}(1.1 \text{ Ga})$  and  $^{87}\text{Sr}/^{86}\text{Sr}(1.1 \text{ Ga})$  values for the LREE depleted Tromøy and Arendal Gabbros (Table 6.4). The more depleted Arendal Gabbro, in its turn, has higher respectively lower  $\epsilon_{\text{Nd}}(1.1 \text{ Ga})$  and  $^{87}\text{Sr}/^{86}\text{Sr}(1.1 \text{ Ga})$  values than the less depleted Tromøy Gabbro (Table 6.4).  $T_{\text{DM}}$  ages of the Vestre Dale Gabbro indicate that the enrichment event took place between 1.69 and 1.88 Ga. As a result, the LILE and LREE enrichments did, in the case of the 1.64 Ga old Flosta Gabbro and the LREE enriched samples of the 1.77 Ga old Jomåsknutene Gabbro (GA146, GA148 and GA456), not result in lower  $\epsilon_{\text{Nd}}$  values. The model ages imply that the lithospheric mantle below Bamble retained its enriched character for more than 0.5 Ga. A similar time interval between enrichment and magmatism has been described for the Proterozoic sub-continental mantle below NW Scotland (Weaver and Tarney, 1981). There, mantle enrichment in LILE and LREE, visualized by the 2.39 Ga old Scourie dyke suite, is supposed to be contemporaneous with the generation of the Lewisian gneisses at 2.92 Ga, some 0.6 Ga earlier.

**Table 6.4**  $\epsilon_{\text{Nd}}$  values and Sr isotope ratios of the Vestre Dale Gabbro (at T = 1.1 Ga) and the Tromøy and Arendal Gabbros (both at T = 1.1 Ga).

Gabbro	$^{87}\text{Sr}/^{86}\text{Sr}(\text{T})$	$\epsilon_{\text{Nd}}(\text{T})$
Vestre Dale	0.7032	+ 1.8 ± 0.5
Tromøy	0.70254 ± 2	+ 5.2 ± 0.3
Arendal	0.70243 ± 2	+ 5.9 ± 0.3

#### 6.4.4 Comparison with other mafic rocks from the SWSD

Having established the trace element and isotopic variations in some of the Bamble gabbros, it may be interesting to check to what extent the inferred features of the Mid-Proterozoic mantle are confirmed by other mafic rocks from the Southwest Scandinavian Domain. The Arendal metabasites (**Fig. 6.1**) are minor, usually concordant, sheet-like bodies with continental tholeiitic affinities (Clough and Field, 1980), occurring across the amphibolite-granulite transition zone. Comparison with the gabbros is hampered by the lack of Y, Nb, La and Sm data and isotope analyses. Like the gabbros, the metabasites have rather flat REE patterns with  $(\text{Tb}/\text{Yb})_{\text{N}}$  ratios between 1.00 and 1.32 (Smalley et al., 1983b). Ti/Zr ratios range between 76 and 118; one sample has a Ti/Zr ratio of 187 (**Table 6.5**). Zr/Nb and Ba/Zr ratios of the most LREE enriched metabasites (in terms of  $(\text{Ce}/\text{Yb})_{\text{N}}$  ratios) compare reasonably well to those of the LREE enriched gabbros (**Table 6.5**). Brickwood and Craig (1987) and Atkin and Brewer (1990) presented mineralogical and whole rock data of some basic intrusives from the northern part of the Bamble Sector (**Fig. 6.1**). These intrusions show similar fractionation trends as the gabbros (Brickwood and Craig, 1987). Trace element ratios are different: most Ti/Zr ratios are generally lower, averaging at 70, whereas Zr/Y ratios between 3.0 and 6.6 are slightly higher than in the gabbros (**Table 6.5**). The intrusions show a considerable range in Zr/Nb ratios (**Table 6.5**). The Zr/Nb ratios of the Averid troctolites are similar to Zr/Nb ratios of the Arendal Gabbro, whereas Zr/Nb ratios of the Bjordam peridotite and gabbro and the Skogen norite compare better to those of the LREE enriched gabbros. Similarly to the gabbros, the increase in Zr/Nb appears to be accompanied by decreasing Ba/Zr and increasing K/Ba ratios, although the Bjordam peridotite has the lowest respectively highest Ba/Zr and K/Ba ratio.

The spread in  $\epsilon_{\text{Nd}}(1.2 \text{ Ga})$  values, displayed by the tholeiitic volcanics of the Telemark supracrustal (**Table 6.5**), is remarkably similar to the spread in  $\epsilon_{\text{Nd}}(1.1 \text{ Ga})$

values observed for the Vestre Dale, Tromøy and Arendal Gabbros. K/Ba ratios of the Gjuve Formation (which forms together with the Morgedal Formation part of the Bandak Group) compare well to the K/Ba ratios of the Tromøy and Arendal Gabbros (Tables 6.2 and 6.5). A possible correlation between Zr/Nb and Ba/Zr ratios and the  $\epsilon_{\text{Nd}}(\text{T})$  values as observed for the Vestre Dale Gabbro and the Arendal and Tromøy Gabbros is less apparent for the basalts, although basalts of the Vemork Formation (which forms part of the Rjukan Group) have the lowest Zr/Nb ratios; but then again these ratios are lower than for the Vestre Dale Gabbro (Tables 6.1 and 6.5). The age of 1.2 Ga, used by Atkin and Brewer (1990) in their calculation of the  $\epsilon_{\text{Nd}}$  values of the Vemork Formation (which is more or less similar to the  $\epsilon_{\text{Nd}}(1.11 \text{ Ga})$  value of the Vestre Dale Gabbro), is probably based upon the Sm-Nd WR age of Rjukan metavolcanics as reported by Menuge (1985). Menuge's age is, however, questionable (Verschure, 1985; Verschure et al., 1990). Recently, Dahlgren et al. (1990) obtained c. 1.5 Ga old U-Pb zircon ages from one of the Rjukan metarhyolites. This demonstrates that any comparison regarding the source evolution of the Rjukan/Vemork metavolcanics and the Vestre Dale Gabbro should be handled with extreme caution.

LILE enrichment has also been reported for Gothian amphibolites from the Østfold-Marstrand Belt (Fig. 6.1; Åhäll and Daly, 1989). The very low  $(\text{La}/\text{Sm})_{\text{N}}$  ratios of these amphibolites, between 0.2 and 0.4, suggest that the source was not enriched in the LREE. Comparison with the gabbros is difficult since only ranges and average values of the trace elements have been published. Zr/Y ratios vary between 1.6 and 2.2 and Ti/Zr ratios between 125 and 140. These are lower, respectively higher than those for the Bamble gabbros.

It is interesting to compare our results with the chemically and isotopically well-documented Sveconorwegian Rogaland anorthositic suite (Fig. 6.1; Duchesne et al., 1985a). The c. 1.0 Ga old massif-type anorthosites are associated with monzonitic rocks with alkali-calcic affinities (Demaiffe et al., 1990). Trace element and isotopic data led Duchesne and co-workers to the conclusion that the massif-type anorthosites crystallized from basaltic magmas, which find their origin in a depleted upper mantle. Extraction from the mantle may already have occurred 0.5 Ga before emplacement (Weis, 1986), i.e. during roughly the same period as the Bamble coronites. Maximum  $\epsilon_{\text{Nd}}(1.0 \text{ Ga})$  and  $\epsilon_{\text{Nd}}(1.05 \text{ Ga})$  values of +4.6 for the Egersund-Ogna anorthosite (Demaiffe et al., 1986) and +4.4 for the Håland-Helleren anorthosite (Menuge, 1988) are much higher than the  $\epsilon_{\text{Nd}}(1.11 \text{ Ga})$  value of the Vestre Dale Gabbro but 1-1.5  $\epsilon$  unit lower than the  $\epsilon_{\text{Nd}}(1.1 \text{ Ga})$  values of the Arendal and Tromøy Gabbros. The lowest initial  $^{87}\text{Sr}/^{86}\text{Sr}$  ratios, obtained for the Egersund-Ogna anorthosite, 0.7033 (Demaiffe et

al, 1986) and Håland-Helleren anorthosite, 0.7035 (Menuge, 1988), are slightly higher than the initial  $^{87}\text{Sr}/^{86}\text{Sr}$  ratio of the Vestre Dale Gabbro. Isotopic variations within the individual anorthosites, reflected by decreasing  $\epsilon_{\text{Nd}}$  values and increasing  $^{87}\text{Sr}/^{86}\text{Sr}$  ratios, are explained by progressive contamination of crustal material (Demaiffe et al, 1986).

**Table 6.5** Trace element and Nd isotope chemistry of mafic rocks from the Southwest Scandinavian Domain. Data from the Arendal metabasites are Smalley et al. (1983b); data from the Telemark Supracrustals (the Vemork, Morgedal and Gjuve Formations) and the basic intrusives are from Atkin and Brewer (1990); SLM amphibolite data are from Åhäll and Daly (1989).  $\epsilon_{\text{Nd}}$  values of the Telemark Supracrustals and the SLM amphibolites have been calculated for T = 1.2 Ga respectively T = 1.76 Ga. Zr/Nb ratios for the Arendal metabasites have been calculated assuming Nb/Ta = 16 (Holm, 1985).

Rock/ Location	Ti/Zr	Zr/Y	Zr/Nb	Ba/Zr	K/Ba	(Ce/Yb) <sub>N</sub>	$\epsilon_{\text{Nd}}(\text{T})$
<b>Bamble</b>							
Metabasites/ <i>Arendal</i>							
Zone A	76-106	-	30-40	1.5-0.9	61-65	2.11-1.25	-
Zone B	118-103	-	26-35	1.8-0.5	46-96	0.93-1.42	-
Zone C	112-95	-	22-15	0.4-3.9	242-23	1.01-2.25	-
Zone D	78-187	-	14-15	1.9-3.5	48-53	3.47-1.84	-
Troctolites/ <i>Averid</i>							
Peridotite	61	6.1	22	0.7	80	-	-
Gabbro/ <i>Bjordam</i>	77	4.5	20	2	26	-	-
Norite/ <i>Skogen</i>	208	3.0	12	1.8	16	-	-
<b>Telemark</b>							
Basalts/ <i>Vemork Form.</i>	75-66	4.7-4.6	8	1.6-0.4	24-30	-	+0.7- +2.1
Basalts/ <i>Morgedal Form.</i>	69-75	3.8-4.9	82-63	1.0-1.6	22-16	-	+2.6- +3.7
Basalts/ <i>Gjuve Form.</i>	75-93	4.2-3.6	30-24	1.1-1.0	46-52	-	+5.0- +5.3
<b>Østfold-Marstrand</b>							
Amphibolites/ <i>SLM</i>	125-140	1.6-2.2	-	-	-	-	+ 4.3

The parental magmas of the monzonitic rocks were derived from melting of basic rocks in the lower crust as the result of anorthositic magmatism (Duchesne et al., 1985b and 1989).  $\epsilon_{Nd}(0.94 \text{ Ga})$  values of the Hydra massif (+5.5- +1.6; Demaiffe et al., 1986) and Lyngdal hyperites (+1.9- +0.4; Demaiffe et al., 1990), indicate that the basic precursors also had a depleted mantle signature. A similar variation in  $\epsilon_{Nd}$  values has been observed among the Bamble gabbros, but the relatively high initial  $^{87}\text{Sr}/^{86}\text{Sr}$  ratios of the monzonites, 0.7061 for the Hydra massif (Demaiffe et al., 1986) and 0.7054 for the Lyngdal hyperites (Demaiffe et al., 1990) make comparison with the Bamble gabbros less appropriate.

From this comparative study, it appears that, despite the rather poor documentation of the basic rocks from the Bamble and Telemark Sectors, at least part of the trace element variations in these rocks show similarities with variations in the Bamble gabbros. Grossly, a distinction can be made between depleted and enriched rocks, which, in case of the Telemark supracrustals, is corroborated by Nd isotopes. The LILE enriched Stora Le-Marstrand amphibolites from the Östfold-Marstrand Belt have distinctively lower Zr/Y and higher Ti/Zr ratios than the other rocks from the Southwest Scandinavian Domain. The Stora Le-Marstrand, the Telemark Supracrustals and the Rogaland anorthosites have clearly positive  $\epsilon_{Nd}$  values. This provides further evidence that the entire mantle below the Southwest Scandinavian Domain had a depleted signature during Gothian times, a conclusion which was already inferred from the Bamble gabbros. In marked contrast, Schärer (1991) inferred a chondritic signature for the 1.7 Ga mantle below the Grenville Province, which constituted one continuous terrain with the Southwest Scandinavian Domain (Gower 1985, 1990).

#### **6.4.5 Origin of the LILE and LREE enrichments**

In order to elucidate the origin of the enrichments, the incompatible trace elements were plotted in so-called spidergrams (Fig. 6.6a-c). The elements are arranged in order of decreasing incompatibility. Since Nd isotope systematics revealed that the gabbros were extracted from a depleted mantle source the elements have been normalized to their abundances in the present-day representant of the depleted mantle, the N-MORB. In this respect, it is good to recall that the gabbros do not represent liquid compositions and that therefore the shapes of the patterns rather than the normalized abundances are of importance.

Besides the already mentioned variable LILE and LREE enrichments, most gabbros are characterized by a negative Nb anomaly; the size of the anomaly is variable.



Similar patterns have been found for the Arendal metabasites and the Telemark supracrustals (Smalley et al., 1983b; Atkin and Brewer, 1990). Samples from the Åmdal Gabbro however lack the Nb depletion. Their pattern compares well to that of the Stora Le-Marstrand amphibolites. Smalley et al. (1983b) and Smalley and Field (1985) explain the various LILE/LREE enrichments in Arendal and Telemark metabasites by partial melting of an originally depleted source which had been variably metasomatized by LILE- and LREE-bearing fluids or partial melts. These authors concluded from the observed depletion in Ta, which is known to show a geochemical behaviour similar to Nb, that this enrichment process and the generation of the magmas was a subduction-related event.

The concept of Precambrian plate tectonics is nowadays generally accepted, although the detailed mechanisms are still a matter of debate (*e.g.* Kröner, 1991). Indeed, LILE/LREE enrichments in combination with negative Nb anomalies are characteristic features of basaltic rocks from **recent** destructive plate margins (*e.g.* Pearce, 1984; Holm, 1985). From the parallel between the chemical variations in the Telemark supracrustals and later plutonic suites, and the variations in modern cordilleran orogens, Smalley and Field (1985) concluded that subduction of oceanic crust and subduction-enrichment of the overlying mantle were active processes c. 1.6 Ga ago. Similarly, Åhäll and Daly (1989) inferred an arc setting for the Östfold-Marstrand Belt during the Gothian from the chemistry of the Stora Le-Marstrand amphibolites. The occurrence of pillow lava in the Stora Le-Marstrand formation, reported by Åhäll (1986), provides definite proof for Gothian oceanic crust. Since the original arc configuration has been erased, confirmation of an Gothian arc setting depends on other, secondary, features. Large volumes of Gothian calc-alkaline rocks are absent in the Bamble Sector, but occur widely spread in the Swedish part of the Southwest Scandinavian Domain (Lindh, 1987). Visser and Senior (1990) tentatively proposed a Gothian subduction event prior to the prograde, continental collision-related, PT-trajectory of the Bamble Sector. However, indications of high-pressure metamorphism characteristic of subduction zones have never been found, although it is possible that they were erased during late Gothian or Sveconorwegian Orogenies.

If the spidergrams indeed reflect an ancient arc setting, the observations of Nijland and Maijer (1991), that the Bamble metasediments were probably deposited in a continental environment, suggest a continental arc setting. The relatively high Zr/Y ratios observed among the gabbros, 3.4 - 4.4, also support a continental arc rather than a oceanic arc setting (Pearce, 1984).

Identification of the source and petrogenesis

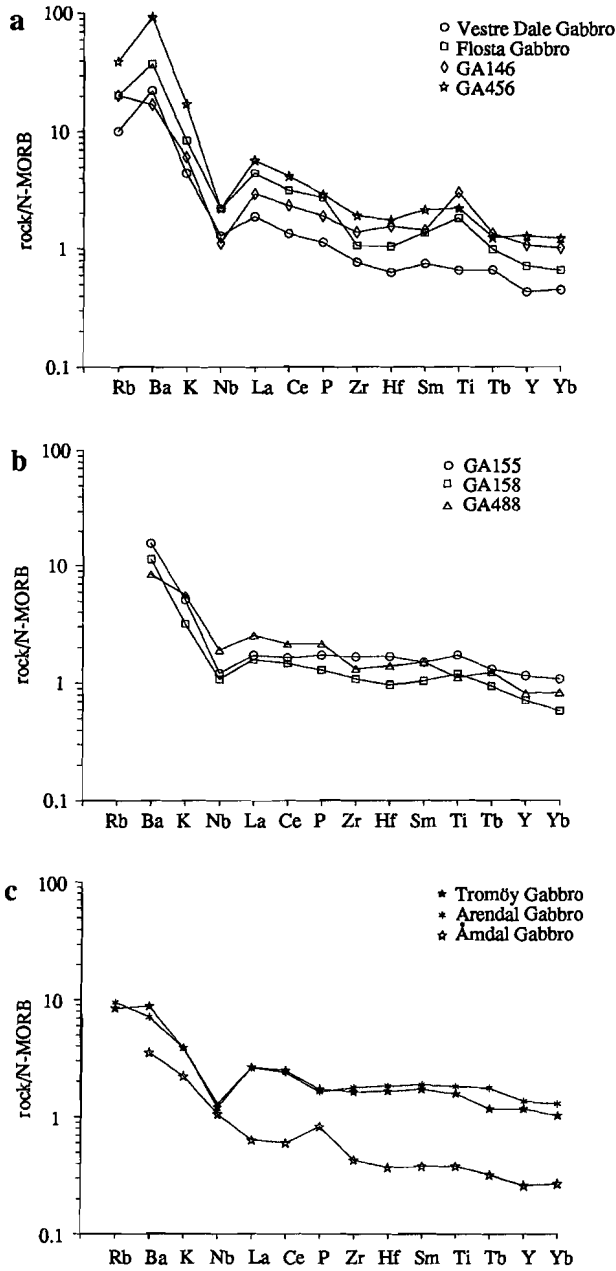


Figure 6.6 Spidergrams of a) the Vestre Dale and Flosta Gabbros (both averaged) and LREE enriched samples of the Jomåsknutene Gabbro; b) LREE depleted samples of the Jomåsknutene Gabbro; c) Tromøy, Arendal Gabbros and Årdal Gabbros. Normalization after Sun and McDonough (1989).

The trace element and isotope chemistry of rocks generated at active continental margins is the result of a complex interaction between the sub-continental lithosphere, the convecting upper mantle, and components derived from the lower continental crust and the subducted oceanic slab (possibly with terrigenous sediment). More than for island arc tholeiites, which have a pronounced slab-related signature, the trace element and isotope characteristics of continental margin rocks is dominated by the composition of the mantle wedge prior to subduction (Pearce, 1984). The high LILE/HFSE (High Field Strength Elements: Nb, Zr, Hf, Ti, Y, Yb) ratios are generally attributed to the introduction of LILE from subducted oceanic crust (Kay, 1980).

The HFSE, on the other hand, are completely derived from the mantle wedge due to their low mobility in the slab-derived component (*e.g.* McCulloch and Gamble, 1991). As a consequence, the variations in the HFSE chemistry of the individual intrusions, as visualized by the range in Zr/Nb ratios, reflect compositional variations in the source region. The Tromøy and Arendal Gabbros have MORB-like Zr/Nb ratios (Sun et al., 1979). The enrichment in Nb relative to Zr, as revealed by the lower Zr/Nb ratios of the other gabbros, may be attributed to the introduction of melts or fluids into the subcontinental lithosphere from the underlying convecting upper mantle. These so-called 'within-plate' mantle contributions (*e.g.* Pearce, 1984) show the greatest enrichments in the most incompatible elements like Ba and Nb, and modest enrichment in the less incompatible elements (*e.g.* Zr, Hf and Ti). The apparent correlation between the Zr/Nb and  $(La/Sm)_N$  ratios of the gabbros (Fig. 6.7), indicate that the 'within plate' enrichment is also accompanied by an increase in the LREE contents. Interestingly, this Zr/Nb- $(La/Sm)_N$  trend resembles the binary mixing curve between the enriched P-MORB and depleted N-MORB made up by MORB's from the Atlantic, Indian and Pacific oceans, as presented by Wilson (1989, p.141).

As argued in section 6.4.2, the contribution of crustal contamination to the trace element chemistry of the gabbros is minor. Crustal contamination is manifested by high values for Ba and Th in spidergrams, but these are not necessarily diagnostic (Pearce, 1984). Ba concentrations of some samples from the Jomåsknutene Gabbro, however, exceed 400 ppm. As a consequence, these samples have much higher Ba/Zr ratios than the other gabbros (Table 6.1 and Appendix 2). This and the relatively low  $\epsilon_{Nd}(1.77 \text{ Ga})$  of GA456 (584 ppm Ba) compared to other samples of the Jomåsknutene Gabbro (+4.6 versus +5.0- +5.8) strongly suggests that part of the source of this gabbro has been affected by crustal contamination.

*Identification of the source and petrogenesis*

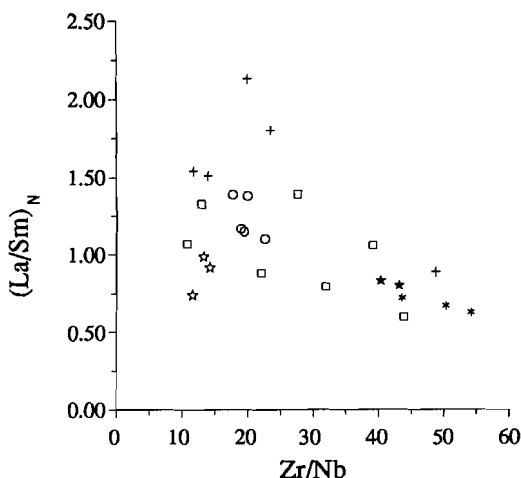


Figure 6.7  $(La/Sm)_N$  vs.  $Zr/Nb$ . Symbols as in Figure 6.2.

So, it appears that the trace element variations observed among the gabbros are largely due to variable enrichments of the mantle wedge, which find their origin in a) the introduction of slab-derived material, related to Gothian subduction and b) the transfer of fluids or partial melts from the underlying mantle. Obviously, the subcontinental mantle below Bamble retained this variably enriched signature for more than 0.5 Ga. This eventually resulted in low  $^{87}Sr/^{86}Sr$  ratios and high  $^{143}Nd/^{144}Nd$  values for the Tromøy and Arendal Gabbros and a high  $^{87}Sr/^{86}Sr$  ratio and a low  $^{143}Nd/^{144}Nd$  value for the Vestre Dale Gabbro. Such heterogeneous nature of the Mid-Proterozoic mantle below southern Norway has also been mentioned by Smalley and Field (1985) in their study on the geochemistry of the Telemark supracrustals and later plutonic rocks.

One point needs some more consideration. If the HFSE have indeed not been derived from the subduction component, then it is at least remarkable that the most enriched gabbros, in terms of the subduction component, are also the most enriched qua 'within plate' component. The increase in  $Ba/Zr$  ratios with decreasing  $Zr/Nb$  ratios, as demonstrated by the Vestre Dale, Tromøy and Arendal Gabbros, suggests that the increase in LILE is accompanied by an increase of the Nb contents. LILE extraction from the subducted oceanic slab is, as mentioned before, not accompanied by extraction of Nb. However, the composition of the subduction component might significantly change if terrigenous sediment is involved in this component. Estimates for the compositions of Proterozoic sediments from the Baltic Shield are yet unknown. The

Zr/Nb ratio of 7.6 for the average upper continental crust (Taylor and McLennan, 1985), however, indicates that incorporation of terrigenous sediment in the subduction component might contribute to a lowering of the Zr/Nb ratios of the mantle source.

## 6.5 CONCLUSIONS

The Jomåsknutene and Flosta Gabbros show the same tholeiitic fractionation trend as the Vestre Dale Gabbro. The Åmdal, Tromøy and Arendal Gabbros, which show hardly any fractionation, also plot on this trend. None of the gabbros crystallized from primary, mantle-derived magmas. The virtually identical Ti/Zr and Zr/Y ratios support the suggestion of a close genetic relationship between the parental magmas of the individual gabbros. The occurrence of LREE depleted as well as LREE enriched gabbros indicate that this is only partly true. The LREE enrichment is accompanied by an increase in the concentrations of LIL elements. It is proposed that this enrichment has been caused by the introduction of LREE/LILE enriched fluids in the mantle during Gothian subduction. The range in Zr/Nb ratios, which are thought not to be influenced by these fluids, indicates that not all of the compositional variations are due to this process. Nd isotope data from the gabbros and mafic rocks from other parts of the Southwest Scandinavian Domain, indicate that the entire mantle had a depleted signature before Gothian subduction. The range in  $\epsilon_{Nd}$  values and  $^{87}Sr/^{86}Sr$  ratios at 1.1 Ga, as revealed by the Vestre Dale, Tromøy and Arendal Gabbros, indicate that the mantle retained its enriched nature after subduction for more than 0.5 Ga.

*Identification of the source and petrogenesis*

**Appendix 1** Whole rock data of 27 selected samples from the Vestre Dale Gabbro (V), the Jomåsknutene Gabbro (J), the Åmdal Gabbro (Å), the Flosta Gabbro (F), the Tromøy Gabbro (T) and Arendal Gabbro (A). -1 for LOI stands for a negative LOI, na = not analysed, dl = below detection limit. See Chapters II and IV for analytical techniques. Bold printed Sm analyses have been obtained by INAA. Bold printed Rb analyses have been obtained by XRF analysis at the Isotope Geology Laboratory.

Sample	WT203	WT209	WT216	WT217	WT225	DT10	GA146	GA148	GA155
Gabbro	V	V	V	V	V	V	J	J	J
SiO <sub>2</sub>	45.29	48.87	46.62	42.56	44.35	40.77	44.40	44.01	46.43
TiO <sub>2</sub>	0.52	1.20	1.84	0.80	0.84	0.28	3.82	0.86	2.17
Al <sub>2</sub> O <sub>3</sub>	13.11	15.81	12.96	9.66	10.86	8.19	11.87	14.20	15.68
FeO	12.92	11.13	13.64	16.47	15.88	16.16	18.12	13.51	13.05
MnO	0.20	0.19	0.22	0.25	0.24	0.24	0.29	0.20	0.24
MgO	17.37	8.03	7.12	19.39	18.25	25.45	5.65	16.38	7.40
CaO	9.01	11.80	10.79	6.42	6.73	5.15	9.99	6.95	9.96
Na <sub>2</sub> O	1.33	2.50	2.32	1.40	1.71	0.80	3.39	2.25	3.21
K <sub>2</sub> O	0.20	0.45	0.67	0.30	0.33	0.10	0.44	0.19	0.37
P <sub>2</sub> O <sub>5</sub>	0.10	0.16	0.15	0.14	0.13	0.09	0.22	0.10	0.20
LOI	dl	dl	1.06	dl	dl	1.44	0.70	0.82	0.84
Total	99.73	99.89	97.39	96.79	98.72	98.67	98.89	99.47	99.54
Co	118	72	65	121	131	165	64	110	65
Ni	364	93	69	449	400	499	35	345	99
Cu	29	71	113	55	61	30	89	17	63
Rb	3	8	19	6	6	dl	11	0	dl
Sr	233	307	288	194	214	134	178	81	208
Y	11	21	25	16	16	4	30	16	32
Zr	39	71	68	57	60	18	102	63	123
Nb	2	4	3	3	3	dl	2.6	dl	2.8
Ba	89	185	153	138	151	56	107	na	99
La	2.52	6.63	6.65	4.20	5.33	1.04	7.33	4.03	4.28
Ce	dl	13.1	17.0	10.70	10.80	2.65	17.56	10.30	12.22
Nd	4.23	9.38	11.41	7.27	7.89	na	11.65	7.12	11.57
Sm	1.20	2.61	3.32	1.97	2.11	<b>0.54</b>	3.78	2.14	3.93
Eu	0.65	1.18	1.29	0.74	0.84	0.33	1.52	0.75	1.55
Tb	0.38	0.63	0.67	0.28	0.48	0.16	0.90	0.46	0.87
Yb	1.10	1.81	1.95	1.21	1.33	0.60	3.08	1.62	3.29
Hf	0.70	1.60	1.66	1.18	1.70	0.42	3.18	1.38	3.43
Mg#	70.6	56.3	48.3	67.8	67.2	73.8	35.8	68.4	50.3

## Appendix 1 (continued)

Sample	GA158	GA456	GA480	GA488	GA487	GA493	GA497	GA498	GA244
Gabbro	J	J	J	J	Å	Å	Å	Å	F
SiO <sub>2</sub>	48.60	46.49	47.15	46.36	43.03	41.77	42.41	42.33	50.33
TiO <sub>2</sub>	1.51	2.80	1.76	1.41	0.53	0.48	0.43	0.38	1.23
Al <sub>2</sub> O <sub>3</sub>	22.81	14.97	16.60	18.38	13.69	10.22	13.54	13.23	17.25
FeO	7.21	14.29	12.47	10.63	13.23	17.08	13.94	14.03	10.25
MnO	0.14	0.25	0.20	0.14	0.17	0.21	0.19	0.19	0.19
MgO	3.05	5.56	7.77	7.70	19.15	23.58	20.12	20.70	8.00
CaO	12.05	8.19	10.39	9.98	6.89	5.54	6.90	6.58	7.83
Na <sub>2</sub> O	3.54	4.27	2.73	3.57	1.82	1.25	1.52	1.50	3.08
K <sub>2</sub> O	0.23	1.25	0.53	0.41	0.17	0.13	0.18	0.14	0.55
P <sub>2</sub> O <sub>5</sub>	0.15	0.34	0.20	0.25	0.11	0.10	0.08	0.08	0.14
LOI	0.58	0.44	dl	0.60	0.32	0.12	0.07	0.37	0.14
Total	99.87	98.41	99.8	99.42	99.11	100.48	99.38	99.53	98.97
Co	49	67	72	64	114	157	124	135	54
Ni	34	66	125	119	435	544	434	462	71
Cu	54	111	76	38	6	dl	dl	dl	25
Rb	dl	22	15	dl	dl	dl	dl	dl	6
Sr	234	326	259	281	82	76	97	89	491
Y	20	36	24	23	9	7	6	6	10
Zr	80	141	118	97	35	33	28	23	42
Nb	2.5	5.1	9.1	4.4	3.0	2.3	2.1	dl	2.1
Ba	72	584	159	53	21	20	24	21	202
La	3.93	14.32	9.60	6.30	1.61	1.57	1.60	1.33	6.24
Ce	10.90	31.31	22.00	16.00	4.80	4.80	3.80	3.40	12.64
Nd	8.54	21.80	na	na	na	na	na	na	7.09
Sm	2.74	5.66	3.97	3.93	1.20	0.94	0.89	0.78	1.61
Eu	1.13	2.02	1.40	1.42	0.57	0.42	0.49	0.47	0.93
Tb	0.63	0.84	0.77	0.82	0.22	0.21	0.21	0.19	0.23
Yb	1.78	3.72	2.02	2.55	0.81	0.87	0.78	0.59	1.26
Hf	1.98	3.58	3.16	2.85	0.88	0.70	0.67	0.65	0.95
Mg#	43.0	41.0	52.7	56.4	72.1	71.2	72.1	72.5	58.3

*Identification of the source and petrogenesis*

**Appendix 1 (continued)**

Sample	GA254	GA256	GA267	GA439	GL62	GL64	GL71	GL74	GL75
Gabbro	F	F	F	F	T	T	A	A	A
SiO <sub>2</sub>	42.28	48.04	48.78	46.63	46.42	46.56	46.31	46.34	46.24
TiO <sub>2</sub>	4.26	2.31	1.39	2.03	1.78	2.00	2.30	2.33	2.30
Al <sub>2</sub> O <sub>3</sub>	13.61	15.18	16.50	16.53	16.33	16.19	14.87	15.12	15.00
FeO	19.03	12.82	9.44	13.19	13.01	13.32	14.88	14.98	14.95
MnO	0.22	0.17	0.19	0.24	0.25	0.26	0.30	0.30	0.30
MgO	5.81	5.99	8.19	7.22	7.67	7.40	6.87	6.83	6.82
CaO	9.20	10.06	10.97	9.00	9.92	9.82	9.77	9.31	9.28
Na <sub>2</sub> O	2.38	2.83	2.79	3.00	2.75	2.48	2.58	2.63	2.96
K <sub>2</sub> O	0.50	0.84	0.56	0.50	0.27	0.28	0.28	0.29	0.30
P <sub>2</sub> O <sub>5</sub>	0.59	0.37	0.18	0.20	0.15	0.20	0.19	0.21	0.20
LOI	0.68	1.37	0.90	0.23	0.35	0.46	0.16	0.17	0.16
Total	98.54	99.98	99.86	98.54	98.90	98.97	98.51	98.34	98.35
Co	95	88	55	78	73	83	85	95	98
Ni	73	154	92	94	123	124	78	88	81
Cu	60	55	39	74	91	99	119	105	93
Rb	8	21	11	12	dl	5	5	dl	dl
Sr	385	407	219	261	214	217	189	195	190
Y	24	24	22	31	29	33	38	39	39
Zr	94	94	88	127	109	121	131	141	141
Nb	8.0	4.0	6.3	2.6	2.7	2.8	3.0	2.6	2.8
Ba	201	295	103	94	43	55	45	46	46
La	12.83	15.83	9.27	7.99	5.86	6.57	6.55	6.45	6.34
Ce	27.39	34.25	20.29	21.69	16.46	18.45	17.70	20.39	19.92
Nd	18.24	20.19	12.36	16.75	na	14.58	15.28	na	16.12
Sm	4.58	4.82	3.37	4.92	3.89	4.52	4.94	5.64	5.19
Eu	1.63	1.73	1.33	1.96	1.51	1.63	2.05	2.06	1.89
Tb	0.71	0.95	0.76	0.89	0.80	0.79	1.18	1.21	1.04
Yb	2.20	2.27	2.27	3.23	2.58	3.16	3.96	3.99	4.32
Hf	2.43	2.80	2.34	3.38	2.62	3.39	3.73	4.55	3.92
Mg#	35.3	45.5	60.8	49.4	51.3	49.8	45.2	44.9	44.9



Appendix 2 Whole rock data and trace element ratios of 17 samples (no REE data available).

Sample	WT208	GA156	GA313	GA315	GA316	GA325	GA336	GA352	GA353
Gabbro	V	J	J	J	J	J	J	J	J
SiO <sub>2</sub>	44.19	46.41	47.31	47.53	49.82	42.17	45.64	46.77	46.75
TiO <sub>2</sub>	0.53	1.61	1.65	1.15	2.15	1.36	2.16	2.68	1.58
Al <sub>2</sub> O <sub>3</sub>	12.92	17.06	17.18	18.12	17.63	13.00	19.75	16.45	18.84
FeO	13.89	12.41	11.06	10.56	10.42	16.15	13.18	13.99	10.65
MnO	0.21	0.24	0.22	0.22	0.18	0.28	0.25	0.24	0.17
MgO	16.48	7.86	6.77	7.27	3.01	13.58	4.59	5.09	5.15
CaO	8.18	9.67	10.63	10.26	9.98	6.68	9.35	8.19	10.46
Na <sub>2</sub> O	1.50	3.12	3.12	3.07	4.57	3.17	2.99	3.70	4.40
K <sub>2</sub> O	0.21	0.25	0.67	0.53	0.74	1.65	0.27	0.90	0.60
P <sub>2</sub> O <sub>5</sub>	0.11	0.14	0.15	0.12	0.34	0.16	0.37	0.43	0.21
LOI	dl	0.67	0.58	0.48	0.33	1.22	dl	1.58	1.32
Total	97.59	99.44	99.34	99.31	99.17	99.42	98.55	100.02	100.13
Ni	369	112	91	95	29	110	45	61	57
Cu	34	71	97	66	50	91	105	95	85
Rb	dl	dl	14	dl	10	21	dl	20	13
Sr	251	182	246	273	290	338	267	339	246
Y	11	24	23	16	43	29	25	34	25
Zr	42	95	100	74	220	125	85	148	96
Nb	2	dl	6.5	5.1	12.3	3.8	dl	5.0	dl
Ba	103	63	157	108	165	466	86	414	103
Mg#	67.9	53.1	52.2	55.2	34.0	60.0	38.4	39.4	46.3
Ti/Zr	76	102	99	93	59	65	152	109	99.0
Zr/Y	3.8	4.0	4.4	4.6	5.1	4.3	3.4	4.4	3.8
Zr/Nb	21.0	-	15.4	14.5	17.9	32.9	-	29.6	-
Ba/Zr	2.5	0.7	1.6	1.5	0.8	3.7	1.0	2.8	1.1

*Identification of the source and petrogenesis*

**Appendix 2 (continued)**

Sample	GA355	GA357A	GA358	GA393	GA451	GA494	GA509	GA429
Gabbro	J	J	J	JG	JG	JG	JG	FL
SiO <sub>2</sub>	42.82	46.41	46.33	46.83	47.45	44.51	47.81	51.53
TiO <sub>2</sub>	1.40	1.30	1.78	2.10	1.76	1.44	2.12	1.98
Al <sub>2</sub> O <sub>3</sub>	11.22	18.11	16.32	17.01	18.16	15.77	16.53	19.29
FeO	17.48	10.50	12.78	12.38	11.82	13.42	13.49	7.48
MnO	0.28	0.21	0.30	0.22	0.22	0.20	0.20	0.13
MgO	13.97	8.57	7.92	6.64	6.20	11.08	7.26	4.60
CaO	8.48	10.69	8.56	8.75	9.00	8.92	8.45	9.02
Na <sub>2</sub> O	2.00	2.48	3.34	3.61	3.14	2.78	3.20	3.88
K <sub>2</sub> O	0.39	0.43	1.05	0.84	0.74	0.26	0.75	0.74
P <sub>2</sub> O <sub>5</sub>	0.22	0.13	0.21	0.24	0.18	0.21	0.28	0.52
LOI	dl	0.26	0.31	1.42	0.11	0.75	0.10	0.39
Total	98.26	99.09	98.90	100.04	98.78	99.34	100.21	99.56
Ni	203	157	136	114	98	204	118	49
Cu	100	43	85	79	79	36	74	20
Rb	13	13	18	13	10	dl	15	10
Sr	285	273	364	378	415	297	344	566
Y	22	18	22	25	20	22	26	20
Zr	93	81	86	93	83	86	108	84
Nb	2.2	4.9	2.5	3.3	3.2	3.6	4.3	7.5
Ba	418	128	654	456	400	68	433	272
Mg#	58.8	59.3	52.5	48.9	48.4	59.6	49.0	52.3
Ti/Zr	90.0	96.0	124.0	135.0	127.0	100.0	118.0	141.0
Zr/Y	4.2	4.5	3.9	3.7	4.2	3.9	4.2	4.2
Zr/Nb	42.3	16.5	34.4	28.2	25.9	23.9	25.1	11.2
Ba/Zr	4.5	1.6	7.6	4.9	4.8	0.8	4.0	3.2

## CHAPTER VII

### THE BAMBLE GABBROS: IMPLICATIONS FOR THE EVOLUTION OF THE BAMBLE SECTOR AND THE UNDERLYING MANTLE.

The main conclusions from this study are:

**I** The five gabbros in this study crystallized from tholeiitic magmas, that were genetically related. None of the parental magmas was primary; the gabbros crystallized from magmas which had already been subjected to some degree of fractional crystallization of olivine and plagioclase. The Vestre Dale, Arendal and Tromøy Gabbros crystallized from one magma each, whereas in case of the Jomåsknutene and Flosta Gabbros more than one magma pulse was involved.

**II** In case of the Vestre Dale Gabbro, one of the most primitive gabbros in Bamble, fractionation of a tholeiitic magma gave rise to a cumulate sequence ranging in composition from troctolitic gabbros via olivine gabbros to olivine-free ferroic gabbros. The other gabbros studied show less extensive fractionation.

**III** Intrusion of the Bamble coronitic gabbros is not exclusively bound to the Sveconorwegian Orogeny; some of the gabbros were emplaced during the Gothian Orogeny. Sm-Nd whole rock dating yielded isochron ages of  $1.77 \pm 0.19$  Ga for the Jomåsknutene Gabbro, and  $1.64 \pm 0.23$  Ga for Flosta Gabbro. The Sveconorwegian Vestre Dale Gabbro has been dated at  $1.11 \pm 0.14$  Ga.

**IV** The parental magmas were derived from a depleted mantle source which had an  $\epsilon_{Nd}$  value of c. +5.5 at 1.7 Ga.

**V** Part of the trace element variations may be ascribed to fractional crystallization processes. Another part of these variations appears to be related to the introduction of LILE and LREE-bearing fluids in the depleted mantle source during the Gothian. The range in initial  $\epsilon_{Nd}$  values among Sveconorwegian gabbros indicates that these fluids variably affected the depleted mantle. It is proposed that these fluids were subduction-related.

**VI** The Gothian as well as the Sveconorwegian gabbros have been amphibolitized to a certain extent. The development of garnet-amphibolites along the margins of the Vestre

Dale Gabbro supports the concept that the Sveconorwegian Orogeny was not a low-grade event.

The obtained data provide new information about the evolution of the Bamble Sector and for the first time about the underlying mantle. It has always been assumed that the maximum age of the crust in South Norway is 1.7 Ga. (Falkum, 1985; Starmer, 1985). The  $1.77 \pm 0.19$  Ga age of the Jomåsknutene Gabbro, although with a large error, implies that crust-forming processes in the Bamble Sector may well have started before 1.7 Ga (Table 7.1; Fig. 7.1). The still unknown basement above which the Bamble supracrustals have been deposited, may therefore be Svecofennian in age. Independent, isotopic support for this suggestion is provided by the U-Pb study on zircons from the Flostå charnockitic gneiss performed by Kullerud and Machado (1991). From the U-Pb data, they inferred a possible 1.73 Ga inheritance age for the gneiss precursor. Indications for crustal growth in other parts of South Norway before 1.7 Ga, are  $T_{DM}$  model ages of charnockitic migmatites from Rogaland, ranging between 1.85 and 1.55 Ga (Menuge, 1988), and the poorly defined 1.76 Ga age (Rb-Sr) for the Håv Group metasediments and metavolcanics from the Kongsberg Sector (O'Nions and Heier, 1972). These considerations contradict earlier claims that no crust older 1.7 Ga is present in South Norway (*e.g.* Falkum, 1985) and imply that crustal growth in South Norway may be contemporaneous with crustal growth in the region east of the Oslo Rift, which started before 1.7 Ga (*cf.* Åhäll and Daly, 1989). More isotope data are required to constrain precisely the timing of crustal growth in South Norway.

The clearly positive initial  $\epsilon_{Nd}$  value of the 1.77 Ga Jomåsknutene Gabbro, and also of the 1.64 Ga Flostå Gabbro, indicate the existence of a depleted mantle reservoir in the early stages of crust formation. The presence of a depleted mantle reservoir beneath parts of Laurentia and the Baltic Shield at that time is nowadays well established (Patchett and Arndt, 1986 and references therein). The observation of Mearns et al. (1986) that crust in Southwest Scandinavian was extracted from a mantle reservoir with a chondritic signature prior to 1.74 Ga may point to the existence of two isotopically different reservoirs beneath Southwest Scandinavia: a mantle reservoir with an  $\epsilon_{Nd}$  value of 0 at 1.74 Ga and a reservoir with an  $\epsilon_{Nd}$  value of *c.* +5.5 at 1.7 Ga. The heterogeneous character of the Mid-Proterozoic mantle, composed of depleted as well as undepleted reservoirs, has also been recognized by Schärer (1991) in his study on the origin of the 1.7 - 1.6 Ga crust in eastern Labrador (Grenville Orogen).

The suggestion that accretion in South Norway was accompanied by subduction processes is corroborated by previous studies in the Bamble and Telemark Sectors (*e.g.* Torske, 1977; Smalley et al., 1983b; Falkum, 1985; Smalley and Field, 1985), although

opinions differ about the timing of subduction (Torske, 1985). Isotope data of the gabbros indicate that subduction during the Gothian was already an active process before 1.7 Ga, i.e. much earlier than 1.6 Ga, postulated by Smalley and Field (1985). From the difference in timing between subduction in the SWSD east of the Oslo Rift, i.e. prior to 1.7 Ga, and west of the Oslo Rift, these authors inferred an east-dipping, westward migrating, subduction zone. The Nd data of the gabbros suggest that pre-1.7 Ga subduction was not restricted to the eastern margin of the SWSD. Possibly, the SWSD formed one, more or less continuous, cordilleran-type orogenic belt during the Gothian (cf. Torske, 1985), along whose entire length subduction took place. The westward increasing intensity of the reworking during the Sveconorwegian Orogeny may explain the scarceness of early Gothian ages in South Norway.

Emplacement of the Sveconorwegian gabbros, which were derived from a variably enriched mantle, occurred during a period of crustal extension in the early Sveconorwegian Orogeny (Fig. 7.1; Table 1), which is mainly characterized by compression (Starmer, 1990a). The Sveconorwegian Orogeny involved rotation of the Baltic Shield relative to the Canadian Shield, which led to mutual collision along the previously continuous southern margins of these two shields (e.g. Gaál and Gorbatshev, 1987; Gower, 1990). Berthelsen (1980) and Falkum (1985) correlate this collisional event with subduction along the southwestern margin of the SWSD. Recently, Smalley and Field (1991) inferred a plate-destructive margin setting for the Bamble Sector during the Sveconorwegian from the trace element chemistry of some Bamble gabbros. This is difficult to reconcile with above evolution. Combined chemical and isotope data of the gabbros, presented in this thesis, bear no evidence for Sveconorwegian subduction.

It is proposed here that during the early Sveconorwegian the extensional regime caused upwelling of the mantle, creating a mafic underplate at the base of the continental crust, from which the Sveconorwegian gabbros have been derived (Fig. 7.1). Interestingly, Nijland and Majer (1992) suggested that the isograd pattern and the structural trend of the Bamble Sector were related to the formation of a thermal dome, which collapsed during the Sveconorwegian Orogeny due to thermal and gravitational instability. They leave the possibility open that the formation of this dome already occurred in the late Gothian. The mafic underplate may have provided the heat for amphibolite - granulite metamorphism in the Bamble Sector. The concept of a mafic underplate as a heat source for the high-grade metamorphism in the Bamble Sector was already postulated by Touret in 1969. The 1.10 - 1.03 Ga high-grade metamorphic event in the Grenville Province has recently been explained in a similar way by Emslie and Hunt (1990).

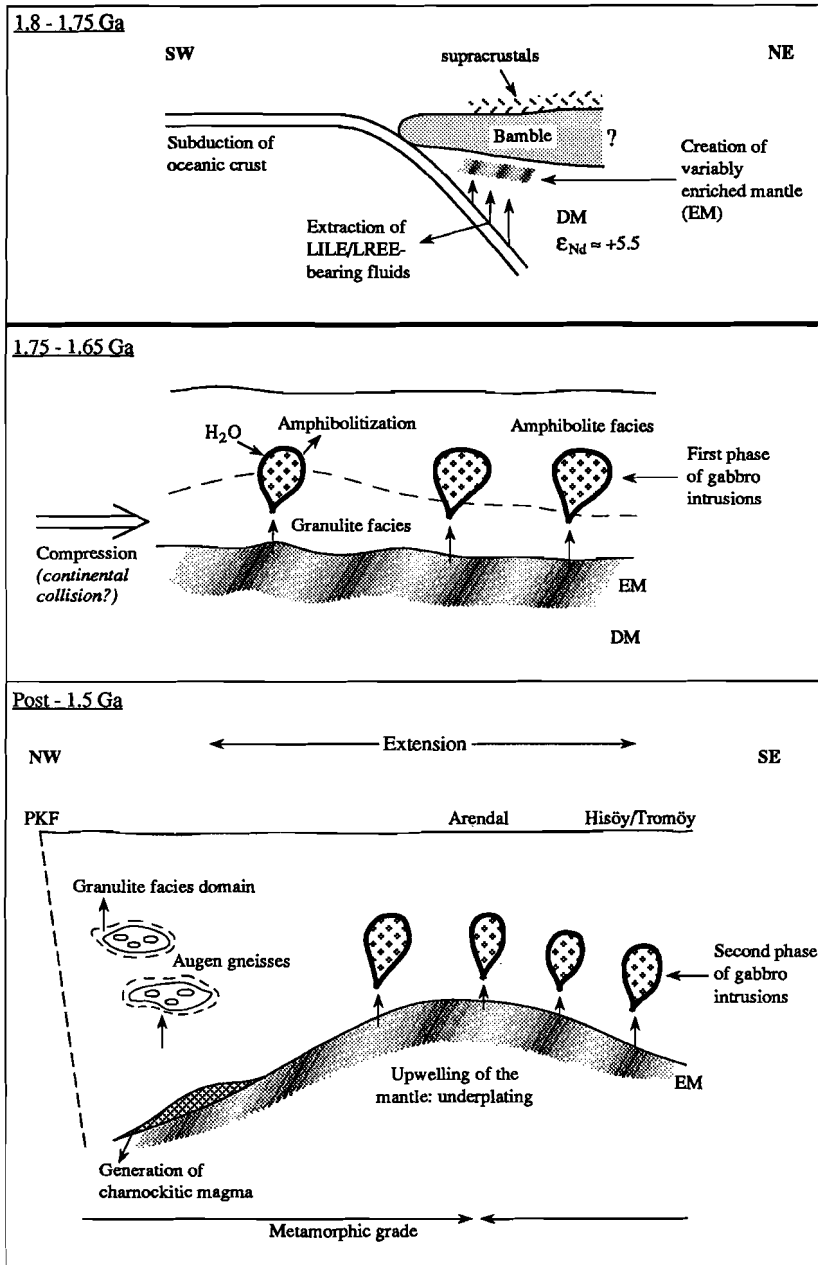
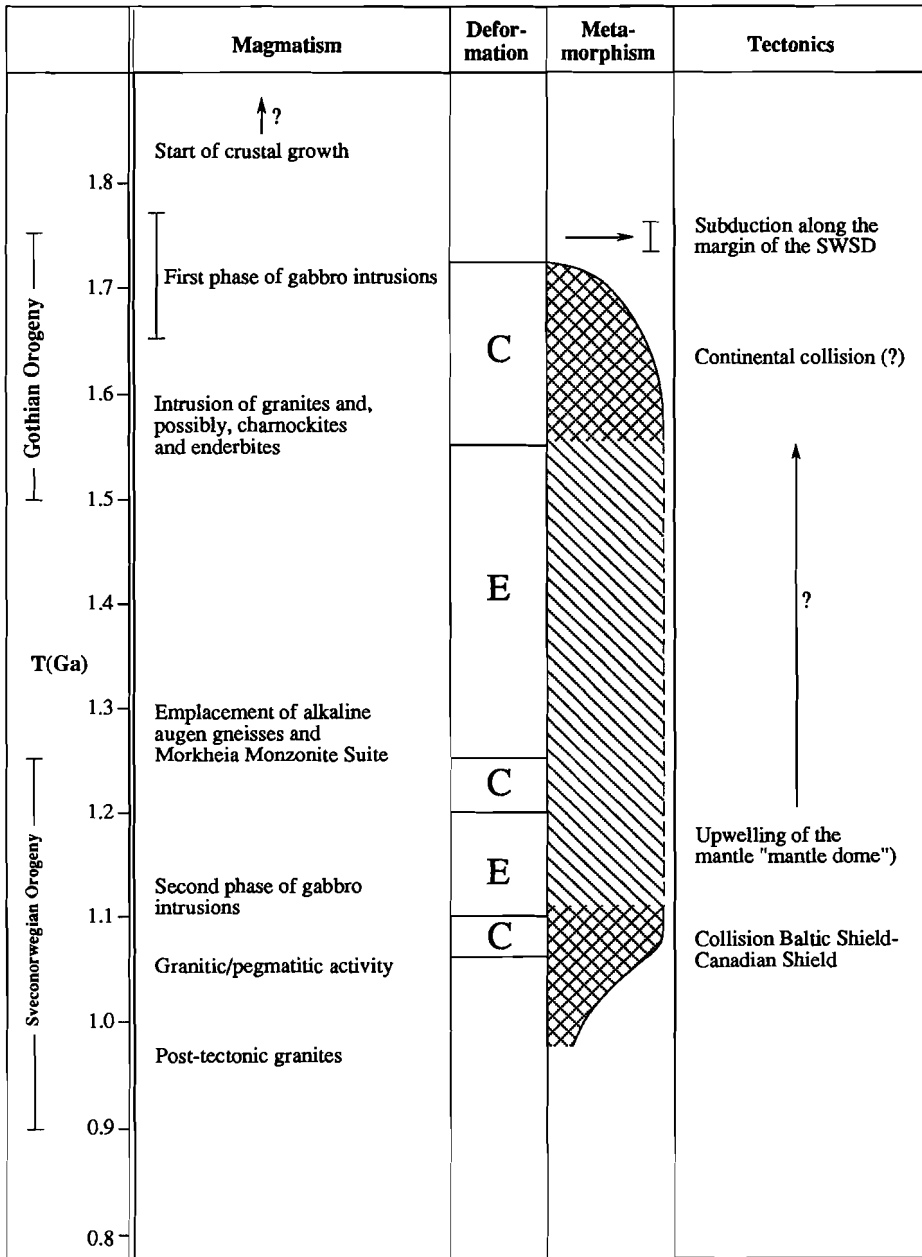


Figure 7.1 Evolutionary scenario for the Bamble Sector during Mid-Proterozoic times. Irregular hatching marks the variable enrichment of the EM.

*The Bamble gabbros: implications for the evolution*

**Table 7.1** Evolution of the Bamble Sector; C: compression; E: Extension; I: Intensity of metamorphism.



## REFERENCES

- Åhäll, K.I., 1986. Pillow lava in the Stora Le-Marstrand formation, southwestern Sweden. *Geol. Fören. Stockholm Förh.* **106**, 105-107.
- Åhäll, K.I. and Daly, J.S., 1985. Late Proterozoic magmatism in the Östfold-Marstrand belt, Bohuslän, SW Sweden. In: A.C. Tobi and J.L.R. Touret (Eds.), The deep Proterozoic crust in the North Atlantic Provinces. *NATO ASI Series C* **158**, Reidel, Dordrecht, pp. 359-367.
- Åhäll, K.I. and Daly, J.S., 1989. Age, tectonic setting and provenance of Östfold-Marstrand Belt supracrustals: westward crustal growth of the Baltic Shield at 1760 Ma. *Precambrian Res.* **45**, 45-61.
- Åhäll, K.I., Daly, J.S. and Schöberg, H., 1990. Geochronological constraints on mid-Proterozoic magmatism in the Östfold-Marstrand belt; implications for crustal evolution in southwest Sweden. In: C.F. Gower, T. Rivers and B. Ryan (Eds.), Mid-Proterozoic Laurentia-Baltica. *Geological Association of Canada Special Paper* **38**, pp. 97-115.
- Alberti, A.A. and Comin Chiaramonti, P., 1976. The metamorphic evolution of Tromøy (Arendal area - South Norway). *Tschermaks Mitt. Petrol. Min.* **23**, 205-220.
- Allègre, C.J., Treuil, M., Minster, J.-F., Minster, B. and Albarède, F., 1977. Systematic use of trace elements in igneous process. Part I: Fractional crystallization processes in volcanic suites. *Contrib. Mineral. Petrol.* **60**, 57-75.
- American Commission on Stratigraphic Nomenclature, 1970. Code of stratigraphic nomenclature. A.A.P.G., Tulsa, Oklahoma.
- Ashworth, J.R., 1986. The role of magmatic reaction, diffusion and annealing in the evolution of coronitic microstructure in troctolitic gabbro from Risør, Norway: a discussion. *Mineral. Mag.* **50**, 469-473.
- Atkin, B.P. and Brewer, T.S., 1990. The tectonic setting of basaltic magmatism in the Kongsberg, Bamble and Telemark Sectors, southern Norway. In: C.F. Gower, T. Rivers and B. Ryan (Eds.), Mid-Proterozoic Laurentia-Baltica. *Geological Association of Canada Special Paper* **38**, pp. 471-483.
- Baadsgaard, H., Chaplin, C. and Griffin, W.L., 1984. Geochronology of the Gloserheia pegmatite, Froland, southern Norway. *Nor. Geol. Tidsskr.* **54**, 111-119.
- Barrie, T.C., Gorton, M.P., Naldrett, A.J. and Hart, T.R., 1991. Geochemical constraints on the petrogenesis of the Kamiskotia gabbroic complex and related basalts, western Abitibi Subprovince, Ontario, Canada. *Precambrian Res.* **50**, 173-199.
- Barth, T.F.W., 1925. On contact minerals from Precambrian limestones in southern Norway. *Nor. Geol. Tidsskr.* **8**, 93-114.
- Barth, T.F.W., 1933. The large Precambrian intrusive bodies in the southern part of Norway. XVI Int. Geol. Congress, Washington, 297.
- Barth, T.F.W. and Dons, J.A., 1960. Precambrian of southern Norway. *Nor. geol. unders.* **208**, 6-67.
- Beeson, R., 1978. The geochemistry of meta-igneous rocks from the amphibolite facies terrain of South Norway. *Nor. Geol. Tidsskr.*, **58**, 1-16.
- Beeson, R., 1988. Identification of cordierite-anthophyllite rock types associated with sulphide deposits of copper, lead and zinc. *Trans. Inst. Mining Metal.* **97B**, 108-115.



- Berthelsen, A., 1980. Towards a palinspastic tectonic analysis of the Baltic Shield. *Mém. B.R.G.M.*, 6th Coll. Int. Geol. Cong., Paris 1980 **108**, pp. 5-21.
- Bingen, B., Demaiffe, D. and Hertogen, J., 1990. Evolution of feldspars at the amphibolite-granulite transition in augen gneisses (SW Norway): geochemistry and Sr isotopes. *Contrib. Mineral. Petrol.* **105**, 275-288.
- Brickwood, J.D., 1986. The geology and mineralogy of some Fe-Cu-Ni sulphide deposits in the Bamble area, Norway. *Nor. Geol. Tidsskr.* **66**, 189-208.
- Brickwood, J.D. and Craig, J.W., 1987. Primary and re-equilibrated mineral assemblages from the Sveconorwegian mafic intrusion of the Kongsberg and Bamble areas, Norway. *Nor. geol. unders.* **410**, 1-23.
- Broch, O.A., 1964. Age determinations of Norwegian minerals up to March 1964. *Nor. geol. unders.* **228**, 84-113.
- Brøgger, W.C., 1934a. On several Archean rocks from the south coast of Norway II. The South Norwegian hyperites and their metamorphism. *Skr. Nor. Vid. Ak. Mat. Nat. Kl. 1*, 1-421.
- Brøgger, W.C., 1934b. On several Archean rocks from the south coast of Norway I. Nodular granites from the environs of Kragerø. *Skr. Nor. Vid. Mat. Nat. Kl. 8*.
- Brøgger, W.C. and Reusch, H.H., 1875. Vorkommen des Apatit in Norwegen. *Z. Deuts. Geol. Ges.* **27**, 646-702.
- Brueckner, H.K., 1972. Interpretation of Rb-Sr ages from the Precambrian and Paleozoic rocks from southern Norway. *Am. J. Sci.* **272**, 334-358.
- Bugge, A., 1928. En forkastning i det Syd-Norske Grunnfjell. *Nor. geol. unders.* **130**, 1-124.
- Bugge, A., 1936. Kongsberg - Bamble formationen. *Nor. geol. unders.* **146**, 1-160.
- Bugge, J.A.W., 1940. Geological and petrological investigations in the Arendal district. *Nor. Geol. Tidsskr.* **20**, 71-112.
- Bugge, J.A.W., 1943. Geological and petrological investigations in the Kongsberg-Bamble formations. *Nor. geol. unders.* **160**, 1-150.
- Chalokwu, C.I. and Grant, N.K., 1987. Reequilibration of olivine with trapped liquid in the Duluth complex, Minnesota. *Geology* **15**, 71-74.
- Chalokwu, C.I. and Grant, N.K., 1990. Petrology of the Partridge River Intrusion, Duluth complex, Minnesota: 1. Relationships between mineral compositions, density and trapped liquid abundance. *J. Petrol.* **31**, 265-293.
- Chauvel, C., Arndt, N.T., Kielinczuk, S. and Thom, A., 1987. Formation of Canadian 1.9 Ga old continental crust. I: Nd isotopic data. *Can. J. Earth Sci.* **24**, 396-406.
- Claesson, S., Huhma, H., Kinny, P. and Williams, I.S., 1991. Provenance of Svecofennian metasediments: U-Pb dating of detrital zircons. *Terra abstracts* **3**, 505.
- Clough, P.W.L. and Field, D., 1980. Chemical variation in metabasites from a Proterozoic amphibolite-granulite transition zone, South Norway. *Contrib. Mineral. Petrol.* **73**, 277-286.
- Conrad, M.E. and Naslund, H.R., 1989. Modally-graded rhythmic layering in the Skaergaard intrusion. *J. Petrol.* **30**, 251-269.
- Cooper, D.C. and Field, D., 1977. The chemistry and origins of Proterozoic low-potash high-iron charnockitic gneisses from Tromøy, South Norway. *Earth Planet. Sci. Lett.* **35**, 105-115.
- Cox, K.G., 1980. A model for flood basalt volcanism. *J. Petrol.* **21**, 629-650.
- Czamanske, G.K. and Bohlen S.R., 1990. The Stillwater Complex and its anorthosites: an accident of magmatic underplating. *Am. Mineral.* **75**, 37-45.

- Dahlgren, S., Heaman, L. and Krogh, T., 1990. Geological evolution and U-Pb geochronology of the Proterozoic central Telemark area, Norway. *Geonytt* **17**, 38 (abstract).
- Dahlgren, S., 1991. Sm-Nd age of the metamorphic mineral assemblage in the Brårvik mafic granulite, Flosta. Excursion log to the 2nd SNF Workshop, Bamble 1991.
- Davidson, A. and van Breemen, O., 1988. Baddeleyite-zircon relationships in coronitic metagabbro, Grenville Province, Ontario: implications for geochronology. *Contrib. Mineral. Petrol.* **100**, 291-299.
- DeLong, S.E. and Chatelain, C., 1989. Complementary trace-element fractionation in volcanic and plutonic rocks: imperfect samples from ocean-floor basalts and gabbros. *Contrib. Mineral. Petrol.* **102**, 154-162.
- Demaiffe, D. and Michot, J., 1985. Isotope geochronology of the Proterozoic crustal segment of southern Norway: a review. In: A.C. Tobi and J.L.R. Touret (Eds.), The deep Proterozoic crust in the North Atlantic Provinces. *NATO ASI Series C* **158**, Reidel, Dordrecht, pp. 411-433.
- Demaiffe, D., Weis, D., Michot, J. and Duchesne, J.C., 1986. Isotopic constraints on the genesis of the Rogaland anorthositic suite (Southwest Norway). *Chem. Geol.* **57**, 167-179.
- Demaiffe, D., Bingen, B., Wertz, P. and Hertogen, J., 1990. Geochemistry of the Lyngdal hyperites (SW Norway): comparison with the monzonorites associated with the Rogaland anorthosite complex. *Lithos* **24**, 237-250.
- DePaolo, D.J., 1981. A neodymium and strontium isotope study of the Mesozoic calc-alkaline granite batholiths of the Sierra Nevada and Peninsular Ranges, California. *J. Geoph. Res.* **86B**, 10470-10488.
- DePaolo, D.J. and Wasserburg, G.J., 1976. Nd isotopic variations and petrogenetic models. *Geoph. Res. Lett.* **3**, 249-252.
- Dons, J.A., 1960. Telemark supracrustals and associated rocks I. In: O. Holtedahl (Ed.), *Geology of Norway. Nor. geol. unders.* **208**, pp. 49-58.
- Duchesne, J.C., Maquil, R. and Demaiffe, D., 1985a. The Rogaland anorthosites: facts and speculations. In: A.C. Tobi and J.L.R. Touret (Eds.), The deep Proterozoic crust in the North Atlantic provinces. *NATO ASI Series C* **158**, Reidel, Dordrecht, pp. 449-476.
- Duchesne, J.C., Roelandts, I., Demaiffe, D. and Weis, D., 1985b. Petrogenesis of monzonoritic rocks dykes in the Egersund-Ogna anorthosite (Rogaland, SW Norway): trace elements and isotopic (Sr, Pb) constraints. *Contrib. Mineral. Petrol.* **90**, 214-225.
- Duchesne, J.C., Wilmart, E., Demaiffe, D. and Hertogen, J., 1989. Monzonorites from Rogaland (Southwest Norway): a series of rocks coeval but not comagmatic with the massif-type anorthosites. *Precambrian Res.* **45**, 111-128.
- Dupuy, C. and Dostal, J., 1984. Trace element chemistry of some continental tholeiites. *Earth Planet. Sci. Lett.* **67**, 61-69.
- Eakin, P.A., 1989. The origin and properties of uranium-niobium-tantalum mineralised hydrocarbons at Narestö, Arendal, southern Norway. *Nor. Geol. Tidsskr.* **69**, 29-37.
- Eliasson, T. and Schöberg, H., 1991. U-Pb dating of the post-kinematic Sveconorwegian (Grenvillian) Bohus granite, SW Sweden: evidence of restitic zircon. *Precambrian Res.* **51**, 337-350.

- Ellam, R.M. and Cox, K.G., 1989. A Proterozoic lithospheric source for Karoo magmatism: evidence from the Nuanetsi picrites. *Earth Planet. Sci. Lett.* **92**, 207-218.
- Elliott, R.B., 1973. The chemistry of gabbro/amphibolite transitions in South Norway. *Contrib. Mineral. Petrol.* **38**, 71-79
- Emslie R.F. and Hunt, P.A., 1990. Ages and petrogenetic significance of igneous mangerite-charnockite suites associated with massif anorthosites, Grenville Province. *J. Geol.* **98**, 213-231.
- Erdmann, A., 1855. Vägledning till bergarternas kännedom - I. Marcus, Stockholm.
- Falkum, T., 1985. Geotectonic evolution of southern Scandinavia in light of a late-Proterozoic plate-collision. In: A.C. Tobi and J.L.R. Touret (Eds.), The deep Proterozoic crust in the North Atlantic Provinces. *NATO ASI Series C* **158**, Reidel, Dordrecht, pp. 309-322.
- Falkum, T., 1990. The Proterozoic evolution of southwestern Fennoscandia - crustal accretion or ensialic rejuvenation. Second symposium on the Baltic Shield, Lund, Sweden, 10 (abstract).
- Field, D. and Rodwell, J.R., 1968. The occurrence of prehnite in a high-grade metamorphic sequence from South Norway. *Nor. Geol. Tidsskr.* **68**, 55-59.
- Field, D. and Elliott, R.B., 1974. The chemistry of gabbro/amphibolite transitions in South Norway II. Trace elements. *Contrib. Mineral. Petrol.* **47**, 63-76.
- Field, D. and Råheim, A., 1979. Rb-Sr total rock isotope studies on Precambrian charnockitic gneisses from South Norway: evidence for isochron resetting during a low-grade metamorphic-deformational event. *Earth Planet. Sci. Lett.* **45**, 32-44.
- Field, D. and Råheim, A., 1981. Age relationships in the Proterozoic high-grade gneiss regions of southern Norway. *Precambrian Res.* **14**, 261-275.
- Field, D., Drury, A. and Cooper, D.C., 1980. Rare-earth and LIL element fractionation in high-grade charnockitic gneisses, South Norway. *Lithos* **13**, 281-289.
- Field, D., Smalley, P.C., Lamb R.C. and Råheim, A., 1985. Geochemical evolution of the 1.6 - 1.5 Ga-old amphibolite-granulite facies terrain, Bamble Sector, Norway: dispelling the myth of Grenvillian high-grade reworking. In: A.C. Tobi and J.L.R. Touret (Eds.), The deep Proterozoic crust in the North Atlantic Provinces. *NATO ASI Series C* **158**, Reidel, Dordrecht, pp. 567-578.
- Fletcher, I.R. and Rosman, K.J.R., 1982. Precise determination of initial  $\epsilon_{Nd}$  from Sm-Nd isochron data. *Geochim. Cosmochim. Acta* **46**, 1983-1987.
- Forbes, D., 1857. Gaeologiske undersøgelser over det metamorfiske territorium ved Norges Sydkyst. *Nyt Mag. Naturvid.* **9**, 165-184.
- Francis, E.H., 1982. Magma and sediment - I. Emplacement mechanism of late Carboniferous tholeiite sills in northern Britain. *J. Geol. Soc. London* **139**, 1-20.
- Frey, M.A., Green, D.H. and Roy, S.D., 1978. Integrated models of basalt petrogenesis: a study of quartz tholeiites to olivine melilitites from southeastern Australia utilizing geochemical and experimental petrological. *J. Petrol.* **19**, 463-513.
- Frodesen, S., 1968a. Coronas around olivine in a small gabbro intrusion, Bamble area, South Norway. *Nor. Geol. Tidsskr.* **48**, 201-206.
- Frodesen, S., 1968b. Petrographical and chemical investigations of a Precambrian gabbro intrusion, Hiåsen, Bamble area, South Norway. *Nor. Geol. Tidsskr.* **48**, 281-306.
- Frodesen, S., 1973. Trace elements in a Precambrian gabbro intrusion, Hiåsen, Bamble area, South Norway. *Nor. Geol. Tidsskr.* **53**, 1-10.

- Frost, B.R., Frost, C.D. and Touret, J.L.R., 1989. Magmas as a source of heat and fluids in granulite metamorphism. In: D. Bridgwater (Ed.), Fluid movements, element transport and the composition of the deep crust. *NATO ASI Series C* **281**, Kluwer, Dordrecht, pp. 1-18.
- Gaál, G. and Gorbatshev R., 1987. An outline of the Precambrian evolution of the Baltic Shield. *Precambrian Res.* **35**, 15-52.
- Gorbatshev, R., 1980. The Precambrian development of southern Sweden. *Geol. Fören. Stockholm Förh.* **102**, 129-136.
- Gorbatshev, R. and Gaál, G., 1987. The Precambrian history of the Baltic Shield. In: A. Kröner (Ed.), Proterozoic lithosphere evolution. *AGU-GSA Geodynamics Series* **17**, pp. 149-160.
- Gower, C.F., 1985. Correlations between the Grenville Province and Sveconorwegian orogenic belt - implications for Proterozoic evolution of the southern margins of the Canadian and Baltic Shields. In: A.C. Tobi and J.L.R. Touret (Eds.), The deep Proterozoic crust in the North Atlantic provinces. *NATO ASI Series C* **158**, Reidel, Dordrecht, pp. 247-258.
- Gower, C.F., 1990. Mid-Proterozoic evolution of the eastern Grenville Province, Canada. *Geol. Fören. Stockholm Förh.* **112**, 127-139.
- Gower, C. F., Rivers, T. and Ryan, B., 1990. Mid-Proterozoic Laurentia-Baltica: an overview of its geological evolution and a summary of the contributions made by this volume. In: C.F. Gower, T. Rivers, and B. Ryan (Eds.), Mid-Proterozoic Laurentia-Baltica. *Geological Association of Canada Special Paper* **38**, pp. 1-20.
- Haas, G.J.L.M. de, Nijland, T.G., Huijsmans, J.P.P., Maijer, C. and Dam, B.P., 1992a. The pre-corona history of a gabbroic intrusion in the Bamble Sector, Vestre Dale, Norway. *Neues Jahrbuch für Mineralogie, Abhandlungen* (in press).
- Haas, G.J.L.M. de, Verschure, R.H. and Maijer, C., 1992b. Isotopic constraints on the timing of crustal accretion of the Bamble Sector, Norway, as evidenced by coronitic gabbros. *Precambrian Research* (in press).
- Haas, G.J.L.M. de, Nijand, T.G., Senior, A. and Dam, B.P., 1992c. Igneous layering and magma replenishment in a 500 m thick gabbroic in the Proterozoic crust of South Norway. Accepted by *Norsk Geologisk Tidsskrift* (with revisions).
- Haas, G.J.L.M. de, Verschure, R.H. and Maijer, C., 1992d. Isotopic age determinations in South Norway III: Rb-Sr isotope systematics of the coronitic Vestre Dale Gabbro and its country rocks, Bamble. Submitted to *Geologiska Föreningens i Stockholm Förhandlingar*
- Hagelia, P., 1989: Structure, metamorphism and geochronology of the Skagerrak shear belt, as revealed by studies in the Hovdefjell-Ubergsmoen area, South Norway. Unpubl. M.Sc. thesis, University of Oslo, 236 pp.
- Hageskov, B., 1980: The Sveconorwegian structures of the Norwegian part of the Kongsberg-Bamble-Östfold segment. *Geol. Fören. Stockholm Förh.* **102**, 150-155.
- Halvorsen, E., 1970. Paleomagnetism and the age of the younger diabases in the Ny-Hellesund area, South Norway. *Nor. Geol. Tidsskr.* **50**, 157-166.
- Halvorsen, E., 1972. On the paleomagnetism of the Arendal diabases. *Nor. Geol. Tidsskr* **52**, 217-228.
- Harley, S.L., 1989. The origin of granulites: a metamorphic perspective. *Geol. Mag.* **126**, 215-247.

- Haskin, L.A., Haskin, M.A., Frey, F.A. and Wildeman, T.R., 1968. Relative and absolute terrestrial abundances of the rare earths. *Internat. Ser. Monograph. Earth Sci.* **30**, 889-911.
- Hebeda, E.H., Andriessen, P.A.M. and Belle, J.C. van, 1988. Simultaneous isotope analysis of Nd and Sm with a fixed multicollector mass spectrometer. *Fresenius Z. Anal. Chem.* **331**, 114-117.
- Helland, A., 1874. Apatit i forekommende i rene stakke og gange i Bamble i Norge. *Geol. Fören. Stockholm Förh.* **2**, 148-156.
- Higgins, M.D. and Van Breemen, O., 1989. Age of the Lac-St-Jean anorthosite intrusion and associated mafic rocks. *Geol. Assoc. Canada, Programs with Abstracts* **14**, p.A84.
- Holm, P.E., 1985. The geochemical fingerprints of different tectonomagmatic environments using hygromagmatophile elements of tholeiitic basalts and basaltic andesites. *Chem. Geol.* **51**, 303-323.
- Huhma, H., Cliff, R.A., Perttunen, V. and Sakko, M., 1990. Sm-Nd and Pb isotopic study of mafic rocks associated with early Proterozoic continental rifting: the Peräpohja schist belt in northern Finland. *Contrib. Mineral. Petrol.* **104**, 369-379.
- Hulzebos-Sijen, N.M.P.E., Visser, D., Maarschalkerweerd, M.H. and Maijer, C., 1990. Two new kornerupine localities in the Bamble sector, Norway. *Geonytt* **17**, 58 (abstract).
- Irvine, A.J., 1978. A review of experimental studies of crystal/liquid trace element partitioning. *Geochim. Cosmochim. Acta* **42**, 743-770.
- Irvine, T.N., 1980a. Magmatic infiltration metasomatism, double-diffusive fractional crystallization, and adcumulus growth in the Muskox intrusion and other layered intrusions. In: R.B. Hargraves (Ed.), *Physics of magmatic processes*. Princeton University Press, pp. 325-384.
- Irvine, T.N., 1980b. Magmatic density currents and cumulus processes. *Am. J. Sci.* **280A**, 1-58.
- Irvine, T.N., 1982. Terminology for layered intrusions. *J. Petrol.* **23**, 127-162.
- Irvine, T.N., 1987. Layered and related structures in the Duke Island and Skaergaard intrusions: similarities, differences, and origins. In: I. Parsons (Ed.), *Origins of igneous layering. NATO ASI Series C* **196**, Reidel, Dordrecht, pp. 185-245.
- Jacobsen, S.B. and Heier, K.S., 1978. Rb-Sr isotope systematics in metamorphic rocks, Kongsberg sector, South Norway. *Lithos* **11**, 257-276.
- Jaques, A.L. and Green, D.H., 1980. Anhydrous melting of peridotite at 10-15 kbar and the genesis of tholeiitic magmas. *Contrib. Mineral. Petrol.* **73**, 287-310.
- Joesten, R., 1986. The role of magmatic reaction, diffusion and annealing in the evolution of coronitic microstructure in troctolitic gabbro from Risör, Norway. *Mineral. Mag.* **50**, 441-467.
- Johansson, L. and Johansson, Å., 1990. Isotope geochemistry and age relationships of mafic intrusions along the Protogine Zone, southern Sweden. *Precambrian Res.* **48**, 395-414.
- Kay, R.W., 1980. Volcanic arc genesis: implications for element recycling in the crust-upper mantle system. *J. Geol.* **88**, 497-522.
- Killeen, P.G. and Heier, K.S., 1975. Radioelement distribution and heat production in Precambrian granitic rocks, southern Norway. *Nor. Vid. Ak. Mat. Nat. Kl. Skr. Ny Serie* **35**, 1-32.

- Kinck, J.J., Huseby, E.S. and Lund, C.-E., 1991. The South Scandinavian crust: structural complexities from seismic reflection and refraction profiling. *Tectonoph.* **189**, 117-133.
- Kjerulf, T. and Dahll, T., 1861. Om jernertsener forekomster ved Arendal, Naes og Kragerö. *Nyt Mag. Naturvid.* **11**, 293-359.
- Klopprogge, J.T., 1987. Fieldwork report of the Åmdal area (Bamble), Norway. Unpubl. M.Sc. thesis, University of Utrecht, 53 pp. (in Dutch).
- Krijgsman, A., 1991. (Meta)-ultramafic rocks from Bamble, Southeast Norway: geology and geothermometry. Unpubl. M.Sc. thesis, University of Utrecht, 46 pp.
- Krill, A.G., Bergh, S., Lindahl, I., Mearns, E.W., Often, M., Olerud, S., Sandstad, J.S., Siedlecka, A. and Solli, A., 1985. Rb-Sr, U-Pb and Sm-Nd isotopic dates from Precambrian rocks of Finnmark. *Nor. geol. unders.* **403**, 37-54.
- Kröner, A., 1991. Tectonic evolution in the Archaean and Proterozoic. *Tectonoph.* **187**, 393-410.
- Kullerud, L. and Dahlgren, S., 1990. Timing of the high grade metamorphism in the Bamble Sector, South Norway. *Geonytt* **17**, 68 (abstract).
- Kullerud, L. and Machado, N., 1991a. End of a controversy: U-Pb geochronological evidence for significant Grenvillian activity in the Bamble area, Norway. *Terra abstracts* **3**, 504.
- Kullerud, L. and Machado, N., 1991b. Flosta charnockitic gneiss. Excursion log to the 2nd SNF Workshop, Bamble 1991.
- Kulp, J.L. and Neumann, H., 1961. Some potassium-argon ages from the Norwegian basement. *Ann. New York Ac. Sci.* **91**, 469-475.
- Kuszniir, N.J. and Park, R.G., 1986. Continental lithospheric strength: the critical role of lower crustal deformation. In: J.B. Carswell, D.A. Carswell, J. Hall and K.H. Wedepohl (Eds.), The nature of the lower continental crust. *Geol. Soc. Sp. Publ.* **24**, pp. 79-93.
- Lacroix, A., 1889. Contribution à l'étude des gneiss à pyroxène et des roches à wernérites. *Bull. Soc. Fr. Min.* **12**, 83-350.
- Lamb, R.C., Smalley, P.C. and Field, D., 1986. P-T conditions for the Arendal granulites, southern Norway: implications for the roles of P,T and CO<sub>2</sub> in deep crustal LILE-depletion. *J. Metam. Geol.* **4**, 143-160.
- Larson, S.Å., Berglund, J., Stigh, J. and Tullborg, E.-L., 1990. The Protogine Zone: a new model - an old issue. In: C.F. Gower, T. Rivers and B. Ryan (Eds.), Mid-Proterozoic Laurentia-Baltica. *Geological Association of Canada Special Paper* **38**, pp. 317-333.
- LeCheminant, A.L. and Heaman, L.M., 1989. MacKenzie igneous events, Canada: Middle Proterozoic hotspot magmatism associated with ocean opening. *Earth Planet. Sci. Lett.* **96**, 38-48.
- Lindh, A., 1987. Westward growth of the Baltic Shield. *Precambrian Res.* **35**, 53-70.
- Lindsley, D.H., 1980. Phase equilibria of pyroxenes at pressures > 1 atmosphere. In: C.T. Prewitt (Ed.), Pyroxenes. *Reviews in Mineralogy* **7**, pp. 289-307.
- Maaløe, S., 1978. The origin of rhythmic layering. *Mineral. Mag.* **42**, 337-345.
- Maijer, C., 1990. Metamorphism in the Froland-Nelaug-Tvedestrand-Arendal-area, Bamble: re-evaluation of the Sveconorwegian as a high-grade metamorphic event. *Geonytt* **17**, 75 (abstract).
- McBirney, A.R. and Noyes, R.M., 1979. Crystallization and layering in the Skaergaard intrusion. *J. Petrol.* **20**, 487-554.

- McCulloch, M.T. and Gamble, J.A., 1991. Geochemical and geodynamical constraints on subduction zone magmatism. *Earth Planet. Sci. Lett.* **102**, 358-374.
- McKay, G.A., 1989. Partitioning of rare earth elements between major silicate minerals and basaltic melts. In: B.R. Lipin and G.A. McKay (Eds.), *Geochemistry and mineralogy of the rare earth elements. Reviews in Mineralogy* **21**, pp. 45-77.
- Mearns, E.W., 1986. Sm-Nd ages for Norwegian garnet peridotite. *Lithos* **19**, 269-278.
- Mearns, E.W., Andersen T., Mork, M.B.E. and Morvik, R., 1986.  $^{143}\text{Nd}/^{144}\text{Nd}$  evolution in depleted Baltoscandian mantle. *Terra Cognita* **6**, 247 (abstract).
- Menuge, J.F., 1985. Neodymium isotope evidence for the age and origin of the Proterozoic of Telemark. In: A.C. Tobi and J.L.R. Touret (Eds.), *The deep Proterozoic crust in the North Atlantic Provinces. NATO ASI Series C* **158**, Reidel, Dordrecht, pp. 435-448.
- Menuge, J.F., 1988. The petrogenesis of massif anorthosites: a Nd and Sr isotopic investigation of the Proterozoic of Rogaland/Vest-Agder, SW Norway. *Contrib. Mineral. Petrol.* **98**, 363-373.
- Michel-Levy, M.A., 1878. Sur une roche à sphene, amphibole et wernérite granulitique des mines d'apatite de Bamble près Brevig (Norvège). *Bull. Soc. Fr. Min.* **1**, 43-46.
- Miller, J.D. and Weiblen, P.W., 1990. Anorthositic rocks of the Duluth complex: examples of rocks formed from plagioclase crystal mush. *J. Petrol.* **31**, 295-339.
- Milne, K.P. and Starmer, I.C., 1982. Extreme differentiation in the Proterozoic Gjerstad-Morkheia Complex of South Norway. *Contrib. Mineral. Petrol.* **79**, 381-393.
- Moine, B., Roche, H. de la and Touret, J., 1972. Structures géochimique et zonéographie métamorphique dans le Précambrien catazonal du Sud de la Norvège. *Sci. Terre* **17**, 131-164.
- Mongkoltip, P. and Ashworth, J.R., 1986. Amphibolitization of metagabbros in Scottish Highlands. *J. Metam. Geol.* **4**, 261-283.
- Morthorst, J.R., Zeck, H.P. and Lundegårdh, P.H., 1983. The Proterozoic hyperites in southern Värmland, western Sweden. *Sver. Geol. Unders.* **Ba30**, 1-104.
- Morton, R.D., Batey, R.H. and O'Nions, R.K., 1970. Geological investigations in the Bamble Sector of the Fennoscandian Shield in South Norway I: The geology of eastern Bamble. *Nor. geol. unders.* **263**, 1-72.
- Munz, I.A. and Morvik, R., 1991. Metagabbros in the Modum Complex, southern Norway: an important heat source for Sveconorwegian metamorphism. *Precambrian Res.* **52**, 97-113.
- Naslund, H. R., 1989. Petrology of the Basistoppen sill, East Greenland: a calculated magma differentiation trend. *J. Petrol.* **30**, 299-319.
- Naterstad, J., Andresen, A. and Jorde, K., 1973. Tectonic succession of the Caledonian nappe front in the Haukelisæter-Røldal area, southwest Norway. *Nor. geol. unders.* **292**, 1-20.
- Naumann, C.F., 1849. *Lehrbuch der Geognosie.* Leipzig, I., 594-596.
- Nelson, B.K. and DePaolo, D.J., 1984. 1700 Myr greenstone volcanic successions in southwestern North America and isotopic evolution of Proterozoic mantle. *Nature* **312**, 143-146.
- Neumann, H., 1960. The apparent age of Norwegian minerals and rocks. *Nor. Geol. Tidsskr.* **40**, 173-189.

- Nijland, T.G. and Maijer, C., 1991. Primary sedimentary structures and infiltration metamorphism in the Håvatn-Barlindåsen-Tellaugstjern area, Froland. Excursion log to the 2nd SNF Workshop, Bamble 1991.
- Nijland, T. and Maijer, C., 1992. Lower crustal transitions I. Changing mineral assemblages and thermobarometric estimates over a classical amphibolite to granulite transition zone, Bamble, Norway. Abstract First Netherlands Earth Scientific Congres, april 23-24, 1992.
- Nijland, T.G. and Senior, A., 1991. Sveconorwegian granulite facies metamorphism of polyphase migmatites and basic dikes, South Norway. *J. Geol.* **99**, 515-525.
- Nijland, T.G., Senior, A. and Maijer, C., 1991. High-grade Grenvillian metamorphism in the Bamble Sector, Norway: Field and petrographic evidence. *Terra abstracts* **3**, 444.
- O'Nions, R.K. and Baadsgaard, H., 1971. A radiometric study of polymetamorphism in the Bamble region, S. Norway. *Contrib. Mineral. Petrol.* **34**, 1-21.
- O'Nions, R.K. and Heier, K.S., 1972. A reconnaissance Rb-Sr geochronological study of the Kongsberg area, South Norway. *Nor. Geol. Tidsskr.* **52**, 143-150.
- O'Nions, R.K., Morton, R.D and Baadsgaard, H., 1969. Potassium-argon ages from the Bamble Sector of the Fennoscandian Shield in South Norway. *Nor. Geol. Tidsskr.* **49**, 171-190.
- Otten, M.T., 1984. The origin of brown hornblende in the Artfjället gabbro and dolerites. *Contrib. Mineral. Petrol.* **86**, 189-199.
- Pasteels, P. and Michot, J., 1975. Geochronological investigation of the metamorphic terrain of SW Norway. *Nor. Geol. Tidsskr.* **55**, 111-134.
- Patchett, P.J. and Bridgwater, D., 1984. Origin of the continental crust of 1.9-1.7 Ga age defined by Nd isotopes in the Ketilidian terrain of South Greenland. *Contrib. Mineral. Petrol.* **87**, 311-318.
- Patchett, P.J. and Arndt, N.T., 1986. Nd isotopes and tectonics of 1.9 - 1.7 Ga crustal genesis. *Earth Planet. Sci. Lett.* **78**, 329-338
- Patchett, J., Gorbatshev, R. and Todt, W., 1987. Origin of the continental crust of 1.9 - 1.7 Ga age: Nd isotopes in the Svecofennian orogenic terrains of Sweden. *Precambrian Res.* **35**, 145-160.
- Pearce, J.A., 1984. Role of the sub-continental lithosphere in magma genesis at active continental margins. In: C.J. Hawkesworth and M.J. Norry (Eds.), *Continental basalts and mantle xenoliths*. Shiva Publishing, Nantwich, pp. 230-249.
- Pearce, J.A. and Norry, M.J., 1979. Petrogenetic implications of Ti, Zr, Y and Nb variations in volcanic rocks. *Contrib. Mineral. Petrol.* **69**, 33-47.
- Pharaoh, T.C. and Brewer, T.S., 1990. Spatial and temporal diversity of early Proterozoic volcanic sequences - comparisons between the Baltic and Laurentian shields. *Precambrian Res.* **47**, 169-189.
- Ploquin, A., 1980. Étude géochimique du Complex de gneiss, migmatites et granites du Telemark - Aust-Agder (Précambrien de Norvège du Sud). Sa place dans l'ensemble épizonal à catazonal profond du Haut Telemark au Bamble. *Sci. Terre* **38**, 1-389.
- Poorter, R.P.E., 1981. Precambrian paleomagnetism of Europe and the position of the Balto-Russian plate in relation to Laurentia. In: A. Kröner (Ed.), *Precambrian plate tectonics*. Elsevier, Amsterdam, pp. 599-622.
- Presnall, D.C., Dixon, S.A., Dixon, J.R., O'Donnell, T.H., Brenner, N.L., Schrock, R.L. and Dycus, D.W., 1978. Liquidus phase relations on the join diopside-forsterite-



- anorthite from 1 atm to 20 kbar: their bearing on the generation and crystallization of basaltic magma. *Contrib. Mineral. Petrol.* **66**, 203-220.
- Priem, H.N.A., Mulder, F.G., Boelrijk, N.A.I.M., Hebeda, E.H., Verschure, R.H. and Verdurmen, E.A.Th., 1968. Geochronological and palaeomagnetic reconnaissance survey in parts of central and southern Sweden. *Phys. Earth Planet. Inter.* **1**, 373-380.
- Priem, H.N.A., Boelrijk, N.A.I.M., Hebeda, E.H., Verdurmen E.A.Th. and Verschure, R.H., 1973. Rb-Sr investigations on Precambrian granites, granitic gneisses and acidic metavolcanics in Central Telemark: metamorphic resetting of Rb-Sr whole-rock systems. *Nor. geol. unders.* **289**, 37-53.
- Ramberg, I.B., Gabrielsen, R.H., Larsen, B.T. and Solli, A., 1977. Analysis of the fracture patterns in Southern Norway. *Geol. Mijnbouw* **56**, 295-310.
- Reynolds, R.C. and Frederickson, A.F., 1962. Corona development in Norwegian hyperites and its bearing on the metamorphic facies concept. *Geol. Soc. Am. Bull.* **73**, 59-72.
- Roeder, P.L. and Emslie, R.F., 1970. Olivine-liquid equilibrium. *Contrib. Mineral. Petrol.* **29**, 275-289.
- Ryan, M.J., 1966. The geology of the area around Ödegårdens Verk, South Norway. Unpubl. Ph.D. thesis, University of Nottingham.
- Schärer, U., 1991. Rapid continental crust formation at 1.7 Ga from a reservoir with chondritic isotope signatures, eastern Labrador. *Earth Planet. Sci. Lett.* **102**, 110-133.
- Sigmond, E.M.O., 1978. Beskrivelse till det berggrundsgeologiske kartbladet Sauda 1:250.000. *Nor. geol. unders.* **341**, 1-94.
- Sigmond, E.M.O., 1984. En megaforkastningssone i Syd Norge. Abstract Sixteenth Geological Wintermeeting Norden, Stockholm.
- Sjögren, H., 1883. Om de norska apatitfjörekomsterna och om sannolikheten att anträffa i Sverige. *Geol. Fören. Stockholm Förh.* **6**, 447-498.
- Skiöld, T., 1976. The interpretation of Rb-Sr ages of late-Precambrian rocks in southwestern Sweden. *Geol. Fören. Stockholm Förh.* **98**, 3-29.
- Skiöld, T. and Cliff, R.A., 1984. Sm-Nd and U-Pb dating of early Proterozoic mafic-felsic volcanism in northernmost Sweden. *Precambrian Res.* **26**, 1-13.
- Skjernaa, L. and Pedersen, S., 1982. The effects of penetrative Sveconorwegian deformation on the Rb-Sr isotope systems in the Römskog-Aurskog-Höland area, SE Norway. *Precambrian Res.* **17**, 215-243.
- Smalley, P.C., 1990. Rb-Sr systematics of a Gardar-age layered alkaline monzonite suite in southern Norway: a reply. *J. Geol.* **98**, 123-127.
- Smalley, P.C. and Field, D., 1985. Geochemical constraints on the evolution of the Proterozoic continental crust in southern Norway (Telemark Sector). In: A.C. Tobi and J.L.R. Touret (Eds.), *The deep Proterozoic crust in the North Atlantic provinces. NATO ASI Series C 158*, Reidel, Dordrecht, pp. 551-566.
- Smalley, P.C. and Field, D., 1991. REE, Th, Hf and Ta in Bamble gabbros (southern Norway) and their amphibolitized equivalents: implications for gabbro tectonic setting. *Precambrian Res.* **53**, 233-242.
- Smalley, P.C., Field, D. and Råheim, A., 1983a. Resetting of Rb-Sr whole rock isochrons during Sveconorwegian low-grade events in the Gjerstad augengneiss, Telemark, southern Norway. *Is. Geosc.* **1**, 269-282.

- Smalley, P.C., Field, D., Lamb, R.C. and Clough, P.W.L., 1983b. Rare earth, Th, Hf, Ta and large-ion lithophile element variations in metabasites from the Proterozoic amphibolite-granulite transition zone at Arendal, South Norway. *Earth Planet. Sci. Lett.* **63**, 446-458.
- Smalley, P.C., Field, D. and Råheim, A., 1988; Rb-Sr isotope systematics of a Gardar-age layered alkaline monzonite suite in southern Norway. *J. Geol.* **96**, 17-29.
- Spera, F.J. 1980. Aspects of magma transport. In: R.B. Hargraves (Ed.), *Physics of magmatic processes*. Princeton University Press, pp. 265-323.
- Starmer, I.C., 1969. Basic plutonic intrusions of the Risør - Söndeled area, South Norway : The original lithologies and their metamorphism. *Nor. Geol. Tidsskr.* **49**, 403-431.
- Starmer, I.C., 1985a. The evolution of the South Norwegian Proterozoic as revealed by major and mega-tectonics of the Kongsberg and Bamble sectors. In: A.C. Tobi and J.L.R. Touret (Eds.), *The deep Proterozoic crust in the North Atlantic Provinces. NATO ASI Series C 158*, Reidel, Dordrecht, pp. 259-290.
- Starmer, I.C., 1985b. The geology of the Kongsberg district and the evolution of the entire Kongsberg Sector, South Norway. *Nor. geol. unders.* **401**, 35-58.
- Starmer, I.C., 1987. Geological map of the Bamble Sector, South Norway. In: C. Maijer and P. Padget (Eds.), *The geology of southernmost Norway - an excursion guide. Nor. geol. unders. Spec. Publ. 1*.
- Starmer, I.C., 1990a. Mid-Proterozoic evolution of the Kongsberg-Bamble belt and adjacent areas, southern Norway. In: C.F. Gower, T. Rivers and B. Ryan (Eds.), *Mid-Proterozoic Laurentia-Baltica. Geological Association of Canada Special Paper 38*, pp. 279-305.
- Starmer, I.C., 1990b. Rb-Sr systematics of a Gardar-age layered alkaline monzonite suite in southern Norway: a discussion. *J. Geol.* **98**, 119-123.
- Starmer, I.C., 1991. The Proterozoic evolution of the Bamble Sector shear belt, southern Norway: correlations across southern Scandinavia and the Grenvillian controversy. *Precambrian Res.* **49**, 107-139.
- Stearn, J.E.F. and Piper, J.D.A., 1984. Paleomagnetism of the Sveconorwegian mobile belt of the Fennoscandian Shield. *Precambrian Res.* **23**, 201-246.
- Støretvedt, K.M., 1968. The permanent magnetism of some basic intrusions in the Kragerø archipelago, South Norway, and its geological implications. *Nor. Geol. Tidsskr.* **48**, 153-163.
- Sun, S.-S. and Nesbitt, R.W., 1978. Petrogenesis of Archean ultrabasic and basic volcanics. *Contrib. Mineral. Petrol.* **65**, 301-325.
- Sun, S.-S. and McDonough, W.F., 1989. Chemical and isotopic systematics of oceanic basalts: implications for mantle composition and processes. In: A.D. Saunders and M.J. Norry (Eds.), *Magmatism in Oceanic Basins. Geol. Soc. Spec. Publ. 42*, pp. 313-346.
- Sun, S.-S., Nesbitt, R.W. and Sharaskin, A.Y., 1979. Geochemical characteristics of mid-oceanic ridge basalts. *Earth Planet. Sci. Lett.* **44**, 119-138.
- Sutcliffe, R.H., Sweeny, J.M. and Edgar, A.D., 1989. The Lac des Iles Complex, Ontario: petrology and platinum-group-elements mineralization in an Archean mafic intrusion. *Can. J. Earth Sci.* **26**, 1408-1427.
- Taylor, S.R. and McLennan, S.M., 1985. *The continental crust: its composition and evolution*. Blackwell, Oxford, 312 pp.
- Theulings, W.T., 1988. Fieldwork report of the Bamble area, Unpubl. M.Sc. thesis,

- University of Utrecht, 40 pp. (in Dutch).
- Theulings, W.T., Ditshuizen, G.P. and Huijsmans, J.P.P., 1986. Petrology, mineralogy and geochemistry of a coronitic gabbro from Vestre Dale, Bamble, South Norway. *Eos* **67**, 1352 (abstract).
- Thompson, R.N., 1975. Primary basalts and magma genesis. II Snake River Plain, Idaho, U.S.A.. *Contrib. Mineral. Petrol.* **52**, 213-232.
- Törnebohm, A.E., 1877. Über die wichtigen Diabas und Gabbro-Gesteine Schwedens. *Neues Jahrbuch*, 379-380.
- Torske, T., 1977. The South Norwegian Precambrian Region - a Proterozoic cordilleran-type orogenic segment. *Nor. Geol. Tidsskr.* **57**, 97-120.
- Torske, T., 1985. Terrane displacement and Sveconorwegian rotation of the Baltic Shield: a working hypothesis. In: A.C. Tobi and J.L.R. Touret (Eds.), The deep Proterozoic crust in the North Atlantic Provinces. *NATO ASI Series C* **158**, Reidel, pp. 333-343.
- Touret, J., 1966. Sur l'origine supracrustale des gneiss rubanés de Selås (formation de Bamble, Norvège méridionale). *Comp. Rend. Ac. Sci. Paris* **262**, 9-12.
- Touret, J., 1968. The Precambrian metamorphic rocks around Lake Vegår (Aust-Agder, southern Norway). *Nor. geol. unders.* **257**, 1-45.
- Touret, J., 1969. Le socle Précambrien de la Norvège méridionale. Unpubl. Ph.D. thesis, University of Nantes, 609 pp.
- Touret, J., 1971a. Le faciès granulite en Norvège méridionale I. Les associations minéralogiques. *Lithos* **4**, 239-249.
- Touret, J., 1971b. Le faciès granulite en Norvège méridionale II. Les inclusions fluides. *Lithos* **4**, 423-436.
- Touret, J., 1979. Les roches à tourmaline-cordiérite-disthène de Bjordammen (Norvège méridionale) sont-elles liées à d'anciennes évaporites? *Sci. Terre* **23**, 95-97.
- Touret, J.L.R., 1985. Fluid regime in southern Norway: the record of fluid inclusions. In: A.C. Tobi and J.L.R. Touret (Eds.), The deep Proterozoic crust in the North Atlantic Provinces. *NATO ASI Series C* **158**, Reidel, Dordrecht, pp. 517-549.
- Touret, J. and Olsen, S.N., 1985. Fluid inclusions in migmatites. In: J.R. Ashworth (Ed.), Migmatites. Blackie Publications, Glasgow, pp. 265-286.
- Tröger, W.E., 1935. Spezielle Petrographie der Eruptivgesteine (Unveränderter Nachdruck 1969). Verlag der Deutschen Mineralogischen Gesellschaft e.V., Bonn, 360 pp.
- Upton, B.G.J., 1987. Gabbroic, syenogabbroic and syenitic cumulates of the Tugtutôq Younger Giant Dike Complex, South Greenland. In: I. Parsons (Ed.), Origins of igneous layering. *NATO ASI Series C* **196**, Reidel, Dordrecht, pp. 93-123.
- Verschure, R.H., 1985. Geochronological framework for the late-Proterozoic evolution of the Baltic Shield in South Scandinavia. In: A.C. Tobi and J.L.R. Touret (Eds.), The deep Proterozoic crust in the North Atlantic Provinces. *NATO ASI Series C* **158**, Reidel, Dordrecht, pp. 381-410.
- Verschure, R.H., Andriessen, P.A.M., Boelrijk, N.A.I.M., Hebeda, E.H., Maijer, C., Priem, H.N.A. and Verdurmen, E.A.Th., 1980. On the thermal stability of Rb-Sr and K-Ar biotite systems: evidence from coexisting Sveconorwegian (ca. 870 Ma) and Caledonian (ca. 400 Ma) biotites in SW Norway. *Contrib. Mineral. Petrol.* **74**, 245-252.
- Verschure, R.H., Maijer, C., Andriessen, P.A.M., Boelrijk, N.A.I.M., Hebeda, E.H.,

- Priem, H.N.A. and Verdurmen, E.A.Th., 1983. Dating explosive volcanism perforating the Precambrian basement in southern Norway. *Nor. geol. unders.* **380**, 35-49.
- Verschure, R.H., Maijer, C. and Andriessen, P.A.M., 1989. Isotopic age determination in South Norway I: The Skår volcanic breccia, Greipstad, Vestagder. *Geol. Mijnbouw* **68**, 253-256.
- Verschure, R.H., Maijer, C. and Andriessen, P.A.M., 1990. Isotopic age determinations in South Norway II. The problem of errorchron ages from Telemark rhyolites. *Nor. geol. unders.* **418**, 47-60.
- Versteeve, A., 1975. Isotope geochronology in the high-grade metamorphic Precambrian of southwestern Norway. *Nor. geol. unders.* **318**, 1-50.
- Visser, D. and Senior, A., 1990. Aluminous reaction textures in orthoamphibole-bearing rocks: the pressure-temperature evolution of the high-grade Proterozoic of the Bamble Sector, South Norway. *J. Metam. Geol.* **8**, 231-246.
- Visser, D., Nijland, T.G. & Maijer, C., 1991. Orthopyroxene-cordierite-garnet-kornerupine-albite-bearing meta-evaporites intercalated with enderbitic gneisses at Færvik School, Tromøya. Excursion log to the 2nd SNF Workshop, Bamble 1991.
- Wager, L.R. and Brown, G.M., 1968. Layered igneous rocks. San Fransisco: W. H. Freeman and Co., 588 pp.
- Weaver, B.L. and Tarney, J., 1981. The Scourie dyke suite: petrogenesis and geochemical nature of the Proterozoic sub-continental mantle. *Contrib. Mineral. Petrol.* **78**, 175-188.
- Weis, D., 1986. Genetic implications of Pb isotopic chemistry in the Rogaland anorthositic complex (Southwest Norway). *Chem. Geol.* **57**, 181-199.
- Welin, E., 1966. The absolute time scale and the classification of Precambrian rocks in Sweden. *Geol. Fören. Stockholm Förh.* **88**, 29-33.
- Welin, E. and Gorbatshev, R., 1978a. The Rb-Sr age of the Varberg charnockite. *Geol. Fören. Stockholm Förh.* **100**, 225-227.
- Welin, E. and Gorbatshev, R., 1978b. Rb-Sr isotopic relations of a tonalitic intrusion on Tjörn Island, southwestern Sweden. *Geol. Fören. Stockholm Förh.* **100**, 228-230.
- Welin, E., Gorbatshev, R. and Kähr, A.-M., 1982. Zircon dating of polymetamorphic rocks in southwestern Sweden. *Sver. Geol. Unders.* **C797**, 1-34.
- Wielens, J.B.W., Andriessen, P.A.M., Boelrijk, N.A.I.M., Hebeda, E.H., Priem, H.N.A., Verdurmen, E.A.Th. and Verschure, R.H., 1980. Isotope geochronology in the high-grade metamorphic Precambrian of southwestern Norway: new data and reinterpretations. *Nor. geol. unders.* **359**, 1-30.
- Wilson, M., 1989. Igneous petrogenesis. Unwin Hyman, London, 466 pp.
- York, D., 1969. The best isochron. *Earth Planet. Sci. Lett.* **2**, 479-482.
- Zeck, H.P. and Wallin, B., 1980. A  $1220 \pm 60$  My Rb-Sr isochron age, representing a Taylor-convection caused recrystallization event in a granitic rock suite. *Contrib. Mineral. Petrol.* **74**, 45-53.

## **CURRICULUM VITAE**

Geert-Jan L.M. de Haas werd op 1 februari 1964 geboren te Goirle. In juni 1982 behaalde hij het diploma Gymnasium- $\beta$  aan het Mill Hill College te Goirle. In september van dat jaar begon hij met de studie Geologie aan de Rijksuniversiteit te Utrecht. In oktober 1983 werd het propaedeutisch examen afgelegd en in april 1987 het doctoraal examen (cum laude) met als hoofdvak Endogene Geochemie en als bijvak Experimentele Petrologie. In de periode van mei 1987 tot en met april 1991 was hij werkzaam bij de vakgroep Geochemie als assistent in opleiding.